NASA Contractor Report 3231

On the Question of Instabilities Upstream of Cylindrical Bodies

Mark V. Morkovin

GRANT NSG-1120
DECEMBER 1979

NASA

NASA Contractor Report 3231

On the Question of Instabilities Upstream of Cylindrical Bodies

Mark V. Morkovin
Illinois Institute of Technology
Chicago, Illinois

Prepared for
Langley Research Center
under Grant NSG-1120

National Aeronautics
and Space Administration

**Scientific and Technical
Information Branch**

1979

CONTENTS

SUMMARY

It has been known since the late twenties (Piercy and Richardson) that unexpectedly high velocity and presumably pressure fluctuations are found in the stagnation region of blunt-nosed bodies placed in wind tunnels with uniform streams. Very recently, visualization techniques have revealed frequent formations of streamwise vortices both steady and unsteady. These fluctuations and vortices are known to increase substantially the heat and mass transfer in the stagnation region when r.m.s. free-stream turbulence exceeds approximately 1% of free-stream speed, U_0, and may also cause increased acoustic radiation. The boundary layer, though perturbed by the streamwise vortices tends to remain laminar in the region of accelerations around the head of the bluff bodies. However, these vortical disturbances are likely to contribute to earlier-than-expected transition to turbulence farther downstream so that prevention of such "seeding" should delay transition.

In an attempt to understand the phenomena behind these important practical flow manifestations, a critical review of the theoretical and experimental evidence was made. Current theory is revealed to be incomplete, incorrect, or inapplicable to the phenomena observed experimentally. The formalistic approach via the "principle" of exchange of instabilities should most likely be replaced by a "forced disturbance" approach. Also, many false conclusions were reached by ignoring the fact that treatment of the base and perturbed flows in Hiemenz coordinate η is asymptotic in nature. Almost surely the techniques of matched asymptotic expansions will have to be used to capture correctly the diffusive and vorticity amplifying processes of the disturbances vis-a-vis the mean-flow boundary layer and outer potential field as η and y/diameter approach infinity. There are also serious uncertainties in the experiments which are discussed in detail.

SYMBOLS

a	velocity gradient at the stagnation point
A	amplitude, stream-tube area
d	diameter of wake generating rod
D	cylinder diameter (or thickness if square)
f	frequency
k	wave number $2\pi/\lambda$ or $(2\pi/\lambda)\cdot\sqrt{\nu/a}$
P,p	pressure
R	radius of cylinder
$Re_{(\ )}$	Reynolds number, based on ( )
t	time
Tu	freestream turbulence in % of V_∞
U, V, W	velocity components in x , y , z directions
U_1, V_1, W_1	Görtler's velocity perturbations, Eq. (11)
V_∞	freestream velocity
x , y , z	rectangular coordinates, see Fig 7
Y	outer variable, y / R
β	dimensionless growth rate
δ	boundary layer thickness
δ^*	displacement thickness
ζ	$\sqrt{a/\nu}\cdot z$
η	Hiemenz variable, $\sqrt{a/\nu}\cdot y$
θ	momentum thickness
λ	wavelength
ν	dynamic viscosity
ρ	density
τ	dimensionless time, i.e., $\tau = at$
φ	angle on cylinder, measured from stagnation plane
Φ_H, Φ_0	Hiemenz stream function, Eq. (2)
ω	vorticity, perturbation vorticity
Ω	mean or base-flow vorticity

Subscripts

H	pertaining to the Hiemenz flow
1	pertaining to Gortler perturbation

1 INTRODUCTION

The purpose of this essay is to summarize and illustrate experimental information on flows in proximity of stagnation regions of cylindrical bodies and to examine critically the notions of flow instability, primarily as they might apply to these flows. The approach is expository, with emphasis on the structure of the phenomena and of the associated equations. The approach is also a searching one, because as new facts are uncovered, new questions also arise, especially with respect to our idealization of the phenomena.

One might call the stagnation flows singular for they are physically complex, e.g. exhibiting singularly increased heat transfer response to even moderate free-stream turbulence, and also because their analyses in effect rely on singular perturbations. A glance at Figs.5, 7, 8, 11 and 12, samples of the most organized features of these flows, will convey an introductory impression of their complexity.

The immediate motivation for focusing on these flows was to understand more about mechanisms which could bring about commonly observed streamwise vorticity in nominally two-dimensional boundary layers, Morkovin (1979). However, this report will not dwell on the facts and scientific or technological consequences of the occurrence of such streamwise vortical flows downstream of blunt (or sharp) leading edges nor on the rather controversial information and theories of the enhanced heat transfer. It will focus primarily on the curious physical and mathematical aspects of these unsteady, vortical, three-dimensional flow fields in stagnation regions. The rather discordant information on the enhanced heat transfer, found for instance in Kestin (1966), Smith and Kuethe (1966), Kayalar (1969), Lowery and Vachon (1975), (1975), Miyazaki and Sparrow (1977), Hoshizaki et al (1975), Swigart (1977) and others, will be brought in only insofar as it provides evidence for specific flow behavior.

There is also much disagreement on the character of stagnation flow fields themselves and especially on their theoretical interpretations and modeling. In order to gain additional perspective, we shall need to consider basic questions of instability phenomena and their mathematical formulation. Relevant issues of temporal versus spatial stability, of receptivity to free-stream disturbances, of its relation to initial value problems of instability and of nonlinearity are discussed in Appendix 1.

However, only the needed, still tentative conclusions are utilized in the body of the report.

The initial free-stream disturbances convected toward the cylinders are generally turbulent but the preseparation boundary layers on the cylinders, while displaying unsteady and random features, do not exhibit basic characteristics of turbulent wall layers (even when enhanced heat transfer is observed). Here, and for stability problems in general, we need to sharpen our concepts and terminology of what constitutes turbulent flows. Appendix 3 proposes operational definitions of turbulence and provides some background for considerations of a class of quasi-laminar flows, such as the boundary layers under study here, which could be called buffeted laminar wall layers.

Some of the experimental and theoretical information discussed in this essay is at least partially contradictory, not an uncommon situation in problems dealing with instabilities, transition to turbulence and turbulence itself. The author presents here points of view close to a perceived consensus of specialists with whom he had discussed the issues over the last three years. Contradictory and unconfirmed results have been recognized as a major block in the progress of transition research so that the U.S. Boundary Layer Transition Study Group adopted a set of guidelines to remedy such uncertainties and avoid miscues for further research, Reshotko (1976), p345. Guideline No. 4 states: "Whenever possible, tests should involve more than one facility; tests should have ranges of overlapping parameters, and whenever possible, experiments should have redundancy in transition measurements". It has been broadened to theoretical research where by a "facility" we understand a theoretical model with its computer program", Morkovin (1978). We shall have to invoke this generalized attitude, designated henceforth as Gen. Reshotko 4, time and again in order to convey proper qualifications on the degree of reliability of various cited results and judgements. Despite this caution, it can happen that future experiments and theories will modify significantly the currently perceived consensus as here interpreted. In fact, a major purpose of describing the new perspective on the stagnation flows is to stimulate further theory and experiments specifically designed to test different elements of this perspective in accordance with Gen. Reshotko 4.

The exposition in Section 2 starts with an account of the piecemeal information on the steady or mean viscous flows around cylindrical objects. In particular the stagnation Hiemenz flow, lacking any characteristic lengths, and its imbedding within outer irrotational flows are described. It is anticipated that an even more severe problem of rigorous matching of inner and outer flows must be faced if the manner in which free-stream inhomogeneities and disturbances bring about unstable responses in the stagnation region is to be understood. In Section 3 the different characteristics and specifications of these disturbances are first examined. An account of experimental observations of steady vortex formations upstream of cylindrical obstacles follows with an attempt at interpretation in terms of prototypes of nonlinear stability theory. The vortical instabilities in the stagnation region are commonly linked with the Taylor vortex instability in annular Couette flow and with the Görtler streamwise-vortex instability in concave boundary layers. In order to gain further insight into instability phenomena in general, the differences in the physical and mathematical structure of these three superficially similar systems are outlined and discussed in Section 4. Consideration of disturbances and forced responses of the systems appears necessary for deeper understanding; see also Appendix 1.

In Section 5, various processes and mechanisms are considered and illustrated through linearized equations. The Görtler-Hämmerlin perturbation model is examined with emphasis on its possible limitations in temporal dependence and in its confinement to the inner domain which lacks a characteristic length. Section 6 contains a careful account of the more detailed stagnation-flow experiments with unsteadiness and turbulence in free stream. An overview of the important issues and the outlook for further progress is contained in Section 7. Useful information on various aspects of Görtler's linear model is given in Appendix 4.

The rather unconventional views presented here in a searching spirit were first written up in May 1976. Eighteen copies of that report were circulated in the United States, Europe, and Japan to elicit critique and suggestions and to provide an opportunity for private prepublication rebuttals for those whose earlier work was questioned in the text. The present report incorporates, then, not only the information and views from publications since

1976 but also the advice and comments of a number of discussors, in particular Profs. G. Inger, E. Roshotko, and I. Tani. Figures based on the reviewed publications are explicitly credited. The original NASA study under Grant NSG-1120 was guided, with understanding, by Ivan Beckwith. The 1979 revision was supported under AFOSR Contract F49620-77-C-013 concerned with instabilities and transition to turbulence.

2 CHARACTERISTICS OF THE OVERALL FLOW

a. Piecemeal Modeling of Viscous Flows around Bodies, Matching and Patching

Before we can study the behavior of disturbances in a flow field we expect to have adequate knowledge of the undisturbed base flow. For slightly viscous flows around bluff cylindrical bodies the theoretical and experimental knowledge is piecemeal, resting on a series of idealizations and characterizations of local behavior. It is instructive for the rationale of handling the perturbed flow to examine the usual approach to the solution of the underlying Navier-Stokes equations for the base flow at Reynolds numbers in excess of say 1000. The Navier-Stokes equations are solved as such only in the immediate vicinity of the front stagnation line, where the classical solution of Hiemenz (Schlichting 1968, pp 87-90) demonstrates the existence of a thin viscous boundary layer without assuming its existence a priori. To continue the Hiemenz solution beyond the stagnation region, approximate boundary layer equations with an assumed outer potential flow are solved up to an ill-defined separation line where the wake begins (e.g. Schlichting 1968, pp 154-162). There is no satisfactory Navier-Stokes solution for the wake and rather crude semiempirical modeling is resorted to for assessments of its significant steady and unsteady influence on the potential flow around and upstream of the cylinder. (Only Tani (1974) allowed for the wake influence in connection with our instability problem).

For the base flow there is a consensus that the conceptual division into the "outer" irrotational flow and the viscous and rotational boundary layer and wake is justified on physical grounds even though careful mathematical treatment of the high-Reynolds number wake and its coupling with the upstream potential flow remains elusive. It is worth pointing out parenthetically a significant contrast between the irrotational base flow and our perturbation flow where vorticity (linearizable or nonlinear) is present upstream of the stagnation region. This complicates the matching between the approach flow and the perturbed flow near the stagnation line. This inner perturbed flow was conceived by Görtler (1955) and explored in much detail by Hämmerlin (1955). It is functionally equivalent to the Hiemenz component of the base flow and will be called the GH flow.

The word "matching" above is used here in the sense of Van Dyke

(1964, p. 89), i.e. applying systematic limiting processes which may assure a smooth continuation of the piecemeal approximations to the solutions of the Navier-Stokes equations. Such dovetailing between the Hiemenz flow and the surrounding potential flow has been generally assumed as possible but has apparently been tried more rigorously only by J. Cole (1968, p. 159). Cole used the inviscid velocity potential and stream function for coordinates, but we fall back on rectangular coordinates x, y, z, with z along the stagnation line, in order to illustrate several aspects of the matching process. But first we should recall some properties of Hiemenz' solution.

b. The Hiemenz Scaling and Embedding

Figure 1 (after Schlichting 1968) depicts some velocity distributions, streamlines and the boundary-layer thickness of the Hiemenz solution (plus the stretching of a material line B_1C_1 into B_2C_2 for later purposes). The figure also conveys the crucial fact that in this flow field, which extends to infinity in the x and y directions, there is no characteristic length L and no characteristic velocity V in terms of which distances x and y and velocities u and v could be measured or made dimensionless. This scaling feature leads to self-similar families of solutions in terms of Hiemenz magnification variable $\eta = \sqrt{a/\nu}\, y$, where a is an arbitrary velocity gradient (or an arbitrary ratio V/L) and ν the kinematic viscosity. The solutions (tabulated and graphed as functions of η in most texts on viscous flows, e.g. on pp 89-90 Schlichting 1968), can be scaled to fit the innermost field near the stagnation line of any irrotational flow approaching a blunt cylindrical body by proper choices of a and ν. As η grows to infinity the viscous Heimenz solutions approach the potential flow

$$U_{H\infty} = ax, \quad V_{H\infty} = -a(y - \delta^*), \quad \delta^* = 0.648\sqrt{\nu/a}, \tag{1}$$

where δ^* is a constant displacement thickness due to the viscous deceleration near the wall at y = o, see Fig. 1. The asymptotic approach to the potential flow is very rapid so that already at η = 2.4 the H flow is within 1% of (1), the definition of δ in Fig. 1. The vorticity layer is thin indeed: the vorticity generated at the wall spreads by weak molecular diffusion and is convected back by the stronger mean approach flow. We should anticipate similar physics for our perturbed flow field.

Figure 2 indicates the manner in which three inviscid potential flows

(expressed in complex notation with $Z = x + iy'$) are related to the limiting Hiemenz flow (1). It is clear that in small neighborhoods of the origin, as $Z \to o$, all three flows merge into (1) if the x axis is shifted by the displacement thickness (which vanishes in the limit $\nu \to o$): $y' = y - \delta^*$. For the cylinder, $a = 2V_\infty/R$, and for the flat plate strip, $a = V_\infty/L$, while the wakes are disregarded. Their presence would primarily decrease the magnitude of the scaling potential velocity gradient at the the origin, $a = [-\partial V/\partial y]_o = [\partial U/\partial x]_o$, the unsolved problem being to determine by how much. (The wakes also introduce u-velocity fluctuations at the stagnation line, dominated by the overall instability of the wakes. This larger-scale motion is not believed to influence the instability of the approach flow, although it is definitely present in most measurements such as in Fig. 9 , discussed in Section 6e.)

Incidentally, the scaling parameter a also appears in the solution for the technologically important heat transfer rates in the stagnation region. Therefore, to provide a reliable reference base for discussion and evaluation of experimentally determined heat transfer rates, $(\partial U/\partial x)_o$ must be evaluated carefully.

c. Outer Scales and Matching of Base and Perturbed Flows

From the preceding illustrations it should be clear that the limit $\eta \to \infty$ does not correspond to free stream conditions. Yet this is an implicit assumption in the various mathematical manipulations of the instability problem as will be seen later. In our illustrations the variables $Y = y/R$ or y/L will be called the outer variable in terms of which the boundary conditions at the upstream infinity can be imposed and satisfied: $Y \to \infty$. The connection to the viscous boundary conditions at the cylinder comes through the adjustable self-similar H solution and its matching with the outer solution, see Cole (1968) p. 159. In simplest Van Dyke terms the matching requires that the limit of the inner solution as $\eta \to \infty$ coincides with the outer solution as $Y \to o$. Here the inner solution would consist of the Hiemenz solution near the stagnation point and of the local boundary layer solutions for other azimuthal positions (where the outer variable would be a curvilinear coordinate equivalent of y/R). Matching involves functional overlap over a region and the explicit

prescription $Y \to 0$ emphasizes that this region is right at the wall.

For the base flow with irrotational behavior upstream of the body the outer limiting process $Y \to \infty$ presents no difficulties. Desirable application of the technique to reattaching shear flows with mean vorticity (Inger 1976, Ginoux 1958, 1971), however, could not well disregard viscous diffusion in the outer flow, and the equivalent of the process $Y \to \infty$ would require extra finesse. An even more serious situation faces us in our instability problem where the up-stream perturbation is vortical and is subject to the vorticity-modifying straining field induced by the body. In the physical problems of interest free-stream turbulence decays steadily in the uniform flow before entering the straining, partly amplifying approach flow. The turbulence characterization as a fixed percentage of V_∞ therefore has little meaning as a boundary condition for $Y \to \infty$. And if we seek true eigenfunction growth, somehow elicited by the presence of free-stream turbulence, as discussed in Appendix 1, where should we prescribe the vanishing of the perturbations? The condition of vanishing disturbances in the Hiemenz limit $\eta \to \infty$ appears inadequate unless all elements of the instability mechanism oculd be shown convincingly to remain confined to the region right at the wall. The eigenvariable η for this viscous-conditioned problem is along the stream direction in contrast to the usual instability problems where η lies across streamlines, see Appendix 1e. Wilson and Gladwell (1978) identify the instability as centrifugal and not only accept the $\eta \to \infty$ matching, but require that the perturbations vary exponentially in η, see Appendix 1e for details. These and other instability issues are discussed further in Section 7 after the relevant steady and unsteady experimental information is reviewed. At this stage, however, it is clear that the behavior of disturbances in the region corresponding to $\eta \to \infty$ and to finite Y will require special attention.

d. The Hiemenz Flow Field

Perturbation equations inevitably involve various characteristics of the base flow, in particular of the inner Hiemenz flow, as coefficients. For reference purposes we therefore recapitulate succinctly the salient features of the Hiemenz solution.

Under the inner $\eta = \sqrt{a/\nu}\, y$ magnification all two-dimensional stag-

nation flows with an irrotational outer stream turn out to be similar, irrespective of the shape of the body, as in Figure 1. For irrotational outer flows the stagnation streamline comes in perpendicularly to the wall, and under the magnification, it is difficult to distinguish between the wall and its tangent plane. The body shape (in particular the leading-edge radius) determines the strain rates at the origin, labeled a in Equation (1). Introduction of a dimensionless stream function $\Phi_H(\eta)$, with appropriate scaling of the dependent variables:

$$U_H = ax\ \Phi_H'(\eta),\quad V_H = -\sqrt{\nu a}\ \Phi_H(\eta);\ \eta = \sqrt{a/\nu}\ y \tag{2}$$

automatically satisfies the continuity equation. The governing equation, that of the x momentum component, is expressible in terms of η alone, for all outer irrotational flow fields, e.g. Schlichting (1968) p. 89:

$$\Phi_H''' + (-\Phi_H'^2 + \Phi_H\ \Phi_H'') + 1 = 0\ . \tag{3}$$

Here the highest order derivative describes the viscous effect as usual, the nonlinear terms (in parenthesis) reflect the inertial acceleration and the last term corresponds to the constant pressure gradient $\partial p/\partial x = \rho a^2$, made dimensionless. The no-slip boundary conditions at the wall are simply $\Phi_H'(0) = \Phi_H(0) = 0$. The blending of the viscosity-conditioned region with the irrotional flow of Equation (1) is accomplished simply by the remaining boundary condition:

$$-\frac{1}{a}\frac{\partial V_H}{\partial Y} = \Phi_H'(\eta) \to 1,\ \text{as}\ \eta \to \infty. \tag{4}$$

Because the Hiemenz scaling, Equation (2), absorbed the usual free non-dimensional parameter Re, characterizing the ratio of viscous and inertial terms, self-similar solutions became possible. As a result the corresponding instability equations and boundary conditions contain no base-flow characteristic parameter either, a parameter which could become "critical" as instability sets in, just as Reynolds number becomes critical in Tollmien-Schlichting instability.

For a circular cylinder of radius R, one may hopefully try to switch to cylindrical coordinates and consistently retain only the lowest order of an expansion in powers of θ so that $x = R\theta$ and $r = R(1+\sqrt{\nu/a}\ \eta/R)$. If, following Tani (1974), one keeps the notation of U and V for the corresponding azimuthal and radial velocity components, one needs only to modify the second of definitions (2) to

$$v_H = - \sqrt{\nu a}\, \Phi_H(\eta) . \quad (1+ \sqrt{\frac{\nu}{a}}\, \frac{\eta}{R})^{-1} \qquad (5)$$

and obtain the governing equation - which is identical to Equation (3). No new R-based parameter appears to regularize the stability considerations, the solution $\Phi_H(\eta)$ remains the same, and only the radial velocity component is slightly modified by the factor $(1+ y/R)^{-1}$ for $0<y<y_m$, corresponding to $0<\eta<\infty$.

The solutions for Φ_H, Φ_H', and Φ_H'' are tabulated and graphed in Schlichting (1968), pp. 90-91. One should wish to supplement these with the solution of the y-momentum equation which yields the pressure field:

$$P_H(x,\eta) = P_H(0,0) - 1/2\rho\{a^2x^2 + v_H^2(\eta)\} - \rho\nu a\Phi_H' . \qquad (6)$$

The main pressure rise in the stagnation region is inertial, as expected, the last term in Equation (6), due to viscous resistance, being very small. The Hiemenz displacement thickness is $\delta^* = 0.648\sqrt{\nu/a}$ and momentum thickness is $0.292\sqrt{\nu/a}$.

3. FREE-STREAM DISTURBANCES AND STEADY UPSTREAM VORTEX FORMATION

3a. Spatial and Temporal Dependance of Free-Stream Disturbances

The notion of instability implies small perturbations from established states of flow, i.e. from the matched approach- and Hiemenz flows of Section 2 in the present problem. There are an infinite number of possible perturbation fields; they can be usefully idealized into several characteristic types. Since there is no evidence that small acoustic disturbances do affect significantly the flow around cylindrical bodies (except at separation of the shear layers which initiate the wake) irrotational disturbances are not usually considered. At a given section y= const. of the approach flow the rotational departures from uniform flow are functions of x and z which can also be (a) time-independent, as for wakes at very low Reynolds numbers, (b) time-periodic, as in the case of non-turbulent von Karman wakes, (c) random-stationary, as free-stream turbulence is usually portrayed in textbooks or (d) a superposition of motions (a), (b) and (c). Appendix 1*f* discusses the spotty and sporadic nature of decaying free-stream turbulence, which at least for the purpose of some instability modeling may perhaps be idealized in terms of separate, energy-sharing coherent structures.

For small disturbances we also have Fourier decompositions at our disposal to reduce the complexity of the functional representation in x, z, and time. Thus for a low-Re wake, diffusing from an x - oriented upstream cylinder (i.e. perpendicular to the z orientation of our stagnation line and parellel to the line B_1 C_1 in Fig. 1) the free-stream perturbation would be $\Delta V = f(z)$, resembling an error function, see the right side of Fig. 3b. The error function is expressible in a rapidly convergent Fourier series so that an analysis with

$$\Delta V = A \cos (2\pi z/\lambda) = A \cos k z \qquad (7)$$

would be meaningful. Alternately, a single row of thin parallel wires with mesh $M = \lambda$, called a zither for short, can be shown to generate a decaying wake in the form (7) with A(y) decreasing exponentially over a significant distance, see Kellogg (1965).

These are of course but simplest illustrations of general Fourier-integral decompositions of arbitrary fields in the wave number space, which are singled out because of their special usefulness for our problem. The disturbance vorticity associated with (7) is parallel to the x axis and

has the magnitude $-Ak \sin kz$. A number of visualization techniques, e.g. Fig. 12 , have disclosed sporadic vortex formations in the stagnation region with a dominant ω_x content, as in Fig. 3a, even when the upstream disturbances were not generated steadily and preferentially as for Fig. 3, but by general turbulence grids at high Reynolds numbers. Thus Equation (7) seems to be on the right track and our main task is to quantify the mechanisms which select this orientation of disturbances and which (more critically) prefer a relatively narrow range of wave numbers k when incoming turbulence contains broad spectra of frequencies and wave numbers.

3b. Knowledge and Specification of Free-Stream Conditions

A quarter-century after Görtler devised the analytical formulation of the problem, and focused on disturbances of the type (7), the second part of the task has not been convincingly carried out and the 1978 voices of Wilson and Gladwell question the accomplishments in the first part. One reason for this is that until a few years ago the experimentalists did not seek the simplest controlled disturbances of the type (7). Instead they tackled directly the most complex unsteady problem of free-stream turbulence and tried to interpret it in terms of the steady formulation (7). Without exception, the wave-number characteristics of the turbulence remained unknown and the complicated function $f(x,z,t;k_x,k_y,k_z,)$ of the preceding Section was specified by a single number, $Tu = \sqrt{(\overline{\Delta V})^2}/V_\infty$ in percent.

Miyazaki and Sparrow (1977) comment that poor specification of Tu (e.g. its y location and decay rate) and inaccuracy of Tu measurements are probably the most serious flaws which face the interpreters of heat-transfer enhancement. Furthermore, when Tu on the order of 3% or higher is claimed, nonhomogeneity in x and z of both Tu and V_∞ can be suspected; the problem then also acquires nonlinear features from the beginning. Even for linearizable Tu values, the unsteadiness and the broad wave-number spectra would make it essentially impossible to ascertain whether part of the response represents a true free eigenfunction behavior, even if space-time correlating techniques were used, see Appendix 1b and 1c.

3c. Steady Vortex Formations Upstream of Obstacles

Any student of vorticity and three-dimensional flows is well advised to ponder the lessons of the beautiful Frontispiece in "Incompressible

Aerodynamics", a remarkable collective effort edited by B. Thwaites (1960). The flow in the Frontispiece featuring a steady five-vortex formation upstream of a cylinder within a laminar boundary layer, is described as "radically different" from its two-dimensional counterparts and its "complexities" are intended as a challenge for the reader. A corresponding seven-vortex formation was studied by Norman (1972) by a single smoke-sheet generator which he moved across the boundary layer to trace the individual streamlines in the plane of symmetry as they wind their ways into the different vortices, e.g. in Fig. 4. There, two near-by streamlines with high total pressure P_t are also outlined by dashed lines. Furthermore arrows are added to emphasize the jet-like character (evident in Norman's movie) of the upstream directed motion along two of the streamlines as they push against the decelerated fluid near the wall.

In 1973, guided by this experience, the present author conjectured that steady separated vortices upstream of cylindrical obstacles could also form away from sidewalls, as in Fig. 3, if the streamlines with the slowest velocities of an oncoming steady laminar wake had sufficiently low stagnation pressure P_t. Such upstream separation must entail a free stagnation point S_f (Fig. 3) where the jet moving upstream from the stagnation point S on the cylinder is brought to rest at a total pressure P_f by the oncoming low-inertia fluid in the center of the wake. The stagnation pressure at the cylinder point S opposite the center of the wake must be lower than that farther along the stagnation line S_ℓ, where the full undisturbed $P_{t\infty}$ is achieved. There is therefore acceleration along S_ℓ toward S in addition to the usual Hiemenz acceleration "around the obstacle", a_H, in the x direction perpendicular to the plane of the lower Figure 3. Apart from the viscosity effects, the magnitude of acceleration a_H tends to limit the maximum velocity that can be generated along the stagnation line toward S, and therefore P_s. The pressure at the free stagnation point, P_f, should be very nearly $p_\infty + \frac{1}{2}\rho(V_\infty - \Delta V)^2$, if p_∞ and V_∞ represent "initial" conditions two or three diameters upstream of the cylinder (often denoted by subscript i). For conditions under which P_s builds up beyond P_f, a reverse flow and vortex formations should ensue as in Figure 3.

3d. Steady - Flow Experiments of Hodson and Nagib

By studing wakes of single and multiple cylinders at low Reynolds numbers as these wakes approached either rectangular or circular

cylinders, Hodson and Nagib (1975) verified the present author's conjecture of Section 3c and provided approximate criteria for the rather sudden appearance of the vortices such as the one seen in Fig. 5a. They also clarified considerably the effect of free-stream unsteadiness on the vortex behavior and on heat transfer rates at various locations of a large cylinder, but these observations will be discussed later. In Fig. 5a, the dye marks the center of a steady subcritical horizontal wake which impinges upon the vertical face of an elongated rectangular cylinder. By making the length of the main cylinder six times its width, D=23.75 mm, the upstream influence of its wake (end of Section 2b) was minimized so that the bifurcation of the oncoming wake at S_f (Fig. 3) and its tight roll-up into a pair of horseshoe vortices was steady to the eye. In the side view of Fig. 5a the horizontal traces of the two vortex cores obscure the fact that the dye did not penetrate the boundary layer of the target cylinder although some of the fluid from the edges of the wake should do so. The flow was always observed simultaneously in the plan view through a 45^{o} mirror arrangement. The reader is referred to Hodson and Nagib (1975) for discussion of the plan-view observations which revealed significant alterations of separation and wake behavior of the main cylinder in the proximity of the vortices. While the implications of such observations for various flow characteristics, including heat transfer, are of interest, for the present purposes the important findings are the existence of steady vortical response to steady upstream nonhomogeneity and what Hodson and Nagib call the threshold of incipient formation of the vortices.

3e. Evidence of Steady-State Threshold and Implications for Theory

Figure 6 presents an ad hoc empirical correlation of the conditions which separate states with and without vortical cells in several series of visualization experiments by Hodson and Roadman (1975) under Nagib's guidance. They were done with smoke in air and dye in water (in a water channel and a towing tank) and with single and multiple wakes which impinged on one rectangular and one circular cylinder. The experiments were carried out with the concept of the vortices as a module in heat-transfer convection rather than with stability theory in mind.

Other attempted correlations involving wake momentum defect and wake vorticity met with lesser success. One should keep in mind that these quantities and the thickness δ of the stagnation boundary layer

are very difficult to measure without probe interference at the conditions needed for visualization and therefore had to be estimated. In Figure 6, $\delta/D = c(\nu/DV_\infty)^{1/2}$, c = 6.59 and 4.66, gives the estimate for the boundary layer thickness at the stagnation line of the rectangular and circular cylinders, respectively; M is the "mesh" or lateral distance between wake-generating multiple cylinders, which provide a variation of ΔV without change in the important lateral length scale after the individual wakes merge; σ is the grid solidity d/M; and the subscript of Re indicates the length on which the Reynolds number was based. The ordinate $(\Delta y/d)^{1/2}$ is related to the strength of the centerline momentum defect empirically - Hodson and Nagib (1975), Nishioka and Sato (1974), Kellogg (1965). The term $Re_d \cdot (\delta/d)$ in the abscissa is proportional to D/δ^*. One would wish that the correlation be more physical but even in this steady laminar case too many parameters enter the formation mechanism. Without theoretical backing, there is no reason then to expect the threshold state to map into a single curve in a two-dimensional representation.

How does this threshold as perceived by Hodson, Nagib, and Roadman relate to instability theory in the light of the discussion of nonlinear effects and diagnostics in Appendix 1h and 1i? Let us assume that the system would allow initially exponential growth in time as its characteristic Reynolds number passes the neutral condition, Re_{cr}, if the disturbances could be kept infinitesimal. This assumption is made in most of the theories thus far. Sutera et al (1963), Sutera (1965), Williams (1968) and Inger (1977) also start with infinitesimal disturbances but suppress time dependence in their analysis. Let us also assume that free-response finite disturbances in the system could be characterized by a single amplitude A(t) and that the system has an inverted bifurcation at Re_{cr} so that its neutral curve has a shape as in Sketch 1. These assumptions allow for the simplest threshold behavior in temporal stability. It is the behavior anticipated by Tani (1974) on the basis of the heat-transfer variations with intensity of free-stream turbulence of Kayalar (1969, Fig. 1). When the free response is characterized by A and a single scale, say a dimensionless wavelength λ^*, a λ^* axis out of the paper has to be added and neutral states then correspond to surfaces in three dimensions rather than simple curves in Sketch 1. The more basic parameters there are, the higher the dimensionality of the neutral states.

* Since δ is proportional to $\sqrt{D\nu/U_\infty}$.

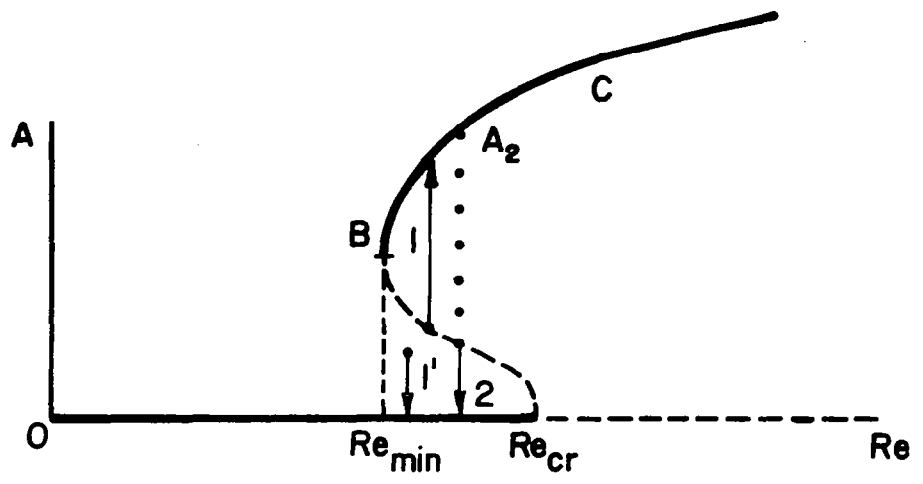

Sketch 1

According to bifurcation theory of the free eigenfunction behavior, e.g. Joseph (1974), the dashed part of the neutral curve separates the domain of stable initial system states (Re,A(0))at the left from the domain to the right, where the states evolve unstably. The unstably developing states to the right of B-Re_{cr} may reach the stable amplitudes of the upper part of the neutral curve B-C provided turbulence does not set in - there is disagreement on the stability of states BC to all disturbances. In temporal instability, any initial state (Re, A(0)) to the left of B-Re_{cr} decays until it settles on the stable line 0-Re_{cr} of zero disturbance energy. The system follows a path such as 1', if Re remains constant.

Actually there were two distinct experimental procedures: Hodson's data in Fig. 6 with a horizontal slash through the symbols denote experiments in which the wake-casting cylinder was fixed, at $y=y_i$, while V_∞ was slowly increased, and his data with a vertical bar through the symbols signify that V_∞ remained constant while y_i increased until the vortices disappeared. According to the simplified theory, as V_∞ increases in the first set, the system would either decay along paths like 1', or, if A(0) were on the B-Re_{cr} dashed line or to the right of it, the path would shoot up to the stable equilibrium B-C, as along path 1 in Sketch 1. Thus, if the temporal nonlinear growth rates past the neutral curve B-Re_{cr} were fast enough, all the experiments of the first set in the region marked

"CELLS" in Fig. 6 should be observed to map into the curve B-C in Sketch 1, with amplitude A dependent only on Re and not at all on the initial amplitude. Corresponding to the region marked "NO CELLS" in Fig. 6, the experimenters should see not just the absence of cells but rapid temporal decay of all normal mode disturbances to the zero energy states corresponding to O-Re_{cr} in Sketch 1. To change V_∞ experimentally entails inevitable time lags. Therefore, identification of the initial time t_o for the system (Appendix 1b) is not feasible for the experiments and one should not expect to make definite conclusions from whatever transient temporal behavior might be observed.

The experiments unquestionably indicate the presence of nonvanishing disturbances thus contra-indicating behavior 1' in Sketch 1; in fact the steady disturbances even grow spatially over part of the region, most likely in accordance with mechanisms discussed in Sections 5a and 5b. Could it be argued that these nonvanishing, spatially growing velocity variations represent a forced rather than a free response of the system to spatial initial conditions of Hodson et al, within a temporal framework? Forced responses are not dealt with in the instability theory and are not present in Sketch 1. But if the interpretation in terms of forced motions were correct how could one maintain that the nonlinear threshold behavior which results from strengthening of this forcing is transformed into a free response describable within the framework of Sketch 1? Since the computable free eigenfunctions of the linear theory would be modified in an unknown manner by nonlinearity in their evolution toward the time-independent modes corresponding to the neutral curve segment B-C, there seems to be little hope of operationally confirming the free-eigenfunction interpretation in this case. Esthetically, the forced-response interpretation would appear self-consistent. Given future computational capabilities it might even be numerically verifiable starting with a time - independent nonlinear perturbation of the Hiemenz flow with constant finite A values in the upstream boundary condition, Equation (7). The aforementioned papers of Sutera et al (1963), Sutera (1965) and Williams (1968) in fact proposed such a forced, steady, weakly nonlinear model and carried out some rather limited computations of uncertain convergence. At present, neither these computations nor the experimental information are adequate to validate the forced response viewpoint in any detail.

Thus far the comparison of experiments in set 1 with behavior portrayed in Sketch 1 dealt with paths of the type 1'. We have already seen that corresponding to paths of type 1 the observable amplitude A should depend only on the Reynolds number. No assessment of the strength of the nonlinear vortices, such as the positions of the free stagnation point S_f in Fig. 3b or 5a, were made in the experiments of type 1. However experiments of type 2, where Re was kept constant and the forcing amplitude gradually decreased by moving the wake-generating rods upstream, do partly bear on the same issue of exclusive Re-dependence of the equilibrium amplitude A past the threshold. To conform to the nonlinear behavior of free eigenfunctions in Sketch 1, the amplitude A_2 would have to remain unchanged on B-C as the rod position y_i increased until a state at or past the unstable neutral curve segment B-Re_{cr} was reached - at which time the amplitude should snap from A_2 to a finite value and then decay along the path 2 in a manner simular to 1'. (The snap from A_2 to below B-Re_{cr} would allow for the possibility of hysteresis in this peculiar open system.)

Again, no specific record was made of amplitude characteristics as y_i was increased, but in type-2 experiments amplitudes (as characterized by the position of S_f) are directly and immediately comparable. According to the memories of the experimenters, A_2 did not remain constant during procedure 2, again contra-indicating behavior 2 and further undermining the basis of the two-dimensional Sketch 1. However, as y_i of a single rod varies, not only the wake disturbance amplitude, but also its scale varies (while for contiguous multiple wakes λ^* remains constant). In a three-dimensional generalization of Sketch 1 to A, Re, λ^* space, procedure of type-2 for a single wake would correspond to a neutral curve in a plane Re=constant starting with A_2 and varying with λ^*. The experimental observations do not therefore rule out a theoretical threshold behavior in a generalized three-dimensional space.

According to the author's simplified reasoning in Section 3c, based on upstream forcing plus enhancement due to adverse pressure gradient (Section 4a) , one would expect slow growth of the vortices (after they are fully formed), as long as the effective strength of the disturbances can be increased. These expectations are not inconsistent with the Hodson-Nagib-Roadman experiments. The general impressions seem to be that

some forcing response is present and that somehow the characteristics of the boundary layer on the cylinder enter the quantitative determination of the geometry of the horseshoe vortices. Whether these features can be incorporated in some modifications of the present linear and nonlinear theories will be taken up in Section 7.

Figure 3b shows a fully formed double vortex which, according to Hodson, corresponds to conditions "sufficiently away from the correlation curve" in Fig. 6. Hodson also comments that "usually a small hairlip is observed at the threshold" (illustrated in Fig. 8 of Nagib - Hodson 1977). This corresponds to a thin cusp of dye extending upstream from S in Fig. 3b when two dye lines are used on either side of the oncoming wake*. If this visualization discloses faithfully all the upstream motion, there would exist a second type of free stagnation point (within the boundary layer?) besides the regular type S_f in Fig. 3b, albeit over a very limited range of parameters. Also, developments past the threshold would not be discontinuous but rather rapid as a function of the steady disturbance strength.

In accordance with Gen. Reshotko 4 one would like to see more detailed independent corroboration of the findings of the Hodson-Nagib experiments, especially since they were not devised to test stability theory. As stated in the Introduction, new information also gives rise to new unresolved issues; the formulation of these issues in this Section should help to focus the new experiments.

---

* It is possible that the slight momentum defect from these two far-upstream slender ejectors was sufficient to modify the critical conditions at the zero-momentum stagnation line and caused the cusp. When the dye source is in the wake-generating rod as in Fig. 5a, the above interference is absent.

4 DIGRESSION ON OTHER INSTABILITIES LEADING TO STREAMWISE VORTICES

(4a) Similarities and Differences between Three Flow Families

It is instructive to compare the growth of the vortices discussed in Section 3e to that of Taylor vortices in an annulus between two cylinders when the inner cylinder rotates, e.g. Stuart (1971, p 348), and to the growth of Görtler vortices in a boundary layer with concave curvature, e.g. Bippes (1972), Tani (1962), and Wortmann (1964). Usually, the stagnation flow is linked to the Taylor and Görtler centrifugal instability, e.g. Stuart (1963, p 505), because the streamlines in Fig. 1 also have concave curvature. We shall see that the analogy may be weak at best (Section 5d) and that there may be significant differences in the stability characteristics of the three flows. Already the geometries of the base flows differ substantially: there is no "upstream", "downstream", or "free stream" in the annulus, while all these stream limits are present in the boundary layer on concave walls, and "free stream" and "upstream" coincide in the stagnation flow. One might expect the structure of the eigenvalue problems to reflect the associated physical differences, but the original formulations in terms of temporally evolving normal modes were essentially identical in the three cases. In particular, the growing vortices were all expressed as $a\omega(\eta)\exp\beta\tau\sin(k\zeta)$, alternating in the spanwise direction ζ. Also, the eigenvariable η was always taken directed across the viscous layers of the base flows. However, in the region of validity of the stagnation Hiemenz flow this η direction (Fig 1) is essentially upstream rather than cross-stream, a key physical difference which is hidden by the formal similarity of the eigenvalue problem.

(4b) Couette Flow Instabilities

The temporal formation seems suited to the physics of the Taylor vortices in the closed annulus domain. Any local vorticity disturbance is not convected away by the stream (as in the concave boundary layer or in the stagnation flow) but remains within the closed confined space. Linear theory for an annulus of infinite length indicates that past a critical Taylor number, T_{cr} ($T=(V_i d/\nu)^2\cdot(d/R_i)$; R_i, V_i, radius and velocity of inner cylinder; d, gap between cylinders) normal perturbation modes of computable wavelength λ_{cr} grow as $\exp\beta\tau$. A number of weakly nonlinear models (Stuart 1971) suggest that the higher terms are stabilizing so that a steady vortical

motion, with $\lambda \sim \lambda_{cr}$, should result. The centrifugally stimulated motion feeds repeatedly back on itself and the strong constraint of mass conservation leads to the topology of an infinite series of vortex cells.

Experimentally, when the inner cylinder of an annulus of finite length L is suddenly started rotating at speeds somewhat above V_{cr}, vortices spread axially inward from the ends, grow very rapidly past their linearized stage, and indeed reach nonlinearly limited finite amplitudes. However, the pattern evolving after the spin-up assumes a non-unique spanwise wave length fairly near that of the theoretical linear λ_{cr} for $L \to \infty$. Its exact value evidently depends on the initial distribution of vorticity in the domain at the time of the sudden spin-up (see Appendix 1b for comments on initial value problems in closed regions). Snyder (1969, p 288) concluded on the basis of imaginative experiments with initial disturbances that "the mode having the highest amplitude initially (always) prevails".

While the rapid initial growth in time appears consistent with the linearized exponential growth (if one keeps in mind that the impulsive acceleration is finite and that instruments have resolution thresholds), the vortex spacings λ/d after two dozen revolutions will exhibit some 20% nonuniformity, presumably related to the initial distribution. Snyder (1969, Fig 6) showed that asymptotic equalization of the individual vortices depends on slow spanwise diffusion through the full chain of cells, with acceptable adjustment time of approximately $L^2/6\nu$. (Unless use is made of high-viscosity fluids "steady state is not reached for periods of from hours to days", and therefore "all past measurements of λ are open to criticism", Snyder, loc. cit., p 286). Snyder's findings were essentially confirmed by the overlapping investigations of Burkhalter and Koschmieder (1974) and Cole (1974).

When the other experimental procedure of slowly creeping up to V_{cr} is employed, the initial velocity perturbations consist of (a) the flows induced at the axial boundaries which do not move in accordance with the ideal Couette velocity distribution, $V=Ar + B/r$, expected far away from the ends (but see Coles and Van Atta 1966), and (b) the nonuniformities induced by the final speed increment ΔV_i of the inner cylinder. The latter influence is probably small, but the boundaries bring forth clearly discernible "anomalous" vortex pairs at the ends at about $0.8V_{cr}$ and continue to induce additional

"ghost" vortices as V_{cr} is approached. However, for sufficiently long annuli, "the speed at which all divisions between cells just become visible has been found to agree well with the calculated critical speed," Cole (1976, p 7). Cole (1974, 1976) and Burkhalter-Koschmieder (1973) provide us with detailed systematic observations and error estimates. The L-independence of the final rapid growth of the center cells in long annuli probably justifies viewing the final vortex formation process as a true instability which may grow nearly exponentially when the center disturbances are still small, in accordance with Taylor's linear normal-mode theory.

The vortical formations induced by the ends are part of the initial conditions for the last ΔV_i increment, but since the no-slip conditions at these boundaries persist, the sidewall motion may be considered as constituting steady forcing by the boundaries. This sidewall action thus bears functional similarity to the role of the upstream rods in the Hodson-Nagib experiments. (There is even scattered evidence that at very high speeds the first seeding of randomness and turbulence starts in the forced, anomalously larger, vorticity formations at the ends, in the Couette case, just as it unquestionably starts in the forced wakes in the Hodson-Nagib and other experiments.) Thus, in presence of the steady forcing and the initial conditions (e.g., the initial flow distributions of Snyder), modes of motion similar if not identical to Taylor's linear normal modes are elicited away from the ends, grow and settle to nonlinearly modified stable modes with wavelengths near the unforced theoretical linear λ_{cr}.

As V_i grows beyond V_{cr} an increasingly broader family of normal modes is admissible according to the linear theory. However, a small subset, judged by measured λ values, is actually observed. Nonlinear theory for infinite L (Stuart, 1971, p 354; Stuart and DiPrima, 1978) suggests that some linearly admissible modes are nonlinearly unstable and that resonance mechanisms among sideband modes and the harmonic of the fundamental are responsible for the narrower range of allowable λ values. For finite L the additional requirement that the number of cells has to be an integer, imposes strong quantization restrictions on the observed modes and leads to hysteresis effects in experiments with increasing and decreasing V_i. These major features of nonlinear Taylor flow behavior probably hold a lesson for anyone

expecting a well-defined λ variation for the stagnation-flow vortices.

In line with our interpretation of the end-wall geometry as forcing, Koschmieder (1975) introduced O-rings, 0.17d in height, at equal distances λ_f along his annulus in order to impose and stimulate preferential growth of vortices on the flow. And stimulated they were: "the first photograph with signs of vortices along the entire column was taken at $0.03T_{cr}$", i.e. at $0.17V_{cr}$ compared to approximately $0.8V_{cr}$ for the flow with normal end effects (Cole 1976). In quasisteady procedures, vortices with $1.47\lambda_{cr} < \lambda_f < 2.0\lambda_{cr}$ were unstable and split up into two vortices in a non-critical, continuous manner. Consistently with nonlinear theory, the range of stable vortices $0.69\lambda_{cr} < \lambda_f < 1.18\lambda_{cr}$ (roughly the same for quasisteady and sudden-start procedures) was narrower than the admissible range of linear modes; see Fig 2 of Koschmieder (1975). In accordance with Gen. Reshotko 4 (section 1), one would wish for corroboration of the nonlinear theory with nonpermanent forcing elements, e.g. vortex generators, which could be withdrawn during the experiment once V_{cr} had been exceeded. It should be the nature of this closed nonlinear system, as it is the implication of Snyder's experiments (1969), that the forced components of those periodic motions with λ_f within the allowed set would decay after the withdrawal of the generators, i.e. the motion would evolve into the allowed λ_f nonlinear mode without rearrangement. Those forced motions with λ_f outside the allowed set would break up and rearrange themselves ultimately into one of the allowable set. In contrast, according to the Hodson-Nagib experiments, it is the nature of our stagnation-flow field that removal of the forcing rods upstream of the cylinder removes the horseshoe vortices near the stagnation line altogether. The disturbances simply are convected out of the open system and so are their response formations.

In terms of bifurcation theory the configuration for the amplitude A(t) of the equilibrium disturbance states of the system with infinite L is supercritical, as in Sketch 2; see Stuart (1971) or Stuart (1977). Below T_{cr}, the quiescent states denoted by the heavy line O-T_{cr} are the equilibrium states and other perturbed states should decay in time along paths like path 1' in Sketch 2. Past T_{cr} the quiescent states along the dotted horizontal axis correspond to unstable equilibrium. Stable equilibrium states

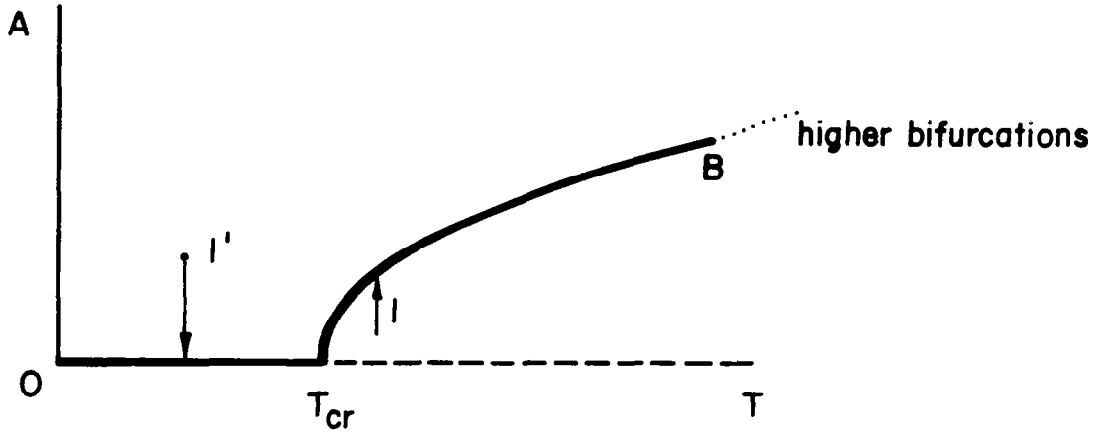

Sketch 2

are now associated with the regularly bifurcating branch T_{cr}-B, with definite non-zero amplitudes. Other pure initial states would approach equilibrium along paths like 1. Again, Sketch 2 describes states completely characterizable by a single amplitude A(t;T); and to accommodate specification of wave lengths λ or wavenumbers k we must generalize the equilibrium curve T_{cr}-B to an equilibrium surface in the A,T,λ or the A,T,k space.

The dots past B in Sketch 2 allow for higher bifurcations, specifically for the so-called wavy instabilities (Stuart 1971, Fig 2) at higher Taylor numbers (which depend sensitively on the ratio of the cylinder radii). The annular vortices develop an integral number of waves in the azimuth which propagate around the annulus so that a fixed probe records a discrete frequency (and weak harmonics). As an example, Coles (1965) observed 3 to 7 waves for R_i/R_o of 0.874 and a length-to-gap ratio of 27.9. As these waves set in, they presumably first grow exponentially in time until they reach new nonlinear equilibria where the vorticity distribution is characterized by terms like $\exp[i(m\theta - i2\pi ft)]$ in addition to the earlier factor $\sin(k\zeta + \text{const})$. We shall see that Hassler's 1972 experiments on the instabilities in the stagnation region also indicate a time-periodic

behavior of the streamwise vortices which has not been previously discussed as a possibility, Section 6e.

The bifurcation diagram of Sketch 2 strictly corresponds to the infinite annulus and does not allow for forced responses, steady or unsteady. Nevertheless, according to our brief account, forced motions are a fact of life in any physical realization of the flow. The concept seems to provide fruitful guidance for experimental diagnostics even though the forced motion cannot be generally treated as a small perturbation. In bifurcation theory, attempts to accommodate finite geometry (but not other forced motions) are sometimes described as studies of imperfect bifurcations. According to p 141 of Stuart's 1977 review, "it is believed (though in no sense proven) that a smooth transition takes place" and that the new equilibrium states correspond to a curve in Sketch 2 which runs somewhat above, but follows the heavy equilibrium lines rather closely, with the maximum deviation in the neighborhood of T_{cr}. Stuart goes on for three pages to describe the difficulties of matching this abstract theory to experiments and the existing discordant views of both.

(4c) Görtler Vortices in Concave Boundary Layers

As pointed out in Appendix 1d, the temporal formulation of the growth of streamwise Görtler vortices in concave boundary layers definitely does not fit the experimental observations: there is no time variation in the early development and the growth is in x. To the author's knowledge the determination whether the instability is subcritical or supercritical has not been made, theoretically or experimentally. We therefore do not know whether to anticipate behavior associated with Sketch 1 or Sketch 2. In fact, there have even been substantial discrepancies in the computed neutral curves for the critical Görtler number G versus wave number k ($G = Re_{th}\sqrt{\frac{th}{R}}$; R, wall curvature; th, momentum or displacement thickness or $\sqrt{\nu x/U}$, depending on the author). A survey of the problem and a collection of contending neutral curves is found in Herbert (1976). Herbert pinpointed inconsistencies in the difficult treatment of streamline curvature as a major contributor to the discrepancies. He also concluded that the gradual thickening of the boundary layer should be a first-order effect, of more importance than for the TS instability. An extended abstract of Floryan and Saric (1979), available at

this writing, suggests that they succeeded in devising a systematic non-singular approach to the curvature problem via the method of multiple scales and the DiPrima-Stuart (1972) scaling of disturbances in streamwise vortices. They also traced some of the past discrepancies to computational errors. Interpretations of experimental results should thus probably start from the new curves of Floryan and Saric.

Experimental study of the Görtler vortices is itself very difficult because measurements of steady perturbations in space are much more insensitive and inaccurate than those of unsteady perturbations at a fixed position. Nevertheless, the hot-wire studies led by Tani (Tani 1962, Tani and Aihara 1969) leave no doubt that there is at first an exponential growth in x which diminishes downstream either due to nonlinear saturation or due to detuning of the normal modes in a thickening boundary layer. Wortmann's (1964) ingenious Tellurium visualization technique in water generally corroborates the findings of Tani and coworkers. He also observes that the normal and spanwise velocity perturbations are twenty to thirty times smaller than that in the streamwise direction, thus providing support for the DiPrima-Stuart (1972) scaling. The rate of rotation of the streamwise Görtler vortices is apparently exceedingly slow (completing barely a 90° turn before transition) in comparison with our stagnation-flow vortices, such as in Figs 5 and 12, also in water. Stereoscopic studies of hydrogen-bubble traces in water by Bippes (1972) indicate that the slow rotation ultimately accumulates bulky ridges of low-inertia fluid along directions where the vortex flow is away from the wall and that a complicated, nearly time-periodic secondary instability develops in proximity of these ridges. For comparison of its characteristics with features of secondary instabilities of nonlinear TS waves and of the wavy-form instabilities of Taylor vortices, see Bippes' 1972 discussion, pp 165-175.

There is some disagreement among the experimenters concerning the nonlinear developments and the nature of the breakdown (which are unlikely to be universal, anyway). However, there is general consensus about the linear behavior. At incompressible speeds without heat transfer, the amplification rates are relatively slow* in comparison to TS amplifications. As the

* Görtler instability is suspected of contributing to transition on the concave walls of supersonic wind tunnels.

experiment of Bippes in Appendix 1a indicates, the more highly amplified normal modes are evidently selected from disturbances present in the layer. However, the maximum of these amplification rates with respect to wave number may be shallow. Thus by driving a disturbance with a wave length twice the preferred one, by winglet devices above the boundary layer, Tani and Aihara (1969) completely preempted the normally observed mode. Presumably, the forced mode was built up to nonlinear levels before the usual mode was of any consequence and thereafter became nonlinearly inhibited. "Mild selectivity to wave length" would explain why the wavelengths observed in four different experiments of Tani and Aihara were "almost independent of free-stream velocity". Evidently, small nonuniformities of flow inherent in a given experimental arrangement can force the Görtler response in their image provided the wavelength is amplified by the instability mechanism.

(4d) Reprise of Comparison of Instabilities with Streamwise Vortices

In Section 4a we listed a number of a priori similarities and dissimilarities of the three families of flows with streamwise vortex formations, which in textbooks are linked by susceptibility to centrifugal instability. All three were originally formulated as temporal instabilities. The experimental evidence reviewed in the preceding sections strongly suggests that only the Taylor instability in Couette flow can be considered temporal in nature and that the Görtler instability is definitely spatial. Even though end-effects cause end vortices to be formed below the linearized critical conditions in Taylor instability, at T_{cr} the vortices all along the annulus grow rapidly--to undoubtedly nonlinear configurations. Spanwise equalization, however, takes place rather slowly by diffusive processes in an adjustment time on the order of $L^2/6\nu$. In the other instabilities such times are not available as the vorticity is transported downstream. For these, we should therefore expect (and indeed do see: Tani 1962) spanwise variations in amplitude and wavelength of streamwise vorticity unless the vorticity is uniformly seeded upstream.

Among the three flows, only stagnation region vortices exhibit velocity components opposite to the direction of the momentum which drives the flows. It is in the development of this local counterflow that the threshold-like phenomenon appears. Neither Taylor nor Görtler vortex behavior seem to provide any guidance for understanding of the Hodson-Nagib experiments and in

particular of the threshold-like behavior in Fig 6. Nor is the model of subcritical instabilities in Sketch 1 truly consistent with the observations, incomplete as they are.

However, in all three systems various aspects of the observed linear and nonlinear behavior seem to require for adequate explanation the presence not only of instability modes but also of forced response to initial and/or complete boundary conditions which are present in any given physical realization. This is the message of the Taylor-flow experiments of Snyder (1969), Koschmieder (1975), Cole (1976), Burkhalter and Koschmieder (1973) and of the selective stimulation of Görtler vortices with upstream grid and with narrow streamwise heating elements in the wall by Bippes (1972), and with winglets placed outside of the boundary layer by Wortmann (1964) and Tani and Aihara (1969). Quantitative mathematical elucidation of the details of the mechanisms constitutes the generalized problem of linear and nonlinear receptivity. Some of the forced responses may decay in time or space, after determining the early development of the normal mode response, as in Bippes' case of the small heating elements, while in other cases the forced response remains a factor throughout. Mathematical clarification of the characteristics of various categories of possible behavior would be helpful. The nonlinear aspects seem to be rather prohibitive at present, but are needed at least conceptually. With hindsight of the preceding sections, we can conjecture that the steady Hodson-Nagib vortices represent in part a forced nonlinear response which may or may not involve a free response, i.e. non-zero solutions of the associated homogeneous system of equations and boundary conditions. The disappearance of the vortices as the wake-producing rods are moved farther upstream seems to support the conjecture.

5 MECHANISMS AND LINEARIZED DISTURBANCE EQUATIONS

5a Prandtl's Inviscid Linearized Formula

That there should be a tendency to accentuate steady-flow defects between neighboring streamlines, ΔV of Fig 3, in regions of adverse pressure gradients has, of course, been known for a long time. That it could lead to local reversal of the flow in absence of a "sidewall" with its no-slip condition (which was present in the case of Fig 4), that is intriguing. Prandtl (1932) considered small steady flow velocity differentials V_1 and V_2 between two stations where stream velocities are V_1 and V_2 and the stream tube areas A_1 and A_2. Assuming that the process of acceleration or deceleration was rapid enough to neglect the slow action of viscosity, he used the conservation of stagnation pressures and of mass flux to derive a first order expression for the relative magnitudes of the defects; see Corrsin (1963),p.553,

$$\frac{\Delta V_2}{V_2} = \left(\frac{A_2}{A_1}\right)^2 \frac{\Delta V_1}{V_1} \quad ; \quad V_1 A_1 = V_2 A_2 \ . \tag{8}$$

Here it is the change in the stream tube areas which reflects the role of the given streamwise static pressure drop or rise, $p_2 - p_1$. Actually, Equation (8) has been used primarily for assessment of channel contraction ratios A_2/A_1 which would depress steady-flow nonuniformities to a tolerable level. It is equally valid for expansion of stream tubes in front of cylinders which takes place in planes perpendicular to their axes. The stream divergence according to the asymptotic Hiemenz solution for the stagnation region is depicted in Fig 1. With Δz in the direction of the cylinder axis, a typical stream tube area $A_1 = \overline{B_1 C_1}\,\Delta z$ expands to $A_2 = \overline{B_2 C_2}\,\Delta z$ and Equation (8) can be rewritten as

$$\Delta V_2 = \frac{A_2}{A_1}\,\Delta V_1 = \frac{\overline{B_2 C_2}}{\overline{B_1 C_1}}\,\Delta V_1 \ . \tag{9}$$

While the result (9) basically rests on the fact that a given increase in pressure along streamlines has much more effect on fluid elements with lower inertia, it can also be interpreted in terms of the companion variable, vorticity, because $\Delta V_1/\Delta z \sim \omega_{x1}$ and $\Delta V_2/\Delta z \sim \omega_{x2}$. Equation (9) then represents the increase in vorticity by stretching of vortex lines, which is the mechanism usually associated with the increased velocity

differences in stagnation regions. However, Equation (8) is clearly valid for non-planar geometries, say upstream of asymmetric three-dimensional bodies, where the corresponding analysis of the vector velocity field would be unwieldy.

5b Forcing by Diffusive Vorticity Convected from Upstream

Figure 7, borrowed from Kestin and Wood (1970), presents schematically computational results of a steady second-order theory as well as the coordinate system, matching that of Fig 1, i.e. with z axis along the stagnation line and the free stream coming from $y \sim +\infty$. Weak periodic steady laminar wakes $-V_1 \cos kz$ (such as generated by Hodson and Nagib's two-dimensional grid in Fig 3) and the free stream, $-V_0$, convect vorticity $\omega_x = -kV_1 \sin kz$ from upstream "infinity" toward the cylinder which is approximated locally by its tangent plane $y = 0$ in Fig 7.

As long as the stream remains unaffected by the pressure field of the cylinder, roughly for $y > 2.5D$, the vorticity perturbation decays exponentially by diffusion $\sim \exp\{-[\nu k^2 (y_i - y)/V_0]\}$ from some initial reference location y_i. For uniform base flow, V_o constant, the sources in the vorticity equation (A2-5) of Appendix 2 are all zero and the vorticity evolution is governed purely by diffusion. This viscous diffusion and decay of vorticity does not cease, of course, as the cylinder is approached. It complicates the formulation of the upstream boundary conditions for the disturbances. The formula suggests that the disturbance amplitudes may have to be prescribed at specific values y_i on the order of 2D if the free-stream forcing is to be taken into account realistically. This is of course way beyond the reach of Hiemenz variable η.

There is a degree of confusion concerning the outer behavior in this direct inflow problem. To the experimentalist the subsidence of vorticity with decreasing y represents a most natural decay. To stability analysts looking outward from the body, the behavior appears as an exponentially divergent growth of disturbances to infinity. Such a divergence is not considered permissible for the normal modes which are presumably rooted in the body boundary layer. In the Hiemenz plane, where the velocity of the base flow is allowed to diverge proportionally to η as $\eta \to \infty$, the diffusive behavior of the vorticity is further camouflaged by straining. Asymptotically algebraic decay (or growth) then replaces the exponential decay obtained

for uniform V_0 .

As discussed in Appendix 1, the normal modes do not develop out of nothing, but in conjunction with the forced response of the system. The outer diffusive behavior of the vorticity represents predominantly the forced response. For the Hodson-Nagib experiments, analyzed at length in Section 3d and 3e, the relation between the forced and free responses remained elusive, but the necessity of paying attention to the forcing was clear. Figure 7, kindly supplied by Professor Kestin, shows explicitly the upstream boundary conditions (which were deleted in the published version) and thereby underscores the peculiar nature of the instability in the direct inflow stagnation region. What looks like a non-homogeneous forced problem is reducible to a homogeneous normal-mode problem by switching the boundary condition V_1 = constant to the condition on the derivative, $dV_1/dy = 0$ as $\eta \to \infty$. Assuming for the moment that the full problem was solvable in the η variable alone, the full solution would presumably consist of the forced solution plus a dovetailing solution of the homogeneous equations with $V_1 = 0$ as $\eta \to \infty$, if such a solution exists. The mechanisms underlying the equations (which differ only in one boundary condition) would in this case be the same.

5c Vorticity Diffusion and Vorticity Stretching

In approaching the cylinder the flow diverges in the yx plane perpendicular to the cylinder axis and the convected ω_x vortex lines are stretched by the Hiemenz flow as already seen in Fig 1. For instance, the vortex line segment $\overline{B_1C_1}$ stretches into segment $\overline{B_2C_2}$ as it is convected with the main flow and thereby generates a vorticity source in the sense of the right hand side of Equation (A2-5). According to Equation (A2-5), the rate of change of ω_x observed as one moves with the material particles toward the cylinder depends therefore to the first order on the race between the dominant stretching source $\omega_x(\partial U/\partial x)$ (equal to $-\omega_x(\partial V/\partial y)$ by continuity) and the diffusion loss rate $\nu(\partial^2\omega_x/\partial y^2 + \partial^2\omega_x/\partial z^2)$. The diffusion due to the curvature of the vorticity profile in the yz plane is governed by the square of its wavelength λ^2 : $\nu(\partial^2\omega_x/\partial x^2) = -\nu k^2\omega_x = -\nu(4\pi^2/\lambda^2)\omega_x$. The squared length controlling the diffusion $\nu(\partial^2\omega_x/\partial y^2)$ is that associated with the approach to the cylinder, i.e. usually a much larger term, on the order of D^2 , except in the immediate vicinity of the cylinder, roughly up to twice the

height of the vortices in Fig 7. Furthermore, above this height this loss, besides being small, is of the same sign as $-\nu k^2 \omega_x$. A slightly conservative estimate of the ratio of the competing local stretching and diffusive rates is therefore $-\lambda^2 \frac{\partial U}{\partial x} / \nu 4\pi^2$ or $+\lambda^2 \frac{\partial V}{\partial y} / \nu 4\pi^2$ everywhere in a narrow wedge-like domain centered on the yz plane upstream of the body, where the above approximations are valid.

Far upstream, $\partial V/\partial y$ is negligible, the above ratio approaches zero, and we recover the exponential decay. The gradient $\partial V/\partial y$ scales with V_0/D since total ΔV is V_0 itself and the only characteristic length is D. For a circular cylinder in potential flow, $\partial V/\partial y$ grows to approximately $1.2V_0/D$ at $y = 0.25D$ and reaches its maximum of $4V_0/D$ at the edge of the boundary layer. There, however, the diffusion term $\nu(\partial^2\omega_x/\partial y^2)$ cannot be neglected so that the maximum $\lambda^2 V_0/\nu\pi^2 D$ of the approximate ratio of the stretching rate to the diffusion rate may be misleading. In particular, we do not expect the ratio to increase indefinitely with wavelength λ. As λ increases, the x-diffusion decreases, so that it will cease to be a controlling factor. Furthermore, as λ increases, the likelihood of building up the stagnation pressure P_S beyond P_f, the free stagnation-point pressure, also decreases--see the discussion in connection with Fig 3b and the dual view at the end of Section 3c.

Clearly, in case of countertrends, general physical considerations such as in the preceding paragraphs need to be replaced by actual solutions of the governing equations. As will be seen in Section 7, such solutions have not yet yielded convincing criteria for the "most amplified wavelength λ". The preceding discussion at least brought out the importance of both the diffusion and vortex stretching as the dominant physical factors in the steady phenomena portrayed in Fig 5a. It also suggests that we can expect net vorticity growth, solely from vortex stretching, especially very near the body.

5d Centrifugal Destabilization

Despite references to concave streamlines, no comparable demonstration of the role of centrifugal destabilization has been reported in the literature. According to Equation (A2-5), there are no additional terms in the Görtler-Hämmerlin vorticity equation beyond those identified above, not even within the boundary layer. Wilson and Gladwell (1978) conclude on the basis of a

generalization of Rayleigh's inviscid instability criteria that "the (centrifugal) destabilizing forces are confined to the region where ω (the base flow vorticity) is appreciable, namely the boundary layer". The same conclusion can be drawn from Stuart's remark (1963, p. 505): "In such a flow, there are certainly regions where the circulation (product of local velocity and local radius of curvature) increases as the local center of curvature is approached normal to the curved streamlines; consequently Rayleigh's criterion suggests instability." In accordance with Helmholtz' theorem this change of the circulation vanishes outside the boundary layer. In other words, curved irrotational flows are neutrally stable.

Wilson and Gladwell identify two types of terms in the x and y momentum equations as due to centrifugal acceleration. However, they conclude that these are relatively smaller and end up with the Görtler-Hämmerlin system of equations.

5e The Görtler Perturbation Mode, Its Temporal Dependence

In 1955, long before any visual evidence of the formation of horseshoe vortex pairs at blunt two-dimensional leading edges was available, Görtler proposed that unstable, vortical, spanwise-periodic perturbations might account for the reported increase in unsteadiness and heat transfer in that region. The linearizably small three-dimensional perturbations were superposed on the Hiemenz flow, Equations (2), so that the velocity and pressure fields were represented essentially as follows:

$$\left.\begin{aligned} U &= ax\{\Phi'_H(\eta) + U_1(\eta)e^{\beta t}\cos k\zeta\} \\ V &= -\sqrt{a\nu}\,\{\Phi_H(\eta) + V_1(\eta)e^{\beta t}\cos k\zeta\} \\ W &= \frac{1}{k}\sqrt{a\nu}\,W_1(\eta)e^{\beta t}\sin k\zeta \\ P &= P_H(x,\eta) + \rho\nu a P_1(\eta)e^{\beta t}\cos k\zeta\ , \end{aligned}\right\} \quad (11)$$

Here and henceforth $\tau = at$ and k stands for the dimensionless wave-number related to the dimensional spanwise wave length λ by $k = (2\pi/\lambda)\sqrt{\nu/a}$ since the spanwise coordinate z undergoes the same magnification as did y, namely $z = \sqrt{\nu/a}\,\zeta$. Substitution of (11) in Navier-Stokes equations and

linearization yields a system of momentum equations and the continuity equation

$$U_1 - V_1' + W_1 = 0 \ . \qquad (12)$$

Undifferentiated $P_1(\eta)$ appears in the z momentum equation and $P_1'(\eta)$ in the y momentum equation. Differentiating the former and eliminating $P_1'(\eta)$ leads to a sixth order differential system in the velocity components which is expected to be subject to six boundary conditions. Mathematical properties of the system and its solutions form a subject beyond the present discussion, much as they influence the question about their relation to the physics of the problem. However, the simplest, nearly self-contained equation is the vorticity equation, which is well worth examining here.

We first note that Görtler allowed for non-propagating temporal instability through the sole unsteady factor $\exp(\beta\tau)$ which cancels out in the continuity equation. The eigen-number β enters all the other equations; in particular in the vorticity equation below it enters as $\beta\omega_1$ and acts as a sink of vorticity, always in unison with the z - diffusion sink $k^2\omega_1$, if the equation is interpreted in a steady system. As discussed in Section 3, the experimental evidence of Hodson and Nagib does not support the exponential time dependence, but neither does it definitely exclude its possibility. Furthermore, hot-wire evidence of Hassler, Figs 9 and 10 and Section 6e, discloses quasi-periodic time variations in response to random turbulence Tu of approximately 0.85% measured at $y_i = 0.83D$ upstream of the cylinder (10 cm or 120 mesh-length downstream of the screen). Such experimental evidence contains unknown contributions from forced motions. At any rate, the Görtler normal-mode system does not allow for such temporal behavior.

5f The Vorticity Equation and the Domain of its Validity

Its mathematical properties and physical interpretation have been central to most analyses, starting with Hämmerlin (1955), who studied in detail a function $g(\eta)$ without identifying it as vorticity. If we enlarge the definitions (11) by $\omega_x = a\omega_1(\eta)\exp(\beta\tau)\sin k\zeta$, its relation to V-W velocity components becomes $\omega_1 = W_1'/k - kV_1$ and through the continuity equation (12) to U_1' as well $(V_1'' - k^2V_1 - U_1')/k$, Hämmerlin's g function. Since the

perturbations are assumed to be small one can obtain an equation for ω_1 directly from Equation (A2-5) in Appendix 2:

$$\omega_1'' + \Phi_H\omega_1' + (\Phi_H' - k^2 - \beta)\omega_1 = 0 \ . \qquad (13)$$

The vorticity stretching source rate $\omega_x(\partial U/\partial x)$ and the diffusion loss rates $\nu(\partial^2\omega_x/\partial z^2)$ and $\nu(\partial^2\omega_x/\partial y^2)$, used for the less restricted approach to the cylinder in Section 5c, become for this specific perturbation pattern (which is immersed in Hiemenz flow) $\Phi_H'\omega_1$, $-k^2\omega_1$, and ω_1'', respectively. (The term $-\Phi_H\omega_1'$ represents the observer derivative as he follows the mean Hiemenz path toward the cylinder.) The ratio of sources to sinks becomes Φ_H'/k^2, independent of ω_1 when k^2 is not too small and $\eta > 6$ for y diffusion to be negligible. In contrast to Section 5c this lower bound on a characterization of the net local amplification increases monotonically as the cylinder is approached.

According to Section 5c, the free-stream disturbances first decay due to vorticity diffusion before vorticity stretching reverses the trend; (see also the experiments of Sadeh, Sutera and Maeder, 1970b). The specification of the boundary conditions for the system and its consequences will be taken up in Section 5g; however we already saw in Section 5b that the problem of computing the response to the prescribed spanwise-periodic inhomogeneity at "infinity" of Fig 7 is included in the homogeneous problem when the derivative of V_1 is made to vanish at infinity. The monotonic rise in the net local amplification associated with the vorticity equation (13) indicates that the system cannot duplicate the occurrence of the minimum where vorticity diffusion is balanced by vorticity amplification. This again reflects the fact that the domain of validity of the Hiemenz and the Görtler-Hämmerlin equations should be measured in small multiples of the boundary layer thickness rather than in terms of the body characteristic length D and that application of the method of matched asymptotic expansions, MMAE, should be considered; see also Sections 2a - 2c.

It is not surprising, therefore, that the study of asymptotic solutions of Equation (13) for $\eta \to \infty$ (which is not the same as for $y \to \infty$, as brought out in MMAE), remained the center of theoretical investigations as well as of contention, e.g. Kestin and Wood (1970), Tani (1974), Iida (1978a,b). Sadeh, Sutera and Maeder (1970a) in fact abandoned attempts to characterize the

approach to free stream through the magnified variable and used "cylindrical coordinates" x,y (i.e. θ or x^2/y^2 very small as in our discussion leading to Equation (5)), to obtain a Reynolds number parameter in the equivalent of Equation (13) for the outer y-field. However, no rigorous matching with the inner field as characterized by Equation (13) was attempted. Sadeh et al (1970a) oversimplified their system so that their Equations (22) and (23) are inconsistent and their subsequent results at best qualitative. In view of the sensitivity of these issues, it is worthwhile to review the untranslated Görtler-Hämmerlin results and the discussion of the outer limits in their η variable.

5g The Outer Boundary Condition on V_1

The no-slip boundary conditions at the wall $U_1(0) = V_1(0) = W_1(0) = 0$ present no difficulties but the outer limit $\eta \to \infty$ does, on two counts. As previously noted, the first is philosophical: do we view the overall problem as an open system where small but nonzero upstream perturbations on V of the form $V_{1\infty} \exp(\beta\tau) \cdot \cos k\zeta$ (with β possibly zero) can be admitted in or beyond the limit $\eta \to \infty$? This would be the view of experimenters and of engineers concerned with observed enhancement of heat transfer. Or do we ask that all perturbations strictly vanish as $\eta \to \infty$ and then arise "spontaneously" along the paths of the fluid elements? This would be the pure normal approach confined to the Hiemenz scales. In Tollmien-Schlichting waves and Görtler vortices, the normal-mode amplitudes are linked to the amplitude of the disturbance environment, though the mathematics of the linkage remains obscure. If a similar linkage existed here, solutions with both types of outer V_1 behavior would presumably be present.

The second difficulty with the outer limit is associated with the singular nature of the η limit in which the base flow velocity itself grows without bound: $V_0 \to \infty$ as $\eta \to \infty$. Since this limit is fictitious (unless MMAE is applied), what is a logical physical requirement for perturbations around it?

Görtler (1955) first asked that all perturbations U_1, V_1, and W_1 approach zero as $\eta \to \infty$, but then observed that the milder requirement $V_1/V_0 \to 0$ should be sufficient, even if V_1 should increase indefinitely.

5h Hämmerlin's Results and Some Implications

The solvability of Görtler's system of equations and boundary conditions was investigated by Hämmerlin (1955). It involved first an assessment of the number of non-divergent linearly independent asymptotic solutions of the asymptotic equations in U_1 and V_1 in which Φ_H was replaced by $Y = \eta - 0.648$ and Φ_H' by unity as Y and $\eta \to \infty$. Hämmerlin then examined the feasibility of matching smoothly at some η_0 the outer solutions (made up of the available, linearly independent outer asymptotic solutions) to the well-behaved inner solutions, $\eta \leq \eta_0$ (made up of six regular linearly independent solutions) and the possibility of simultaneously satisfying the wall boundary conditions. For the continuous wave number spectrum $0 < \beta + k^2 < 1$, Hämmerlin found an extra degree of freedom for the coefficients of the linearly independent solutions. Equivalently, for a chosen positive value of $\beta + k^2 < 1$, one "amplitude" can be chosen arbitrarily at η_0, and then there would be a unique set of solutions such as those of Inger (1974) in Fig 17. For $(\beta + k^2) > 1$, the extra degree of freedom disappeared because a previously convergent solution diverged and had to be discarded by setting its coefficient to zero. Hämmerlin considered the possibility that the resulting nine homogeneous equations in the nine constants could have discrete eigensolutions but concluded that this could only be settled numerically. In a limited numerical search with H.J. Maehly on a 1955-type computer no eigenvalues were found.

For the so-called neutral, i.e. steady, solution, $\beta = 0$, Hämmerlin's asymptotic solution for V_1 involved algebraic variation with the dominant term $(\eta - 0.648)^{k^2-1}$. This would be allowable for $k^2 < 2$ according to Görtler's weaker boundary condition $V_1/V_0 \to 0$ as $\eta \to \infty$. However, according to Hämmerlin the boundary condition $V_1' \to 0$ (needed to make $W_1 \to 0$ through Equation (12)) requires that $k^2 < 1$ so that the above term would also decay to zero. Thus for perturbations of Hiemenz' flow as $\eta \to \infty$, $V_1' \to 0$ implies $V_1 \to 0$. According to Inger (1974 and private communication), that is the case for his solutions such as those in Fig 17.

The implication of this is that the forcing boundary condition of Fig 7 cannot be satisfied with $V_1 \neq 0$ within the Hiemenz flow, where V_0

itself diverges as ($\eta \approx 0{,}648$). Wilson and Gladwell (1978) believe that all instability mechanisms should occur within the Hiemenz scale and reject Hämmerlin's algebraic approximation to V_1 as unphysical. They maintain that any linearizable vorticity influence upstream from the boundary layer must decay exponentially outward with η . As discussed in Section 5b, this algebraic solution has the earmark of diffusive vorticity strained in the convective Hiemenz motion downstream toward the body. If so, discussion in Section 5f and Hämmerlin's conclusion concerning $V_1 \to 0$ as $\eta \to \infty$ indicate that responses to unavoidable oncoming disturbances in this open system and their possible linkage with free normal modes cannot be accomplished in the Hiemenz plane and that at least a two-region asymptotic matching process may be required to improve the correspondence of Görtler's model with experimental observations. Even then nonlinearity and unsteadiness (quasi-periodic or randomlike) are likely to stand between the theoretical model and the physical phenomena. In this writer's opinion, however, the main stumbling block is the confinement to the Hiemenz plane. It is for this reason that he does not discuss the painstaking, weakly nonlinear treatment of Iida (1978a, 1978b). It does not seem to improve the physical picture, presumably because it is locked in the η variable.

6 EXPERIMENTS WITH UNSTEADY DISTURBANCES

6a Possible Mechanisms of Enhanced Heat Transfer at the Stagnation Line

As noted in Section 3b, all the reported experiments other than that of Hodson and Nagib had unsteady free-stream perturbations which clearly do not correspond to the assumed perturbations of Equation (11). Most investigations, largely motivated by experimental observations of heat transfer rates in excess of the theoretical (laminar) predictions, Schuh (1953), naturally focused on the technologically important cases at higher Reynolds numbers where the oncoming stream is usually turbulent. However, the existence of steady vortical flow fields, such as in Figs 3 and 5a, suggests that increased heat transfer rates could be due to (a) increased "mixing" in steady nonlinear horseshoe vortex formations associated with steady nonhomogeneity of the oncoming flow; (b) increased heat transfer rates across temporally thinner shear layers associated with some unsteady aspects of the flow; or (c) additive or more than additive effects of simultaneous conditions (a) and (b). Small perturbation theory of Fourier-decomposed unsteady stagnation boundary layers yields only small second-order heat transfer effects, e.g. Lighthill (1954), so that effect (b) alone is unlikely to account for the observations.

6b Visual Evidence of Hodson and Nagib and of Sadeh and Coworkers

It is instructive to watch the movies which Hodson and Nagib made while gradually introducing unsteadiness in the oncoming low-Reynolds number wakes such as in Fig 5b. One finds that even though the modulation of the vortex formations is relatively slow, the relaxation times in this through-flow system are extremely short in comparison with those in Taylor vortices; see Section 3g. The sequence of frames shown in Fig 8 was recorded at the intervals of time shown in the figure. Here the steady wake of Fig 5a was replaced by a periodic but still laminar von Karman vortex street at Re_d of 90 by increasing the speed threefold. At 111 diameters downstream of the wake generating rod the fluctuations are rather weak, e.g. Kovasznay (1949), and this small, relatively high-frequency vorticity variation appears to change the mean stagnation region vortex cells very little. (For lower forced frequencies the effect could well be more substantial.)

Special interest centers on the response of the "amplifying system" to a moderate local disturbance marked P whose progress through the system is documented in Fig 8 and is described by Hodson and Nagib as follows: "The vortex flow module is always present on the average but is kicked out of position into the 'free stream' by the perturbation. When this occurs a large amount of the fluid in the vortices, which is marked by the dye, is ejected away, providing a very efficient mechanism for the mixing of the flow in the stagnation region with that in the free stream. It is conjectured that this mechanism also leads to added enhancement of heat transfer from the bluff body." The break up of the vortex pair and the ejection are seen in stages 5 and 6 of Fig 8. They are rapid and nonlinear and should give rise to some very thin temporal boundary layers. In Fig 8, the "disturbance" P marks a relatively small change in the oncoming unsteady but rather regular vorticity pattern so that the events can be clearly identified, contorted as the streaklines are. Apparently, when the disturbances are strong enough to cause mildly unsteady horseshoe vortex pairs to form we can expect sharper vortex interactions as the oncoming vortex pattern changes. Hodson and Nagib also mention interaction with vortices in neighboring cells when multiple wakes are observed.

Sadeh, Brauer, and Garrison (1977) and Sadeh and Brauer (1978) present visualization studies using a single smoke filament injected just 0.32D upstream of the stagnation line. The short length of the history-integrating smoke streakline facilitates somewhat the interpretation of the motions in the region of interest which is viewed from the side, from the top, and from the rear. However, the momentum defect from the injection tube and its support system (enhanced by the adverse pressure gradient) is convected directly at the stagnation line and interferes with the sensitive motions over half of the span. The Reynolds number Re_d of the wake generating rods was 650, yielding a much more random onflow than that of Fig 8. Since the rods were only 18.3 mesh-lengths upstream of the main cylinder, there was ample upstream nonhomogeneity (category a) and unsteadiness (category b). Each study describes detailed analysis of 62 frames of motion picture film, each frame with elaborate interpretative sketches. A companion motion picture, available on loan from NASA, makes one appreciate the complexity of

the erratic response of the rolled-up vortex structure to oncoming turbulent eddies and the possible interaction with the neighboring horseshoe vortices. At these upstream wake conditions visual information concerning the oncoming eddies (such as that in Fig 8, where the disturbance P is identifiable) is not obtainable, which hampers the interpretation of the responses and interactions.

This writer has some reservations concerning a few passages of less critical interpretation* and the smoke ejector interference. The reader would benefit from studying the reports first-hand and could then judge for himself. Even if the reservations were correct, the net evidence amply demonstrates that increased turbulence intensifies distortions and vortex interactions such as described above in connection with Fig 8. In particular, in the top views, (Fig 11 of Sadeh and Brauer corresponding to sequential views of Y streaklines in our Fig 5b), "an additional feature of utmost significance hitherto unexplained is unfolded". To this observer, the sequence of stills and the associated sketches in their Fig 11 seem to portray variants of strong interaction between the one visible half of the dancing horseshoe vortex pair, the invisible oncoming upstream-modulated vorticity and probably the invisible neighboring vortex pair. The strongest interaction does not appear dissimilar in nature to that in the last three frames of present Fig 8 (where, however, the neighboring vortices are altogether absent).

Whatever the best perception of the motions may be, their very complexity raises the question of adequacy of analytical modeling. These motions can hardly be considered quasisteady and mildly nonlinear. Could they possibly be portrayed with satisfactory accuracy by the first two or three terms of poorly convergent, weakly nonlinear approximations grafted on steady neutral solutions ($\beta = 0$) of the GH equations (11)? Do we have to adopt statistical

---

* Seldom do two independent observers agree fully on the interpretation of single, history-integrating streaklines in randomly modulated flows with strong vorticity. Also some of the disagreements may be a matter of terminology. The one important issue, which is discussed in Appendix 3, concerns the criteria for calling the boundary layer on the large cylinder turbulent in the classical sense.

techniques from turbulence theory because of the randomness? Is the formation of the horseshoe vortex structures at all explainable within such theories?

6c Controlled Onset of Unsteadiness and Change in Heat Transfer

While the steady nonlinear cellular motion pictured in Figs 5a and 7 may bring forth heat transfer rates in excess of those in a regular stagnation boundary layer, the unsteady motions described in the preceding section are likely to enhance the heat transfer even more. In other words, the observed increased heat transfer rates in presence of free-stream turbulence appear to be more likely due to category (c) in Section 6a than to category (a) alone. Hodson and Nagib devised a heat transfer experiment which covered the change from steady to unsteady controlled wake disturbances. The control was accomplished by moving the wake generators from outside while the tunnel was running and thereby inducing or suppressing the nonlinear horseshoe vortices at will.

They constructed a two-dimensional zither-like mesh of fine wires (diameter of 0.127 mm or 0.005 in.; solidities 0.05 and 0.10) and cast their wakes on an instrumented circular hollow pyrex cylinder (diameter of 50.8 mm or 2 in.) in the arrangement of Fig 3b. As the wind-tunnel speed was slowly increased these wakes experienced transition to an unstable state revealed by an oscilloscope trace from a continuously monitoring hot-wire anemometer. This occurred near Re_d of 25, depending on the proximity of the zither wires to the adverse pressure gradient generated by the cylinder. A gold strip less than 10^{-6} mm thick was baked onto the front of the cylinder, covering angles $-11^\circ < \varphi < 11^\circ$. Whenever the hot wire would indicate instability of the wakes, the strip-chart recorder measuring the temperature of the gold strip would register a sharp decrease. Thus, substantially increased cooling by the air stream took place when unsteadiness set in. Since the vorticity released into the wakes of the "zither" wires increases continuously with Reynolds number, even in presence of an essentially two-dimensional instability, and since the strength of steady vortex cells, such as in Fig 5a, also increases continuously with Reynolds number, the sudden change in cooling

can be ascribed* to the onset of unsteadiness.

For methodology and detailed quantitative results the reader is referred to Hodson and Nagib (1975) or Nagib and Hodson (1977). Their results relevant to flow instabilities are as follows: for steady wakes of the zither, the average Nusselt number over the gold strip increased by 5% at Re_d of 19 and by 10% at Re_d of 24 when the zither was brought to the y/d range of formed vortex cells. As already mentioned, a discontinuous increase in Nusselt number occurred in this y/d range when multiple Karman vortex streets were sensed near Re_d of 25. At Re_d of 27, the increase of Nusselt number due to combined effects of the cells and the Karman-street unsteadiness was about 23%. At Re_d values of 31, 37 and 42 the rise leveled off at approximately 29%, with increased scatter. The experiment demonstrates, therefore, that the formation of steady vortex cells does increase heat transfer rates in the stagnation region, category (a), and that presence of rather regular unsteadiness increases them more, category (c). We should keep in mind that the wakes at these low Re_d values below 42 are not turbulent. The conditions probably correspond closer to the unperturbed patterns of Fig 8 than to the disturbed pattern after the perturbation P interacts with the vortex. These are difficult experiments and corroboration of the results and their extension to higher Re_d values would be desirable.

6d Experiments in a Towing Tank

Our account would not be complete without discussing and digesting the most detailed experimental information thus far on the vortex structure in a turbulent environment, that from Görtler's Institute for Applied Mathematics and Mechanics in Freiburg, Germany. The reader really should examine the German originals of Hassler (1971) and Čolak-Antić (1971) to appreciate the foresight, special technique, and care it takes to elicit the small-scale details of this unstable and unsteady phenomenon in vivo. Its unsteadiness

* Evidence from continuous changes in variables (velocity increase and decrease past the critical condition; back and forth motion of the wire grid without stopping and opening the wind tunnel) is of course more convincing in diagnostics of instability effects than from discrete changes in variables (such as installations of different grids). Discrete changes in parameters, which require stopping of the wind tunnel, invariably bring about unmonitored changes in some conditions of the flow or instrumentation and increase scatter substantially. This and the need to fair discrete data impair our ability to document cause and effect in instability phenomena from discrete changes in variables.

dictated the use of hot-wire anemometry; the need for λ magnitudes on the order 6 - 15 mm for adequate spatial resolution and visualization called for water as a medium. The hydrogen-bubble visualization experiment of Čolak-Antić and the hot-wire explorations of Hassler were therefore carried out in a water tank 0.23 x 0.28 x 3 m. Water provided relatively high Reynolds numbers and visualizability at low speeds, 5 - 40 cm/s, but at the price of (a) special techniques and constant recalibrations because of the conductivity of the medium and (b) the need to move the cylinder model with all instrumentation (including turbulence screens, traversing mechanisms, the hydrogen-bubble cathode wire and the camera) on a sliding carriage along the channel.

Two details are of particular relevance to the data to be examined: (1) the hot-wire signal itself was used as a guide to minimize the vibrations induced by the carriage motion so that these did not influence appreciably the 0 - 80 Hz spectrum of interest; (2) the bare 90% platinum-rhodium hot-wire sensors had a diameter of 5 microns and lengths of 1 - 2 mm and were welded onto conical prongs of like material. In Figs 9-10 and 13-16, due to Hassler, the wavelength was 7+ cm (i.e. the wire averaged the signal over roughly one-fourth of a vortex cell), the boundary layer was 1,8 mm thick (Fig 14), and the closest probe position was 0.5 mm from the cylinder, 12 cm in diameter. Thus when we consider the results in the plane of symmetry (from which the angle φ is measured), we should again allow for the possibility of some probe interference: the flow is instability-prone and the probe does force upon it additional boundary conditions including an additional momentum defect. For larger $\varphi \sim x/R$, the component U of the base flow (Fig 1) builds up and the danger of upstream interference rapidly decreases,

Since the wire senses only the velocity normal to itself, the same Fig 1 or Equation (1) also helps us to assess the relative wire sensitivity to the U and V components of the velocity. The flatter the streamline, the larger is the response to U, a fact to remember in interpreting the figures because Hassler always calls the signal u, irrespective of local streamline orientation.

6e An Unexpected Quasiperiodic Behavior

Figs 9 and 10 of Hassler disclose the presence of various types of

unsteadiness, which over the 0.16 second intervals (2,4 cm of cylinder travel) may display quasiregularity, some of it of unknown origin. These fluctuations are conditioned by free stream turbulence characterized by Tu of .85% (same for all the figures of Hassler) but unfortunately not by a spectrum; see discussion in Section 3b. Even though the 12 cm cylinder had a 24 cm long splitter plate attached at its rear, the wake oscillated at approximately 8 Hz (see lowest of Figs 10, past separation). For cylinders without splitter plate, upstream influence of both sets of vortices in the alternating wake produces appreciable fluctuation near the front stagnation line, at double the wake frequency. The small sample at 15.6 Hz in the upper trace of Fig 9 for $\varphi = 0°$ suggests that the effect may appear even in the presence of the splitter plate.

Because of the acceleration around the cylinder, the boundary layer thickens very slowly so that little error is committed if one uses a single scale $\delta \sim 1.8$ mm, even at $\varphi = 45°$. Then the indicated y positions can be converted to the Hiemenz scale: $\eta \sim 1.3 - 1.4y$, for rough comparison with Figs 17, 18, and 20 of eigenfunctions of the steady linear theory. The linearized vortex height corresponds to $W_1 = 0$. The trace at y = 5 mm in Fig 9 with the largest unsteadiness corresponds then to approximately twice that height where the steady V_1 perturbations have dropped 30 - 40% from their maximum. These traces exhibit a remarkably regular mysterious frequency of about 86 Hz (60 - 70 Hz in other longer samples, according to Hassler's private communication). It is helpful to recall that Fig 9 portrays the behavior in the stagnation plane so that small vorticity perturbations are convected from the region of the lowest trace against the pressure gradient to the region of the uppermost trace. The lowest trace corresponds to η of about 27, i.e. to the asymptotic region of the Hiemenz flow beyond the confines of Figs 1, 7, and 18.

As we move away from the interference-sensitive stagnation plane to $\varphi = 15°$ ($x \sim 1.6$ cm $\sim 8.8\delta$) the mysterious frequency is still present, randomly modulated, according to the first trace of Fig 10. Here the signal would represent mostly the temporal fluctuation in U, if it were comparable in magnitude to that in V. The remaining three traces make it clear that the temporal tangential fluctuations damp out farther around the cylinder: the

boundary layer remained laminar despite its spanwise corrugations and despite the relatively high free-stream turbulence of 0,85%.

The higher frequency oscillations of Figs 9 and 10 are representative of the quasiperiodic behavior mentioned in Section 4b in connection with wavy instabilities in Couette Flow. The turbulence level of 0.85% here is undoubtedly much lower than the unspecified level of Sadeh and Brauer, who saw no quasiperiodic patterns. However the same level of turbulence is high enough to hide the periodic Tollmien-Schlichting response in non-stagnation boundary layers in most investigations. Hassler's diagnostics seem convincing enough to exclude as possible causes the relative vibrational motion between the hot-wire and the cylinder-attached velocity gradients, and purely electrical effects. Unsteadiness there should be as a response to the grid turbulence, but what mechanisms would selectively amplify a narrow band of frequencies just at the outer edge of the boundary layer? The linear instability formulation of Görtler does not allow for such temporal periodicity. Could it possibly be associated with secondary instability of the nonlinear vortex formations as in the wavy instability of Taylor vortices (Section 4b) and the Görtler vortices (Section 4c)? Unfortunately, the plans to verify that the effect is indeed generic and to study its parametric dependence in a larger towing tank at Freiburg have fallen through with the closing of the laboratory.

6f Visible Patterns of Čolak-Antič

Čolak-Antič's two snapshots of the hydrogen bubble "time lines", Figs 11 and 12, display the "top view", vertically downward onto the cylinder, with the leading edge seen tangentially at the upper edge of the photographs. The corresponding velocities V_∞ of 11.9 and 19.4 cm/s bracket the 15 cm/s velocity of all the Hassler data in Figs 9-10 and 13-16. The lines of bubbles are released at equal intervals at $\varphi = 11^\circ = 0.19$ rad, $y = 2$ mm, i.e. just beyond the edge of the boundary layer and away from the sensitive stagnation plane. Once formed upstream of this station, streamwise vortices should follow the pattern of Figs 7 and 20 even if they "dance around a little". If the bubbles were released at the height of the vortex centers where $W_1 = 0$, a short time Δt later the bubble line $\Delta y = V_1 \cdot \Delta t$ would resemble the profile of the V_1 curve in the lower Fig 20 except that the bubble density would

increase or decrease depending upon the local narrowing or widening of the stream tubes in the y - z crossplane. For bubble release above or below the height of the vortex centers the bubble time lines are also subject to spanwise distortions due to W_1 motion indicated in the lower Fig 20. Ultimately, had they had enough time, most bubbles would migrate toward the vortex centers according to the streamlines of the upper Fig 20. At the speed of 11.9 cm/s of Fig 11 the upwelling motion between the vortex pairs (near cos kz = 1 of Fig 20) is clearly visible and the Ω shapes suggest that the bubble line was released below the vortex centers. The bubble lines also distort in the streamwise direction because of the variation of mean and perturbation tangential velocities U(y) as is especially visible in Fig 12. At the higher Reynolds number of Fig 12 the irregularities seem to be more pronounced, including a tendency for stronger vortex pairs to interact and even absorb neighboring weaker vortex pairs. Some of this behavior is not as surprising as it might otherwise be after the lessons of the Hodson-Nagib movie associated with Fig 8.

6g On the Causes of Spatially-Fixed Mean Patterns in Nominally Homogeneous Turbulence

If free-stream turbulence were truly homogeneous one would expect vortex pairs to arise and disappear irregularly along the stagnation line as the different free-stream vorticity formations sweep in and out of the stagnation region, giving instantaneous impressions similar to that of Fig 12. If the amplification along the paths had a sharp peak in wave number for the more complex unsteady perturbation equations here operative, one would expect a preferential wavelength to occur rather frequently but randomly along the span. However, true homogeneity would dictate no spanwise preferential location of vortex pairs, not even on a nonlinear basis. It is difficult to imagine an upstream influence from a finite-size vortex structure (which is being washed out of the stagnation region) strong enough to force the independent oncoming free-stream vorticity formation to replicate its pattern. That oncoming vorticity formations are rather powerful even in presence of strong mean vorticity fields was illustrated in Hodson-Nagib, Fig 8. And yet substantial spanwise regularity in the mean does frequently occur in nominally homogeneous fields, as the remaining figures of Hassler will demonstrate. To the present writer this suggests that even subtle steady departures from

spanwise homogeneity in the oncoming stream do get picked up in an amplifying process and enforce a steady mean pattern, (The effect could be likened to that of a minute mean drift making itself felt in face of random molecular motion, except that in this analogy the drift would be amplified.) When occasionally a rare experimenter investigates the character of turbulence downstream of a turbulence grid or screen, with care great enough to resolve small mean changes in presence of large A.C. signals, he invariably finds that there is more inhomogeneity and nonisotropy than expected, e.g. Bradshaw (1965) and Grant and Nisbet (1957). In particular, the idea that parallel rods can generate a turbulent field 10 - 40 mesh lengths downstream, homogeneous for the purposes of experiments in stagnation regions, must be considered a myth.

6h Hassler's Averaged Quantitative Field

In the face of the unsteadiness exhibited in Figs 9 and 10, Hassler averaged the signals over one-second intervals (trace lengths over six times those in Figs 9 and 10) and labeled this averaged velocity component normal to the hot wire $\bar{u}$. Fig 13 displays the spanwise variations of $\bar{u}$ at $\varphi = 4^c$, $x \sim 0.41$ cm $\sim 2.3\,\delta$. A vertical cut at $x = 2.3\,\delta$ in Fig 1 tells us that $\bar{u}$ partakes more and more of $-\sqrt{\nu a}\, V_1$ than of $ax \cdot U_1$ (Equation 11) as y increases. Note also that $\sqrt{\nu a} \sim 0.42 \cdot a\delta$ for Hiemenz flow and that according to Fig 17 the maximum of U_1 is very small and close to the wall at $\eta \sim 1.2$ or $y \sim .09$ mm . Thus Hassler's averaging indicates vortical motion with $\lambda \sim 7+$ mm, $k \sim 0.65$ (using $\delta = 2.4\sqrt{\nu/a} = 1.8$ mm), below $y \sim 3.6$ mm $= 2\delta$ or $\eta \sim 4.8$. While Hassler could document only the peak-to-valley spanwise variation of the mean velocity normal to the wire, denoted by $\bar{u}'$, we can safely infer the mean pattern of motion without direct W_1 information because of Čolak-Antič's visual evidence under essentially the same conditions in the same laboratory.

The quantitatively determined mean strength of the vortices, measured in terms of $\bar{u}'$, is substantial; see Fig 14. For $\varphi = 4^c$ the maximum of the ratio $\bar{u}'/\bar{u}$(y=10mm) is approximately 0.2 (0.1 in the U_1/U_0 , V_1/V_0 notation of Equation (11)). A "zero-length" hot wire would indicate still sharper minima and maxima in Fig 13 and therefore higher $\bar{u}'$. The "instantaneous vortices" seen by Čolak-Antič must have then been much stronger to yield Hassler's average numbers despite their spanwise shifting and dancing.

6i The Extent of the Hiemenz and the Görtler-Hämmerlin Domains and Decay in x

The reader who wishes to develop a more concrete feeling for the nature of the imbedded Hiemenz-flow approximation will enjoy the exercise in interpreting the mean "normal" $\bar{u}$ profiles at $\varphi = 4^{\circ}$ and 0° in Figs. 13 and 16, respectively, in terms of the theory; i.e., Equations (1) and (2) and the field of Fig. 1 when modified for the stagnation region of a circular cylinder by Equation (5).

For $y < 1$ mm in Fig. 14, the signal $\bar{u}'$ should reflect mostly the behavior of the theoretically increasing component $ax.U_1$ with downstream distance or φ, but it decreases instead. Presumably this is associated with the curvature of the streamlines which now become convex: we are apparently beyond the domain of validity of the Hiemenz and Görtler-Hämmerlin flows. The cooling of the hot wire by the V_1 component may have also contributed to this trend. Note, however, that the decay of $\bar{u}'$ at $y = 0.5$ mm in Fig. 14 is much less rapid than at $y = 2$ mm, the height monitored in Fig. 15 as a function of φ.

Fig. 15 tells us that spanwise variations, $\bar{u}'$, decay more or less hand in hand with the temporal fluctuations of Fig 10 as the flow accelerates around the cylinder. While the choice of the monitoring height may exaggerate the decay, it is unlikely that strong streamwise vortical activity would take place below this height. The time lines in Čolak-Antić' Figs. 11 and 12 which were generated at the same height of 2 mm at $\varphi = 11^{\circ}$, may be displaced somewhat inward by the base velocity V_0 at this early station, but the main upwelling Ω motion in these figures probably occurs near $y = 2$ mm or even farther out. The genuineness of the decay is also born out by mean heat-transfer measurements and by the refusal of the boundary layer to become turbulent for $\varphi < 60^{\circ}$ at Reynolds numbers below Re_D on the order of 3.10^6. At first glance Figs 11 and 12 of Čolak-Antić seem to contradict the decay of Fig. 15, but his time-line distortions probably represent primarily the nearly frozen integrated effect of past history. It is difficult to judge the local time-rate of the distortion which is proportional to the local strength of the motion. Čolak-Antić agrees with this interpretation.

6j The Mysterious Wavelength Doubling at the Stagnation Line

The lowest curve depicting variations in the stagnation plane in Fig 16 seems to show an effect opposite to the tendency to coalescence of vortex pairs observed in Fig 12 for larger φ values. The development of this new mysterious effect as the flow approaches the cylinder in the stagnation plane is documented in intriguing detail in Fig 16. At $y = 10$ mm $\sim 5.6\delta$. mean hot-wire measurements (which now correspond purely to $-\sqrt{av}(V_0+V_1 \sin kz)$) sense only the same pure wavelength, manifest at $\varphi = 4°$ in Fig 13, but somewhat more irregular. At $y = 0.5$ mm an irregular but definite and puzzling double structure is evident--the explanation for the four points at $\varphi = 0°$ marked with a question mark in Fig 21, transcribed from Tani (1974).

How can this near-doubling be viewed in consonance with the rest of the concepts described here? It could be a manifestation of a true discrete eigenvalue selection in a borderline situation where two modes with λ_1, say, and $\lambda_2 = 2\lambda_1$ would be near equally likely and the randomness of the free-stream disturbances would shift the flow between the two patterns in time. Since the fields associated with the smaller-scale vortices also reach out less in the y direction, it would be possible for the time-averaged measurements to sense the larger λ_1 mode alone at larger distances such as $y = 10$ mm. While not impossible, the situation has no counterpart among linear shear-flow instability systems, nor among prototypes of nonlinear systems such as discussed in Sections 3 and 4.

An alternative is the coexistence at all times of larger eddy formations for large y values with smaller formations near the wall. This pattern is even harder to imagine and believe. Presumably the mean streamline pattern would have to be somehow generalized from that in upper Fig 20 to accommodate first a row of free stagnation points at distances λ_1 apart at a height near 7 mm. Closer to the wall a second set of free stagnation points would apparently be called for. The two sets would have to mesh in such a way as to satisfy the topological consistency of the streamlines and achieve stable equilibrium everywhere. Recalling the discussion in Section 3c one tends to be pessimistic.

Any explanation must not only clarify how the mean vortices could suddenly split in midstream as the flow approaches the stagnation line but also how they could suddenly disappear as the flow leaves the stagnation line in the x direction. According to Fig 13, at $\varphi = 4°$, i.e. $x = 4.1$ mm $= 2.3\delta$, the smaller vortices are no longer sensed by the probe.

In the opinion of the writer, the most probable explanation is that the appearance of the second set is induced by the additional boundary conditions due to the presence of the probe. Stagnation regions and nearly separating (i.e., nearly stagnant) boundary layers are notoriously sensitive to probes approaching the wall. Here in the stagnation plane the absence (or smallness) of U to relieve the situation compounds the danger of localized probe interference. As the probe is shifted to $\varphi = 4^\circ$ where its momentum defect is no longer convected toward the stagnation line, the vortex formations in the stagnation plane cease to be influenced and the false signals disappear. In a 1977 lengthy private review of the likelihood of the various possibilities, Dr. Hassler also agreed that the last one appears as the most probable at this stage of our research. The question mark was placed in Fig. 21 to warn of the probability that only the wavelengths reported for $\varphi = 4^\circ$ had best be used for comparison with theoretical modeling.

Another explanation for the measurements of Fig. 16, was pointed out by Ivan Beckwith and Dennis Bushnell, of NASA Langley, after reviewing a draft of this report. In presence of the vortices spaced λ apart, a subset of counter rotating vortices with a wave length $\lambda/2$ may be induced by viscous effects and could exist beneath the most unstable mode of vortices. Due to the structure of the mean flow (Fig. 1) this subset of vortices would move closer to the wall with increasing φ, so that at $\varphi = 4^\circ$ they would presumably be found only for $y < 0.5$ mm. Such vortices have been predicted by numerical solutions of the Navier-Stokes equations and observed experimentally in flows inside cavities beneath a shear layer or near horseshoe vortices upstream of an obstacle immersed in a boundary layer. This explanation is somewhat related to the second of those listed above.

7 OVERVIEW OF ISSUES

7a Is There a True Instability?

Perhaps the best point of departure for this Section are the theoretical findings of Wilson and Gladwell (1978). Having rejected the algebraic solutions utilized by all others (e.g. in Figs 7, 17, and 18), they show numerically that that Görtler equations then yield only stable solutions. They add, "There is, however, considerable experimental evidence that instability of this kind can occur," and "It must be concluded that this instability is, as yet, not satisfactorily explained".

Is it clear that the observed phenomena really constitute an instability in the usual fluid-mechanical sense where a linearized system of equations describes the basic mechanisms and admits exponential growth in time or space? Do we have a well-posed mathematical problem? Wilson and Gladwell tellingly point to the severely limited upstream feedback from the body boundary layer and yet find it "appropriate to assume that all disturbances are proportional to $\exp(\beta\tau)\exp(i\,k\,\zeta)$ ". Our Section 4b on Taylor vortices described the conditions physically appropriate to $\exp\beta\tau$ growth with β real: disturbances are not convected away but reinforce themselves in the closed domain. What physical agent could make all the fluid disturbances grow in unison exponentially in time, even far upstream, in our problem? Experimental evidence illustrated in Fig 8 suggests that the upstream influence is indeed very limited. Vorticity perturbations are convected in, interact, and are convected out. Rapid variation of the base flow in the direction of convection also distinguishes our flow from quasi-parallel flows where $\exp\beta\tau$ (with β complex) may be rationalized. It was the purpose of the studies of the three flows with streamwise vortices in Sections 3 and 4 to compare the actual instability characteristics which were originally considered analogous. Sections 4a and 4d, in particular, underscore the special character of the stagnation flows which make it unlikely that $\exp\beta\tau$ is appropriate. The experiments of Hodson and Nagib in Section 3e, however, did not definitely exclude $\exp\beta\tau$ as a possibility.

7b Implications of Controlled Steady Experiments of Hodson and Nagib

The same experiments show that steady flows corresponding to the steady free stream forcing portrayed in Fig 7 exist. When V_1 is small, the forced and free response (if any) remains below the resolution limit of the visualization

experiments. As V_1 is gradually increased, a threshold-like behavior leads to the appearance of mature nonlinear vortices with λ set by the forcing disturbances in these experiments with limited λ range. The onset of the steady vortices evidently corresponds to a mild but definite increase in the heat transfer rate in the stagnation region (Section 6c). In accordance with Generalized Guideline 4 (Section 1) it would be desirable to replicate and improve the Nagib-Hodson-Roadman experiments and focus on the stability questions rather than heat transfer modules; (see Section 3e for relevant issues). In particular, the widest range of the ratio λ/δ should be tried to uncover any special scale receptivity of the stagnation boundary layer as Bippes has done for Görtler vortices (Appendix 1a) and Koschmieder for Taylor vortices (Section 4b).

7c Forced Motion, Free Response, and Linkage

Given the nonlinearity of the observed phenomena, can we recognize a pattern of known instability behavior in these steady experiments? In Section 4b the author proposed a forcing experiment in the non-unique Taylor-cell regime using a spanwise arrangement of vortex generators withdrawable through the wall of the fixed external cylinder. Withdrawal of the generators after the nonlinear cells with admissible λ's are established will remove only the steady forced contribution to the flow but not the stable cells themselves. Withdrawal of the vorticity forcing rods in our stagnation flow removes the whole phenomenon. Forcing and receptivity are central to our problem.

In the Görtler instability in concave boundary layers and in the Tollmien-Schlichting instability, the receptivity in these open systems includes the difficult subproblem of penetration of the disturbances into the shear layers. Its resolution for rotational disturbances may require a solution of an auxiliary set of equations. In the stagnation flow problem the disturbances are convected directly into the boundary layer along the streamlines of Fig 1 and this process is governed by the same differential equations as the postulated instability. In the steady linearized case, this leads to the Görtler equations with $\beta = 0$. If we could resolve the weak-disturbance cases of Hodson-Nagib experimentally, how much forced motion and how much free instability response would we observe? In the TS and Görtler instabilities above, the experimentally observed modes, presumably indistinguishable from normal modes, rise with the disturbance amplitude. In controlled acoustic excitation of a free mixing layer, the stimulated

normal-mode vorticity is linearly proportional to the forcing acoustic pressure gradient around the point of separation (before nonlinearity sets in). Does a similar linkage exist in our problem in the linear regime (if there is a linear instability)?

7d A Crucial Limitation of the Hiemenz Plane

At first thought the direct-inflow aspect of our problem should make a theoretical answer to the question far easier than in the other systems (Section 5b). The penetration subproblem is not a problem. But the search for an answer is thwarted by the limitations of the formulation of the problem in the Hiemenz plane alone (Section 5h). If U_1 and $W_1 \to 0$ as $\eta \to \infty$, then $V_1' \to 0$ by continuity and so does V_1 for the algebraically decaying solution, which should be linked to vorticity incoming from upstream. Thus treatment of the problem without using at least two asymptotically matched regions precludes answers to our quantitative search for a forced solution and a linked, free response (if any).

The threshold behavior in the Hodson-Nagib experiments indicates that interesting answers could be sought through nonlinear formulation of the problem, which should then also include other higher order effects such as body curvature effect, etc. The initiative of Tani (1974) and Iida (1978a,b) in this direction is therefore interesting. However, this effort, too, is hampered by confinement to the Hiemenz scales.

7e Continuous Spectrum and Optimum λ

If the algebraically decaying eigensolutions are admitted, a continuous spectrum of eigenfunctions for $0 < k < 1$ exists. Many of their "physical" characteristics for the "neutral" or steady solutions, $\beta = 0$, are discussed in Appendix 4: "Miscellaneous Observations on the Görtler Model". Since, uniquely, the eigenvariable is colinear with the motion, the increasing functional values as η decreases (say, for ω_x in Fig 17) can be viewed as spatial amplification. Much can be learned about the complex motion by studying the relative shapes of the U_1, V_1, W_1, ω_x, and P_1 eigenfunctions as dependent on the wave number k. It would be interesting to know more about energy transfer in these flows, in particular production and dissipation, which are now computable.

The presence of the continuous spectrum is most likely due to the absence of a characteristic length in the Hiemenz base flow (Section 2). Extension to two or more asymptotically matched regions would probably supply an extra condition and thereby criteria for an optimum λ . At least two sets of researchers are working along these lines at this writing. The path is strewn with traps: the matching should be rigorous. A critique of one such attempt by Kestin and Wood (1970) can be found in Wilson and Gladwell (1978). Tani (1974) also pointed out that the crucial assumption of Kestin and Wood to the effect that the vorticity $\omega_x(\eta)$ has no zeros in the whole η domain is incorrect (see Appendix 4). There has been no rebuttal to the latter criticism. Iida (1978a) proposes two weak criteria for λ selection based on integral properties of the eigenfunctions in the Hiemenz domain.

7f Agents of Instability

Focusing on the instabilities associated with the vorticity in the boundary layer (rather than on the vorticity coming in through the open streamtubes). Wilson and Gladwell (1978) diminish the degree of freedom among the independent solutions of the Görtler equation by rejecting the algebraically decaying solution as unrepresentative of the possible instability mechanisms. They show numerically that for $0 < k \lesssim 10$ the least negative β in the $\exp\beta\tau$ factor is $-1,3754$, whatever such global decay implies physically (Section 7a). Having removed the continuous spectrum and believing that the short upstream influence is fully covered in the Hiemenz range, Wilson and Gladwell see no reason for using matching and inner Hiemenz η and outer, y/D , scales, advocated above for different purposes.

They also demonstrate that centrifugal instability is not a factor in stagnation-flow instability despite frequent invocation of the analogy in the literature. Examination of the terms in the vorticity equation (Section 5a-5c and Appendix 2) identifies the stretching of any x - oriented vorticity, as it is convected toward the body, as the dominant destabilization in the steady motion. It is the Brown University group, Sutera, Kestin, Maeder, Sadeh, Williams, Wood, etc. who emphasized that this mechanism (so familiar in turbulence) is at work here where others invoked centrifugal instability. However, it was not made clear whether they viewed their eigensolutions as forced motion, free normal modes, or both. This could make a difference in starting the computations at large η values -- see the paragraph "Computer Differences?" in Appendix 4.

7g Experimental Information in Unsteady Environments

The preceding issues dealt with steady or exponentially growing behavior in presence of Fourier-analyzed steady spatial nonhomogeneities in the spanwise z direction. Most free-stream environments are also temporally nonhomogeneous, in fact more or less turbulent. The Hodson-Nagib experiments with controlled onset of Kármán instability in the upstream forcing wakes (Sections 6b and 6c) provide some insight into sporadic, more violent vortex interactions which are possible even for relatively low unsteadiness levels (e.g. Fig 8). The careful stereoscopic hydrogen-bubble visualization of Čolak-Antič for mild, presumably isotropic and nominally homogeneous turbulence add more physical insight (Section 6f and Figs 11 and 12). Hassler's unique hot-wire information at slightly higher $Tu \sim 0.85\%$ (Sections 6d, 6e, 6g, and 6h) brings forth two questions: what mechanisms select the dominant temporal quasi-periodicity (Figs 9 and 10) and the prominent average spatial quasi-periodicity (Figs 18 and 20) at 240 meshlengths downstream from a nominally homogeneous turbulence screen? These most detailed of the available experiments, carried out in a reasonably controlled and monitored environment, give indications that the spatial vortex structure scales to some extent with the thickness of the boundary layer δ, Fig 21. The grosser experiments of Brun et al (1966) and Kestin and Wood (1970) with less assurance of homogeneity are in general agreement with the results of Hassler and Čolak-Antič concerning the one feature of preferred average λ, Fig 21.

At higher intensities of turbulence with distinct mean nonhomogeneity, Sadeh and Brauer (1978) demonstrated visually how complex and violent the vortex interactions can be. There is little chance to model these types of highly nonlinear unsteady nonhomogeneous turbulent flows rationally for some time so that the conceptual issues perhaps should be addressed in flows with $Tu < 1\%$.

7h Interpretation of Experiments with Unsteady and Turbulent Free Stream

Do these motions represent forced response, true instability, or a combination of both? If we cannot reach an answer to these questions in the case of steady disturbances, we shall not be able to do so for this more complex motion. The limitations of the confinement in the Hiemenz plane are undoubtedly just as operative. We can certainly say from the visualizations that forced motions are present, probably to an increased degree; see, for instance, the strong forced vortex interaction in Fig 8. Čolak-Antič and Hassler agree that in their case

the disturbed motion subsides as the vortices are stretched around the cylinder with increasing φ (Figs 10, 14, and 15). Such damping is often observed in thin laminar boundary layers despite the continued vorticity stretching which, however, occurs in the proximity of the wall. Time-line and streakline visualization portrays the integrated history of the fluid elements, not their local rates of deformation, so that Figures like 12 and the stills of Sadeh and Brauer (1978) often give false impressions of excessive activity. Even at relatively high body Reynolds numbers the agitated motion does not cause turbulent bursts intrinsic to the scales of the body boundary layer. Thus the enhanced heat transfer subsides around the cylinder until a genuine transition in the buffeted laminar boundary layer of the body takes place at high Reynolds numbers. The simplest telltale sign of transition is the onset of high frequency oscillations in the boundary layer on the scale of 0.1 δ to 0.001 δ and less; (see also Appendix 3).

Does the evidence in Fig 21 of vortex scales on the order of 2 - 4 δ prove that there exists genuine laminar instability in the stagnation region in the sense of Section 7a, alongside the forcing motion? It suggests the possibility of unstable response but by no means demonstrates its presence. The forced response, after all, is also a solution of the motion in presence of the boundary-layer field and must reflect some of its characteristics such as the thickness. (Similarly the frequencies in decaying Wygnanski-Champagne puffs in a pipe at Reynolds numbers below 1800 will scale with the pipe shear layer without constituting true instabilities of the shear layer.)

7i Whither Further Progress?

This brings us back to the question we posed in Section 7a in connection with the apparent impasse of the Wilson-Gladwell findings: is there a true instability in the steady and unsteady cases? The question is unlikely to be answered experimentally because the instruments read the whole motion, and it is impossible to decompose the signals without knowing much about the characteristics of the ingredients. Theoretically the most promising approach seems to be the search for the linkage between the forced and free responses (if any) for the steady environment, which means breaking out of the Hiemenz scales constraint (Sections 7c - 7d).

For the unsteady problem it might be worthwhile to explore changes in the structure of the linear problem (forced or free) which would ensue if one replaced

$\exp \beta\tau$ (β real) with $\exp(i\gamma\tau)$ (γ real or complex) in Görtler's formulation, Equation (11). Kayalar (1969) set up some general equations along this line but studied only the case with $k = 0$, i.e. the bulk oscillation without vortex formation. Could there perhaps be any new ways of transferring energy to the disturbed flow due to special phase relationships?

Since the Hassler hot-wire information is currently unique, it should serve as a springboard for still more incisive and more controlled experiments, in accordance with the Generalized Guideline No. 4 of Section 1. If two-probe space-time correlations could be accommodated for this interference-prone geometry, the experiments should prove most rewarding.

Without improved information on detailed motion and on coherent motion we can say little about correspondence of unsteady reality with theoretical models. For instance, to use any comparison of optimal λ values, drawn from steady linear theory in the Hiemenz plane, with the measurements in Fig 21 in unsteady, highly nonlinear flows as sufficient evidence for a model is an exercise in unwarranted extreme faith. Analyzing the present experimental information makes one feel very humble and conscious of the need for rigorous experimental procedures and rigorous inferences.

7j Applicability of the Information

Although the original motivation for scrutinizing the stagnation flows came from applications, the emphasis in this report has been on the basic information. Reliable, rational semi-empirical prediction methods for a host of applications cannot be expected without deeper appreciation of the physics and mathematics of the problems.

The most immediate applications deal with heat and mass transfer in stagnation regions of bluff bodies. When the leading edge is quasi-cylindrical and normal to the flow, the present account of the experiments and theory provides us with some conceptual understanding of the underlying mechanisms. It should appeal to the intuition of the engineer. Both the vortex roll-ups associated with spatial nonhomogeneity in the environment and the unsteady vortex interactions in a homogeneous turbulent environment contribute to an increase in scalar property transfer (Sections 6a - 6c), without the body boundary layer becoming turbulent. Unless the body boundary layer undergoes transition to its own intrinsic turbulence, the heat transfer enhancement subsides with increasing

φ . The motions associated with the enhanced heat transfer evidently bear a resemblance to the general pattern of motion envisaged by Görtler in 1955. The vorticity-stretching mechanism is part of the dynamics, as has also been recog- by Bearman (1972) and Hunt (1973).

The subject of transfer mechanisms and boundary layer instabilities at swept-back cylinders and axisymmetric bodies is a separate matter. There seem to be some similarities and some important differences so that drawing analogies is not recommended without further studies.

APPENDIX 1

RECEPTIVITY, INITIAL VALUE PROBLEMS, TEMPORAL AND SPATIAL NORMAL-MODE APPROACH AND NONLINEARITY

a. The Problem of Receptivity to Disturbances and Some Illustrations

In a detailed study of the growth of Görtler streamwise vortices in boundary layers on a concave surface in water Bippes (1972) deliberately stimulated disturbances of different spanwise wavelengths λ by local heating at the wall. When the imposed λ was substantially larger than the eigenwavelength λ_m of maximal amplification the initially dominant flow response was in vortical motions with the forcing periodicity λ, followed by slow spatial development of ultimately dominant motions near λ_m. When Knapp and Roache (1968) irradiated the laminar boundary layer on an axisymmetric ogive-cylinder body with an acoustic frequency f_1 in a relatively broad band near the maximally excitable Tollmien-Schlichting frequency f_m, the response apparently developed into that of free TS eigenwaves at the forcing frequency f_1. When loud sound at frequency f_2 near $f_m/2$ was beamed at the boundary layer, the response appeared to be a TS wave of frequency $2f_2$, again near f_m. When Loehrke (1970) gave a sudden pulse to a spanwise stretched thin wire (0.038mm in diameter), vibrating in the flow direction within a 4mm thick Blasius boundary layer, a slowly broadening wave packet of TS waves with frequencies around f_m grew and traveled downstream.

These are but three examples of selective responses of unstable shear layers to identified forcing disturbances. Complicated responses with wavenumber spectra in the region of most-amplified eigenfuctions are known to evolve in presence of low-intensity turbulence in the free stream for both the TS and Görtler instabilities. The intensity of the response grows with the intensity of the free-stream disturbances and leads to earlier transition to turbulence in the shear layer. In open flow systems: duct flows, free shear layers, and boundary layers (in wind tunnels or in free flight), the upstream regions generally contain nonvanishing acoustic, vorticity or entropy fluctuations which penetrate the shear layers and excite their responses. These responses evidently include free eigenfunction motions (normal modes) which dominate in unstable shear layers. The processes of penetration, excitation of forced

and free responses ("internalization" of the disturbances) constitute the receptivity problem as identified by Morkovin (1969) and discussed by Reshotko (1976). Rigorous experimental elucidation of receptivity and its convincing theoretical modeling represent an important step in our further understanding and estimation of transition to turbulence, see Morkovin (1978).

b. Temporal Initial Value Problems

Receptivity is sometimes linked to initial value problems of linear instability. For such problem formulation it is assumed that the disturbances have already penetrated the shear layer and that they are known throughout the region at some initial time t_o. The evolution of the forced and free responses is sought for $t>t_o$ generally in the easier temporal formulation. The motion associated with any normal mode k then grows (or decays) uniformly throughout space in proportion to $\exp(\beta_k t)$. This approach has the virtue of potentially identifying the forced response which presumably has little to do with the build up of disturbance energy to nonlinear levels. (However, this motion may possibly play a role in the initiation of subsequent secondary instabilities which seem to be necessary, but not necessarily sufficient, for onset of turbulence). Quantitative linking of the disturbance at t_o with initial amplitudes A_k at t_o of the amplified normal modes of the free response would be conceptually helpful to the understanding of one element of receptivity. The equally important element of receptivity, associated with the transformations of the disturbances as they penetrate the shear layer and adjust to it, is absent in the initial value problems.

c. Spatial Initial Value Problems

We must keep in mind that the analytic problem is exceedingly difficult and that without substantial idealization it becomes intractable. But whatever the useful conceptual lessons of initial value problems in time are, it should also be recognized that the approach does not seem to be adaptable to a number of important situations. For instance it does not fit the cited cases of Loehrke, or Knapp and Roache, and of Bippes, nor Bippes' case of excitation of Görtler instability by free-stream turbulence. In the cases of Loehrke and Bippes, the disturbances were introduced artificially directly into the boundary layer at fixed streamwise locations, and the forced and free responses evolved spatially

rather than in time. Apparently, the single-frequency, constant-amplitude acoustic excitation of Knapp and Roache also developed according to the spatial instability formulation, but involved furthermore the penetration and internalization problems. For these cases an initial-value problem in the streamwise direction x would be more appropriate although it is mathematically less well posed. (The handling of the downstream boundary conditions is not rigorous and remains ad hoc at this writing). Numerical experimentation on computers with either linearized or full Navier-Stokes equations, e.g. Fasel (1976), Fasel etal (1977) and Orszag (1979), suggests that additional insight into receptivity could be gained with this approach for two-dimensional and simple three-dimensional disturbances, given enough funds and computer capacity. The word experimentation is used on purpose to emphasize that one loses the generality of analysis and that there are also problems of resolution and convergence. On the other hand nonlinearity can be handled. At this writing, however, no published contributions to the receptivity problem have appeared based on the spatial initial value problem.

d. Issues in Spatial and Temporal Growths in Normal-Modes Techniques

In principle, the temporal or spatial initial value problems can provide a quantitative sequential link between the internalized initial disturbances and the free normal modes which ultimately dominate the unstable motion. However, most linear instability analyses merely assume exponential temporal or spatial growths of normal modes of specific functional form and focus on the analytic-numerical problem of determining the eigenvalues and some typical eigenfunctions. Again the assumed temporal or spatial formulation may not fit the physics of the problem and may lead to serious difficulties in interpretation. Thus, in our first example of receptivity, the streamwise Görtler vortex instability was originally assumed to grow as $\exp\beta t$, while Bippes (1972) and others find only growth in x. For Tollmien-Schlichting propagating instabilities Gaster's transformations establish a direct link between spatial and temporal growth of the normal modes which is valid for relatively slow amplification rates in non-decelerating quasi-parallel boundary layers, Gaster (1962).

For a system to be capable of both exponential growth in t and x, implicit in the Gaster transformation, the linearized stability equations

must have coefficients independent of both t and x, i.e. they should correspond to a strictly steady and parallel base flow of infinite extent. For slowly growing boundary layers the slow x variation leads to second-order corrections which do not vitiate the physical interpretation. For non-parallel base flows with rapidly converging or diverging streamlines, such as our flow toward the stagnation line, the exponential disturbance growth in the streamwise direction is precluded by the variable coefficients in the governing equations. Since the coefficients remain constant in t, the $\exp\beta t$ factor for the solutions is available - and used by default. Its meaning deserves careful scrutiny.

For quasi-parallel boundary - layer instabilities of the TS and Görtler type, the eigenvalue problems develop in the cross-stream y direction. Free-stream vorticity and entropy disturbances travel along mean streamlines of the base flow and influence the fluctuations within the shear layer either by vortical Biot-Savart induction across streamlines or by slow penetration along with the external streamlines because of the departure from strict parallelism. (Acoustic disturbances, of course, can always propagate across streamlines).

e. Some Special Features of the Eigenvalue Problem for Stagnation Flows

Here again the contrast with the stagnation flow near the plane of symmetry x - 0 in Fig. 1 is striking. All vorticity and entropy disturbances are directly convected into the region of presumed instability. Furthermore, unlike in the boundary-layer cases, they are subjected to a known straining field (due to the base flow) during this convection. This means that forced response of the flow to upstream disturbances should be easier to calculate. However, the singular fact that the independent variable y or η in the eigenvalue problem is here in the direction of the stream and thus ties together the whole upstream history of the flow suggests that the physics of the eigenrelations is basically different. Geometrically, this is associated with the streamline bifurcation and the 90% turn at the stagnation line, not present for other instabilities.

Sensing the peculiarity of the variable, Wilson and Gladwell (1978) argue on p. 517 that "the instability, if any, is the centrifugal instability" which can take place only as the concave streamlines reach the vortical region of the base flow, i.e. the viscous layer. They believe that the upstream influence (working against the inflow) of a mechanism

confined to the viscous layer should be dying out exponentially and thereby they change the character of the eigenvalue problem.

Wilson and Gladwell consider the possible role of free-stream disturbances and the effect of the upstream straining only in their closing remarks and negatively so. A major part of their argument is based on direct misreading of the German text of Hassler (1971) and Čolak-Antić (1971). Their experiments did not have "exceedingly small free-stream vorticity" because they towed a turbulence-generating grid ahead of their cylinder in the otherwise quiet water tank. The reported measured intensity is 0.85%, i.e. substantial enough to be dominant in other instabilities. The other part of the Wilson-Gladwell reasoning is taken up in the final discussion of the phenomenon.

f. Reflections on Receptivity to Turbulence Leading beyond Initial Value Problems

Since time and again interpretation of instability experiments hinges on the role of free-stream turbulence, it is worth-while to reflect on the nature of such turbulence and on how the inherent variability of its local intensity and scale may interact with potentially exponential responses in shear layers. It appears likely to this observer that receptivity to free-stream turbulence involves a problem more complex than can be handled by either of the initial value problem formulations. Already the first experiments on TS waves, those of Schubauer and Skramstad (1947), disclosed that free-stream turbulence elicits modulated wave-packet response in boundary layers. Free-stream turbulence in uniform flows is a decaying field, spotty in space and time (and only nominally isotropic and homogeneous when time or ensemble averaged). Especially in the latter stages of decay, there are sporadic occurrences of higher-amplitude events and of patches with different scales, occasionally referred to as inner intermittency. A boundary-layer response in the form of finite TS wave packets is therefore consistent with such spotty, time-modulated, three dimensional, forcing disturbances. Within a given wave packet there is energy transfer in space and time. Because of this energy sharing the primary packets induced in the upstream region of a growing boundary layer by a spotty sporadic vorticity formation as it is convected downstream near and within the boundary layer will probably have to be characterized by a finite spacetime domain, Δx, Δz, Δt.

We note that information on temporal averages of free-stream turbulence or even on its three-dimensional spectra (if obtainable) would be of little help for the above picture of response to weak turbulence. Rather, for fundamental studies of receptivity at least two-probe, space-time correlations of the exciting and response signals are indicated.

g. Apparent Consequences of Substantial Amplitude Variations in x and t: Gaster Experiments

The exploration by Gaster and Grant (1975) of simpler wave packets generated by sudden puffs through a small hole in a plate supporting a growing Blasius boundary layer and its theoretical modeling, Gaster (1975), taught us much about the linearized development of three-dimensional TS wave packets. It appears now, Gaster (1978) (subject to Gen. Reshotko 4), that the finiteness of the wave packet in $\Delta x, \Delta z, \Delta t$, brings about "dramatically" different nonlinear development and an earlier secondary instability (also called breakdown of TS waves). This comes from comparisons of the behavior of the wave excited by the sudden puffs and those excited by "continuous puffing" through the same hole at the central frequency f_m of the pulsed wave packets. Strictly speaking this is not a receptivity effect, because the linear development (which is present because the disturbance is linearizably small) is modeled satisfactorily. However the effect warns us that there may be dangers of misinterpretation when we use the otherwise attractive procedure of studying responses to single-frequency normal modes.

h. Subcritical Instability, Threshold Phenomena and Receptivity: The Duct-Flow Case

When the environment disturbances are larger and involve some nonlinear processes the problem of receptivity gets even more complicated. It is likely that the cited $2f_2$ frequency response of the boundary layer of Knapp and Roache to a forcing acoustic disturbance f_2 resulted from nonlinearity in the sound. The harmonic $2f_2$ component may have been hidden in the background noise and yet brought out by the exponential amplification of the TS mechanism. Analysis of weakly nonlinear, slightly stable systems, e.g. Stuart (1971) p. 359, shows that "nonlinear effects may permit the existence of a threshold amplitude" above which instability can grow even though the system parameter is below the critical value for

linear (infinitesimal) instability.

Hard evidence of such subcritical instabilities may elude our measuring instruments especially if it develops temporally in a truly parallel flow. For instance it has been stated in numerous papers that TS waves in two-dimensional Poseuille flow cannot be observed because the growth of the instability would be so rapid that only the final turbulent state of equilibrium would be ascertainable. And indeed for more than half a century no investigator was successful in preventing transition to turbulence above 60 to 90 percent of the infinitesimal critical Reynolds number, - until Nishioka, Iida, and Ichikawa (1975) brought down their free-stream turbulence to approximately 0.01% and maintained laminar flow beyond Re_{cr}, see Morkovin (1978, pp 7-9) for discussion of the issues . By introducing controlled, nearly two-dimensional disturbances through a vibrating ribbon, Nishioka etal also set the stage for a spatially growing initial value problem and demonstrated the spatial subcritical threshold behavior of their TS waves. It is instructive with respect to the character and role of disturbances that Karnitz, Potter and Smith (1974) were able to reach only 0.87% of Re_{cr} with free-stream disturbances of approximately 0.3% and reported privately that any loud voices or even finger snapping near the Poiseuille duct would switch the flow from laminar to turbulent near that Reynolds number. Theory has established that this flow exhibits subcritical bifurcation so that we are forewarned in our interpretations of the influences of disturbances. But what about interpretation of behavior in presence of disturbances in systems that have not been adjudged subcritically unstable? Or by observers who are not familiar with the peculiarities of nonlinear instability?

i. Diagnostics, Thresholds, and Visualization Evidence

The awareness of the possiblility of threshold phenomena is an essential ingredient of diagnostics of instabilities. The willingness and capability of devising deliberate perturbations (the general "spoiler" technique, Morkovin 1969) is another mainstay of instability diagnostics. From such explorations by Hodson and Nagib (1975) it appears that the stagnation flow does show threshold behavior with respect to steady low-Reynolds number disturbances, see Section 3d and 3e.

An important question with respect to diagnostics relying on visualization techniques is their capability of resolving disturbances in their

linearizable stages. General information from hot-wire anemometry, primarily for TS type instabilities, suggests that velocity fluctuations below approximately 1% of local maximum velocity exhibit behavior consistent with linearized equations, e.g. apparent local exponential growth, absence of higher harmonics (within resolution of instrument), independent superposability of disturbances with different frequencies, no threshold with respect to subsequent stabilization etc. With care and know-how, monochromatic fluctuation amplitude of the streamwise velocity component can be measured quite reliably to 0.01% of the local maximum velocity so that the 1% estimate cannot be grossly in error and certainly is not on the order of 3%.

Comparison of various visual indications of spatially growing narrow-band TS type waves with hot-wire traverses of the same controlled fields lead one to conclude that visualization almost surely does not resolve the fluctuations in their linearizable stage.* The conclusion is reinforced by studying Bippes' 1972 stereographic measurements of steady Görtler vorticies growing in x. The implication of these considerations is that when using visualization diagnostics we should be conscious that we are probably seeing only the nonlinear regimes, and that a threshold phenomenon may have taken place. Generally, then, we should distinguish between linear receptivity following a threshold jump when making our diagnoses.

* Actually the issue is sufficiently important in diagnostics to warrant quantitative research for the several visualization techniques: smoke, hydrogen bubbles, thin oil films which indicate stress lines at the wall, evaporation and sublimation techniques. It is possible that steady streamwise vortices may be disclosed in their linear stages by the cumulative effect of evaporation and sublimation over sufficiently long time periods.

APPENDIX 2

ON VORTICITY AND PRESSURE RELATIONS

For "incompressible" flows with constant viscosity but variable (for instance stratified) density, application of the skew curl operation to the Navier-Stokes momentum equation, $\underline{\nabla} \times \underline{M}$, leads to an equivalent of a local angular momentum equation, expressed in terms of vorticity $\underline{\nabla} \times \underline{u} = \underline{\omega}$

$$\frac{D(\underline{\omega}/\rho)}{Dt} - \frac{\nu}{\rho} \nabla^2 \underline{\omega} = \frac{\underline{\omega}}{\rho} \cdot \underline{\nabla}\,\underline{u} - \frac{1}{\rho}\,\underline{\nabla}\left(\frac{1}{\rho}\right) \times \underline{\nabla}\, p \ . \qquad \text{(A2-1)}$$

This skew operation is said to decouple vorticity from its companion, the pressure, which in the momentum equation appears as $\underline{\nabla} p$, i.e. operated upon by a symmetric operation.

When we use the symmetric divergence operator on the Navier-Stokes momentum equation, $\underline{\nabla} \cdot \underline{M}$, we banish skew entities by virtue of $\underline{\nabla} \cdot \underline{\omega} = 0$ and arrive at the pressure equation, companion of the vorticity equation (A2-1) (now with density constant)

$$-\nabla^2 p = \sum_i \sum_j \frac{\partial^2 u_i u_j}{\partial x_i \partial x_j} = \sum_i \sum_j \frac{\partial u_i}{\partial x_j} \frac{\partial u_j}{\partial x_i} \ . \qquad \text{(A2-2)}$$

For compressible flows both the vorticity and the pressure equations get much more complicated, but only Equation (A2-2) changes its nature by becoming hyperbolic: the operator on the left hand side of the generalized equation (A2-2) becomes the wave operator $(1/a^2)(\partial^2 p/\partial t^2) - (\nabla^2 p)$, (e.g. Phillips, (1960)), where a^2 is the speed of sound squared. It is then possible to use the equation as a vehicle for analysis of aerodynamically generated sound, with the non-homogeneous right-hand-side terms of the wave equation interpreted as effective generators, attenuators, and redistributors of sound, generally called "sources". As a fluid becomes "more incompressible", its speed of sound, a , increases indefinitely and the hyperbolic wave operator reduces to Laplace's operator in Equation (A2-2). Thus for idealized incompressible fluids any pressure changes, however caused, act "instantaneously" at any distance and come back "instantaneously" from any "reflectors" in the field. This mutual instantaneous interaction within the whole field conveys one of the essential

properties of the resulting elliptic differential equation. Since it at times camouflages causes and effects, it is often helpful to think of slightly compressible fluids with large but finite speed of sound. The instantaneous action concept is also present in the Biot-Savart law of induction of velocity by a "source-like" vortex. Such action must in fact be transmitted "hand in hand with the companion agent, the pressure", and often it is useful to think of it as propagating at the speed of sound, e.g. for linearized supersonic flows.

The concept of sources comes from the fruitful study of linear differential equations with their right hand side given by the Diract delta or source function, such as

$$\frac{1}{a^2}\frac{\partial^2 p}{\partial t^2} - \nabla^2 p = \delta(\underline{x} - \underline{x}_0 \, , \, t - t_0) \, , \tag{A2-3}$$

$$\frac{\partial T}{\partial t} - \kappa \nabla^2 T = \delta(\underline{x} - \underline{x}_0 \, , \, t - t_0) \, . \tag{A2-4}$$

The latter equation is the familiar parabolic heat equation for non-deforming (stagnant) fluids or solids where κ stands for Kelvin's diffusivity or Maxwell's thermometric conductivity, e.g. Carslaw and Jaeger (1947), Chapter I. The inquisitive reader will also find a lucid presentation of the power of the source concept in Chapters X and XIII of Carslaw and Jaeger. For non-stagnant fluids, the local derivative operator $\partial/\partial t$ is replaced by the material derivative operator D/Dt so that the left-hand-side operator in the heat equation (A2-4) becomes identical with the operator in the vorticity equation (A2-1) if κ is replaced by ν, the kinematic viscosity.

It is instructive to linearize equation (A2-1) around a two-dimensional base flow $U_B(x,y), V_B(x,y), \Omega_{Bz}(x,y)$ for the x-perturbation component of vorticity ω_x and put it in the above form:

$$\frac{\partial \omega_x}{\partial t} + U_B\frac{\partial \omega_x}{\partial x} + V_B\frac{\partial \omega_x}{\partial y} - \nu\nabla^2\omega_x = \omega_x\frac{\partial U_B}{\partial x} + \omega_y\frac{\partial U_B}{\partial y} + \Omega_{Bz}\frac{\partial u}{\partial z} \tag{A2-5}$$

The intrinsically three-dimensional terms on the right-hand side thus act as effective sources of ω_x. The first term is the ω_x stretching source due to base-flow straining while the other two terms are due to rotation of ω_y and Ω_{Bz} onto the ω_x direction. These two terms, however, are automatically

zero for the outer Hiemenz flow where $\partial U_B / \partial y = \Omega_{Bz} = 0$. The two terms cancel each other exactly in the Görtler-Hämmerlin flow for which V_B and w remain independent of x. In these cases the vorticity stretching indeed dominates the behavior of ω_x.

APPENDIX 3

ON TURBULENCE CONCEPTS USEFUL

IN DIAGNOSTICS OF LAMINAR-TURBULENT TRANSITION

TURBULENCE implies spatially and temporally irregular nonlinear three-dimensional vortical motion resulting in transport of momentum (heat or mass) much larger than that due to molecular processes in laminar motion at the same mean Reynolds number (Rayleigh number or Taylor number, etc.). For point measurements turbulent character implies continuous three-dimensional power spectra decaying monotonically past some characteristic wave number (frequency). Turbulence may be present locally within large-scale organized motions (nearly regular, nearly periodic).

TURBULENT-LAMINAR INTERFACES occur at sufficiently high Reynolds numbers as sharp gradients in flow characteristics between irrotational (exterior) flows and turbulent shear flows (jets, boundary layers, wakes, plumes, etc.); also between laminar shear flows with regular oriented vorticity and neighboring shear regions which had undergone transition to irregular three-dimensional vortical motion (boundary layers, pipe flows, Couette flows with counter-rotating cylinders, etc.).

TURBULENT SPOTS are formed through isolated localized fine-scale, higher-order-instability breakdowns of laminar shear flows. Through the ensuing turbulent-laminar interfaces turbulence spreads into adjacent laminar neighborhoods and is simultaneously convected with a "mean speed". In boundary layers "TRANSITION" begins at the upstream locations of the sporadically forming turbulent spots and ends where the spots have grown together leaving no laminar lacunas.

INTERMITTENCY refers to repeated crossings of laminar-turbulent interfaces at a fixed observer point. It is usually characterized by γ, the fractional time (between 0 and 1) of turbulent behavior at the point.

In TURBULENT BOUNDARY LAYERS identifiable violent motions called "bursts" erupt sporadically near the wall. A disproportionally large portion of turbulent energy and Reynolds stress is generated in the burst activity. Bursts do not take place in boundary layers below some still poorly defined Reynolds number $Re_{\theta\ min}$ depending on pressure gradient, three-dimensionality, etc.

Interfaces associated with turbulent boundary layers or spots at low Reynolds numbers (just past $Re_{\theta_{min}}$) are diffuse, and it is difficult to determine operationally whether a boundary layer is a laminar, randomly buffeted boundary layer or a self-sustaining turbulent boundary layer.

BUFFETED BOUNDARY LAYERS. When upstream turbulence impinges upon a boundary layer below $R_{\theta_{min}}$, the resulting motion has all the specified earmarks of turbulence, except that the scales of the motion exceed the boundary layer thickness. The mean gradients near the wall are then less steep than if the boundary layer itself was intrinsically turbulent. The transport of momentum (heat or mass) in such laminar buffeted boundary layers is therefore enhanced, i.e. more than if the boundary layer were not buffeted and less than if it were turbulent on its own scales. As the buffeted boundary layer grows, the transport of momentum (heat or mass) will increase as its own transition takes place. Laminar buffeted boundary layers occur frequently at leading edges of bodies and are of technological importance, e.g. in turbomachinery.

One can speculate that in high-speed Couette flow periodically oscillating Taylor cells with periodic instabilities in wall boundary layers or in shear layers between cells can also be buffeted by neighboring turbulent regions. Since turbulence sets in at discrete locations, coexistence of laminar and turbulent regions should be expected. The temporal spectrum in such a doubly periodic cell near another partly turbulent cell would consist of two discrete lines plus a continuous spectrum as is observed.

APPENDIX 4

MISCELLANEOUS OBSERVATIONS ON THE GÖRTLER MODEL

Geometrical configurations often possess preferred vortical formations. Görtler's "spontaneous" pattern, Equations (11), or its forced counterpart (say, generated by weak merged wakes from the dotted grid in lower Figure 3) certainly describe a family behavior which is present in many physical situations but not necessarily all. Kayalar (1969) proposed a different set of streamwise vortical patterns,without theoretical or experimental backing. Inger (1975) discussed another "forced disturbance model" of streamwise vortices, which may be too simplified, e.g. $V_1(\eta) = 0$, and saw little evidence for their existence. In this section, agreements on Görtler formations and the corresponding physical fields are reviewed in detail.

The Detailed Fields

The general flow pattern, though to second order in the small quantities, is represented in Figure 7 and upper Figure 20 according to Kestin and Wood (1970). The η variation of the perturbation velocity components and the pressure for $k = 2/3$ in Figure 17 was borrowed from Inger (1974) where additional profiles for $k = 0.2$, 0.5 and 1 , as well as for cases of very cold and very hot cylinder walls can be found. The lower part of Figure 20 for x = constant was constructed to show schematically the relation between the full flow streamlines in the upper part of Figure 20 and the linearized P_1, V_1, W_1, ω_1 profiles of Figure 17. The circles with + and - signs locate the local maxima and minima of the linear pressure perturbation with the ones near the wall being typically 4-6 times stronger than those near the edge of the boundary layer. The arrows show the relative magnitude of the physical perturbation velocity V_1 (which is opposite to V) according to Equation (11).

Nonlinearity

The W_1 field and the rotational patterns of lower Figure 20 are directly comparable with the upper figure, except for the second order effects present in the latter. However, for the full vertical-velocity and pressure picture we must superpose their counterparts on the base Hiemenz flow. The amplitudes of the linear eigensolutions in Figure 17 are arbitrary as long as they are "small". One could normally dare to assume ratios of maxima in the boundary layer of V_1/V_0 , P_1/P_0 , etc. to be on the order of 0.2 for the linear regime and up to 0.4 for second order analysis and still retain good pattern resemblance. However at the value of η corresponding to the free stagnation point in the Kestin-Wood upper Figure 20, where $\Phi_0 + V = 0$, $\Phi_0 \sim 5$ and therefore V is locally a rather massive "disturbance". That such large steady disturbances commonly occur in the real world has been shown by Hodson and Nagib (1975), e.g. upper Figure 5.

The Pressure Fields

The flow away from the pressure minima at $k\zeta = 0$ and 2π in lower Figure 20 could be puzzling until one makes some estimates of the Hiemenz pressure rise from the + circle to the - circle that must be superposed. According to Equation (6) this $\Delta p \sim \frac{1}{2}\rho V_0^2$ (at +) $= \frac{1}{2}\rho a \nu \Phi_0^2 (+)_1$. Because it takes a V perturbation of $|\Phi_0(+)| \sim 5$ to cause stagnation at the + circle, and because the largely viscous pressure perturbation P_1 is likely to remain nearly proportional to the first power of the velocity perturbation, this quadratic inertial pressure rise Φ_0^2 will surely make the full static pressure at the - circle larger than that at the + circle. The pressure at the + circle near the wall at $z = \lambda/2$ will then be the highest achieved stagnation pressure. The relative magnitudes of the stagnation pressures at the three stagnation points S_ℓ, S and S_f in upper Figure 20 should then be in the same descending order as at S_ℓ, S and S_f in lower Figure 3 discussed in connection with the threshold vortex appearance in Section 3e. In the linearized viscous solution (lower Figure 20), the local pressure minima seem to be induced by vortex associated entrainment (viscous pumping) away from the regions in question.

Does Vorticity ω_x Have a Zero?

According to lower Figure 20, the standing vortices have cores with solid body rotation as witnessed by the linear distribution of velocities from zero at their centers. But there are no pressure minima at these centers, as there would be in vortices resulting from roll up of thin vorticity sheets. It is a topological necessity for these vortices to induce W_1 velocities as shown, velocities which generate their own thin vorticity boundary layers at the wall of a sign necessarily opposite to that of the standing vortices. Thus the upper figure, borrowed from the 1970 paper of Kestin and Wood, demonstrates the impossibility of a key statement of theirs in the same paper, to the effect that ω_x does not change signs between $\eta = 0$ and $\eta \to \infty$ (we shall return to the implications of the statement in Section 7). All linear vorticity computations (including those of Kestin's coworkers Sutera (1965), Figure 4, and Williams (1968), Figure 11) disclose the sign reversal as in Figure 17 here, but the topological argument transcends linearity.

The Smallness and Limited "Reach" of U Fields

Thus with minor exceptions, there is a general accord on the consistency of the Görtler vorticity and velocity patterns and their occurrence in steady real flows, Hodson and Nagib (1975). All the computed perturbation profiles: Sutera (1965), Williams (1968), Inger (1974) and Tani (1974) also agree on the shapes of the profiles, their sign changes and on the smallness of the amplitude and the limited η extent of the U_1 perturbation (Figure 17). Sutera and Inger observe that U_1 acts as if it were decoupled from V_1

and W_1 . Since velocities in the y and z directions and the pressure in Görtler's model, Equations (11) are independent of x , the coupling of the U_1 equation with the others is solely through the convective derivative $V_1 \partial U_0/\partial y \sim -V_1 \Phi_0''$, which vanishes outside of the Hiemenz boundary layer near $\eta = 4$. Thus the U_1 equation is indeed independent of the rest, outside of the unperturbed boundary layer. Hämmerlin (1955) used that fact to start his asymptotic analysis. The single independent nondivergent asymptotic solution for the second order differential equation in U_1 has the leading term $Af(k)\exp\left[-\frac{(\eta - 0.648)^2}{2}\right] \cdot (\eta - 0.648)^{-(k^2+3)}$. The quadratic exponential decay signals the quenching of the coupling source. (A is one of the free coefficients of the linearly independent solutions discussed in Section 5 in connection with Hämmerlin's smooth matching of the regular inner solutions and the outer asymptotic solutions.) The extensive outer reach of V_1 and W_1 variations relative to that of U_1 underscores the inviscid nature of the basic amplifying processes (Equation (9), Section 5, or $-\omega_x \partial V/\partial y$): the U_1 component is stimulated only through the gradient $\partial U_0/\partial y$ which is generated within the viscous boundary layer.

Contrast with Görtler's Vortices on Concave Walls

In 1955, before computers could numerically experiment with complex equations and grind out results on which the present discussion is partly based, Görtler conjectured about the analogy between the vortices in the stagnation region and the "other" vortices bearing his name, arising in boundary layers on concave walls. The latter are driven by centrifugal instability, just like the famous Taylor vortices exterior to a rotating cylinder, whereas streamline divergence and adverse pressure gradients are essential here. It is unfortunate that this early conjecture is being perpetuated in widely used texts and reference books. The structure of the "other" Gortler vortices is vastly different. In particular the U_1 component, instead of being smaller than V_1 and W_1 by factors on the order 20 (for reasons already discussed) is orders of magnitude larger as pointed out by A.M.O. Smith (1955) and Betchov and Criminale (1967). In one case Smith computed the ratios U_{1max}/V_{1max} and U_{1max}/W_{1max} to be 285 and 667, respectively!

The Spanwise Flow Field

The dimensional steady-state velocity in the x direction, $ax\Phi_0'(\eta) + axU_1(\eta)\cos k\zeta$, also have x as coefficient, making the perturbation term still smaller in the region of validity of the approximation. The normal component of velocity, $-\sqrt{a\nu}\,(\Phi_0 + V_1 \cos k\zeta)$, grows only as η^2 from the wall because $V(0) = V'(0) = 0$. The spanwise component is by far the largest in the vicinity of the wall at $x = 0$. In other words, the solutions suggest that considerable velocity "can be generated along the

stagnation line toward S " despite the streamwise "leak" promoted by acceleration a_H (see the end of Section 3c) but that this motion does not build up a larger stagnation pressure p_S because of the viscous pumping effect near S . The streamline pattern near the stagnation line should therefore look as depicted in Figure 6 in Inger (1977).

The Temperature Field and its Limited "Reach"

The slow streamwise removal of matter from the stagnation region should also make the steady-flow heat transfer at the wall more limited than intuitive ideas comparing molecular "mixing lengths" of the undisturbed Hiemenz flow with the "vortex-size mixing lengths" of the perturbed flow would at first suggest. Insofar as the fluid churns without substantial streamwise motion the heated elements return to the wall decreasing the original ΔT between the fresh fluid and the wall and therefore the capacity for subsequent heat flow. In the steady nonlinear regime there is undoubtedly a much larger thermal boundary layer thickness than could be accommodated by the Hiemenz flow, but quasi-periodic nonlinear removal of heated matter from the region appears as an additional mechanism that could help to account for the observed effects as conjectured by Hodson and Nagib (1975) — see Section 6a and Figure 8.

If the dimensionless difference of temperature from its wall value is $\Delta T = \{T_\omega - T(\eta)\}/(T_\omega - T_\infty)$ and its linear perturbation is $\theta_1(\eta)$, the differential equation for the latter, in the Hiemenz flow, reads:

$$\theta_1'' + Pr\Phi_0\,\theta_1' - k^2\theta_1 = -Pr\Delta T'\,V_1$$

where Pr is the Prandtl number. Comparing this with Equation (13) for ω_x , we readily identify the thermal diffusion in η and ζ directions as θ_1'' and $-k^2\theta_1$ and the convective derivative $-V_0\,\partial\theta/\partial\eta$ as $Pr\Phi_0\,\theta_1'$. The source-like term on the right represents modifications of the otherwise stratified temperature by the cellular "mixing motion" V_1 and plays the role of the stretching term $-(\partial V_0/\partial\eta)\omega_1 = \Phi_0' \cdot \omega_1$ in Equation (13). Both $-\Delta T'V_1$ and its aforementioned counterpart in the U_1 equation, $-(\partial^2 U_0/\partial\eta^2)V_1$, vanish outside of the boundary layer whereas the stretching term continues to infinity as $+\omega_1$ in the Hiemenz flow. So like U_1 , θ_1 is decoupled from the inviscid amplified vortical motion outside of the boundary layer and for Prandtl numbers near unity, i.e. for most gases, has η profiles very similar to that of U_1 in Figure 17. Typical profiles of linearized temperature perturbations can be found in Sutera (1965), Figure 9, and Williams (1968), Figure 16. The isotherms of the combined mean and perturbation field are essentially cosine like with higher temperatures occurring at $z = 0$ and λ , where the perturbed flow is away from the wall (i.e. something like the V curve itself in lower Figure 20, but less exaggerated). The isotherms are straight at the wall because of the constancy of temperature imposed by the authors as boundary condition and again past η of

4, the edge of the thermal diffusion from the wall in the V counterflow. They are the waviest near $\eta \sim 1.2 - 1.4$, the maximum of the θ_1 profile.

Computer Differences? Guideline No. 4

In the preceding section we relied heavily on computers to elicit the general properties and features of the velocity, pressure, and temperature fields. But computing is still an art rather than science in complex instability problems. Could differences in computational details and errors due to approximations be also amplified? Comparison of the results of Sutera (1965), his Figure 4, and Inger (1974), our Figure17, indicate substantial differences in relative variations for the one case computed by independent programs: $k = 2/3$. (Inger actually used a compressible code, but the results in Figure 17 are for $\Delta T = 0$, $\Delta\rho = \Delta\mu = 0$, and yield the same Hiemenz base flow as a check.) Sutera's maximum of V_1 and zero of W_1 (vortex center height) are located at $\eta \sim 2.4$, while Inger's are at $\eta \sim 3.0$. From its maximum at $\eta = 2.4$ to $\eta = 8.5$, Sutera's V_1 drops by a factor of 5 while Inger's V_1 drops only by a factor of 2 between $\eta = 3$ and 9 . The ratio of the negative inner maximum of W_1 to its positive outer maximum (Figure 17) is approximately 2.7 for Sutera and 4.6+ for Inger. It seems that we can trust the general features discussed in the preceding section but not necessarily the magnitudes.

It is not clear whether the differences creep in from error amplification, from handling of the conditions at "computer infinity" or from other causes.

The Condition at Infinity: Reprise

To start his integration toward the wall from a finite η , Inger uses asymptotic solutions which insure $V_1(\infty) = 0$. Sutera like all the Brown University investigators formally asks that $V_1'(\infty) = V_1''(\infty)$ etc. $\to 0$ as $\eta \to \infty$ and speaks only of boundedness of V_1 at large η not of vanishing of V_1 . The details of his procedure are not clear nor is it clear whether he agrees with the analysis of Hämmerlin (1955) which indicates that for $k < 1$, $V_1'(\infty) \to 0$ implies $V_1(\infty) \to 0$ as Görtler (1955) pointed out — see Section 5h. All these investigations deal with Hiemenz base flow. For non-Hiemenz outer flow, $V_1'(\infty) \to 0$ would not necessarily imply $V_1(\infty) \to 0$ as mentioned in Section 5.

Tani and Iida, as reported by Tani (1974), make an explicit statement that the condition $V_1 \to 0$ as $\eta \to \infty$ is incompatible with their differential equations which generalize the Görtler-Hämmerlin system in several respects. First a circular cylinder is considered (with allowance for the wake) by introducing cylindrical coordinates and obtaining the factor $(1+\sqrt{\nu/a}\,\eta/R)^{-1}$, which modifies the limit of V_0 as $\eta \to \infty$, see Equation (5) in Section 2d. Since for large η , $\Phi_0 \sim \eta - 0.648$, $V_0 \to -aR = 1.765\, V_\infty$ (rather than ∞ or V_∞) as $\eta \to \infty$. Tani and Iida also account for the second-order boundary-layer

effects of nonzero curvature and for displacement thickness. The detailed equations are not shown in Tani (1974) but it is likely that the first effect is the governing one as regards the approach to infinity. The same modifying coordinate factor of Equation (9) is present in the definitions of the perturbations V_1 and W_1.

Flow Fields for Decreasing k -- More Computer Differences?

Tani and Iida's 1974 non-Hiemenzian system included a mixture of first-order and higher-order terms, which presumably caused $V_1(\infty)$ to be a nonvanishing constant dependent on the wave number k. The smallest $V_1(\infty)$ occurred for $k=0.35$, corresponding to a longer wavelength $\lambda = 2\pi/0.35\sqrt{\nu/a} = 27.70\,\delta^* \sim 7.49\,\delta$. Thus each vortex cell is just less than four Hiemenz boundary layer thicknesses wide. The corresponding η profiles in Figure 18 indicate the location of the linearized vortex center to be near η of 4.5 or almost two boundary-layer thicknesses out. It is curious that Inger's adiabatic solutions with Hiemenz base flow (which have $V_1(\infty) \to 0$) for the sequence $k = 1.0,\ 0.667,\ 0.5,\ 0.2$ show no outward shift of the vortex centers. The one striking trend in Inger's sequence is the strong relative decrease of V_1 with respect to W_1 as k decreases. In fact his V_1 vanishes for all practical purposes at four Hiemenz boundary layer thicknesses from the wall for $k = 0.2$: according to him, longer wavelengths flatten out the motion and inhibit the normal velocity perturbations. Tani and Iida's solutions in Figure 18 ($V_1(\infty) = \min \neq 0$, curvature taken into account, etc.) appear then quite different, in particular in regard to the vigorous V_1 motion relative to the W_1 motion for such a relatively long wavelength.

Iida (1978a) systematically sorted out the orders of magnitudes in the Tani-Iida model in preparation for his weakly nonlinear treatment (1978b). To the first order ($O(A\cdot\varepsilon^0)$, in Iida's notation), Hämmerlin results of Section 5h were recovered. The only first-order profile printed in Iida's paper is for $k = 0.5$, so that a direct comparison with Fig 18 to observe the differences is not possible. However, comparison with Inger's 1974 $k = 0.5$ profiles reveals that Iida's results do not follow Inger's trend described above. In fact, Iida's ratio $V_1\max/W_1\max$ exceeds two, just as in Fig 18, whereas Inger's falls below 0.5!

The Hainzl-Hämmerlin Contradiction and Possible Resolution

One more clue for the far-field near-field relationship, $\beta = 0$, should be mentioned, especially since it seems to have been forgotten. Görtler was well aware of the basic difficulties brought on by the parameterless, unbounded Hiemenz base flow. At his instigation Hainzl (1965) turned to a circular cylinder and first found "a new rigorous solution of the steady Navier-Stokes equations as a replacement for the Hiemenz flow". Physically, Hainzl's new base flow, see Fig 19, represents an incompressible field induced by applying infinite suction along the rear stagnation line. If the $\eta = \sqrt{\nu/a}\,y$ magnification were applied, this flow could not be distinguished from Hiemenz', in rectangular coordinates fitted to the front stagnation line, and presumably from that of Tani and Iida in cylindrical coordinates for which V_0 is given by Equation (9). In

1968, Görtler privately described the situation as puzzling,

One can surmise that the puzzle centers on the asymptotic behavior of the stream function in the limits $\eta \to \infty$ and $y \to \infty$. Neglecting the displacement effect for the limiting processes to follow Hainzl's stream function (Equation (5)) for $y > 4\sqrt{\nu/a}$, i.e. beyond the boundary layer thickness δ ,is

$$\Phi_H(\eta) = \ln\left(1 + \frac{y}{R}\right) = \ln\left(1 + \sqrt{\frac{\nu}{a}}\frac{\eta}{R}\right) . \qquad (15)$$

For y values large with respect to δ but small with respect to R , $\Phi_H \sim y/R = \sqrt{\nu/a}\,\eta/R \sim \Phi_0$ of Hiemenz. The corresponding expression for the base velocity V_0 beyond the boundary layer is according to Equation (9) $V_{0H} = -\sqrt{a\nu}\left[\ln(1+y/R)\right](1+y/R)^{-1}$ which in the intermediate limit $\sim -\sqrt{a\nu}\,\Phi_0(\eta)(1+\sqrt{\nu/a}\,\eta/R)^{-1}$, the Tani-Iida expression. As η grows large, the latter approaches $-aR$, not V_∞ , when the Hiemenz approximation is imbedded in a potential flow with uniform upstream V_∞ , nor zero, the correct y limit of V_{0H} when the Hiemenz flow is imbedded in Hainzl's new field solution. In the light of our discussion in Section 5c of the vorticity amplification source $-\omega_x\,\partial V_0/\partial y$ there is ample opportunity for differences in results depending on which limit is taken and how carefully any matching of functions is performed. In Hainzl's case, vorticity disturbances oncoming from large y are first inviscidly depressed (cf narrowing of stream tubes coming from far upstream in Figure 19) as well as depleted by diffusion. Only for y/R of less than 0.5 or so (in the θ wedge of convergence of the perturbation equations) is there inviscid amplification. How far does $\eta \to \infty$ really extend when the Hiemenz flow is analytically contained in a given external flow, such as that of Hainzl, and one is using a computer? The puzzle could be explained if Hämmerlin (1955) worked within the limit of the inviscidly amplifying region near the cylinder and Hainzl apparently beyond it for his base flow.

REFERENCES

Bearman, P.W. (1972): Some Measurements of the Distortion of Turbulence Approaching a Two-Dimensional Bluff Body, J. Fluid Mech., Vol. 53, p. 451. See also AGARD Conf. Proc. CP-93, 1971 and references therein to other shapes.

Betchov, R. and Criminale, W.O. Jr. (1967): Stability of Parallel Flows. Academic Press.

Bippes, H. (1972): Experimentelle Untersuchung des laminar-turbulenten Umschlags an einer parallel angestromten konkaven Wand, Sitzungsber. Heidelberger Akad, der Wissensch. Math-naturwissen, Klasse, 1972, 3Abh. Springer Verlag, Also NASA Tech. Transl. TM-75243, 1978.

Bradshaw, P. (1965): The Effect of Wind-Tunnel Screens on Nominally Two-Dimensional Boundary Layers, J. Fluid Mech., Vol. 22, p. 679.

Bradshaw, P. (1966): The Effect of Initial Conditions on the Development of a Free Shear Layer, J. Fluid Mech., Vol. 26, p. 225.

Bradshaw, P. (1969): The Analogy Between Streamline Curvature and Buoyancy in Turbulent Shear Flow, J. Fluid Mech., Vol. 36, No. 1, pp. 177-191.

Brun, E.A., Diep, G.B. and Kestin, J. (1966): Sur un Nouveau Type de Tourbillons Longitudinaux dans l'Ecoulement autour d'un Cylindre (On a New Type of Longitudinal Vortices in the Flow around a Cylinder). C.R. Acad. Sci. Paris, Vol. 263, pp. 742-745.

Burkhalter, J.E. and Koschmieder, E.L. (1974): Steady Supercritical Taylor Vortices after Sudden Starts, Phys. Fluids, Vol. 17, pp. 1929-1935.

Burkhalter, J.E. and Koschmieder, E.L. (1973): Steady Supercritical Taylor Vortex Flow, J. Fluid Mech., Vol. 58, pp. 547-560.

Carslaw, H.S. and Jaeger, J.C. (1947): Conduction of Heat in Solids, Oxford Univ. Press, London.

Čolak-Antić, P. (1971): Visuelle Untersuchungen von Langswirbeln im Staupunktgebiet eines Kreiszylinders bei turbulenter Anströmung (Visual Investigations of Longitudinal Vortices in the Stagnation Region of a Circular Cylinder Exposed to a Turbulent Stream), DLR Mitteilung 71-13, Bericht über die DGLR-Fachausschuss-Sitzung "Laminare and Turbulente Grenzschichtung (Report on the DGLR-Specialist Session: "Laminar and Turbulent Boundary Layers"), Göttingen, pp. 194-220.

Cole, J. (1968): Perturbation Methods in Applied Mathematics, Blaisdell Publ. Co. (Div. Ginn & Co.)

Cole, J.A. (1974): Taylor Vortices with Short Rotating Cylinders, J. Fluids Engin., Vol. 96, pp. 69-70.

Cole, J.A. (1976): Taylor-Vortex Instability and Annulus-Length Effects, J. Fluid Mech. Vol. 75, pp. 1-15.

Coles, D. and Van Atta, C. (1966): Measured Distortion of a Laminar Circular Couette Flow by End Effects, J. Fluid Mech., Vol. 25, pp. 513-519.

Corrsin, S. (1960): Turbulence: Experimental Methods, Handbuch der Physik, Vol. VIII/2, Springer Publ.

DiPrima, R.C. and Stuart, J.T. (1972): Non-Local Effects in the Stability of Flow between Eccentric Rotating Cylinders, J. Fluid Mech., Vol 54,pp 393-415

Fasel, H. (1977): Investigation of the Stability of Boundary Layers by Finite-Difference Model of the Navier-Stokes Equations, J. Fluid Mech,Vol. 78, pp. 355 - .

Fasel, H., Bestek, H. and Schefenacker, R. (1977): Numerical Simulation Studies of Transition Phenomena in Incompressible, Two-Dimensional Flows, Symp. on Laminar-Turbulent Transition, AGARD Conf. Proc. AG-224, pp. 14-1 to 14-8.

Floryan, J.M. and Saric, W.S. (1979): Stability of Görtler Vortices in Boundary Layers with Suction, AIAA Paper 79-1497.

Gaster, M. (1962): A Note on the Relation between Temporally-Increasing and Spatially-Increasing Disturbances in Hydrodynamic Stability, J. Fluid Mech., Vol. 14, pp. 222-224.

Gaster, M. (1975): A Theoretical Model of a Wave Packet in the Boundary Layer on a Flat Plate, Proc. Roy. Soc. A., Vol. 347, pp. 271-289.

Gaster, M. (1978): The Physical Process Causing Breakdown to Turbulence, Proc. Twelfth Symposium on Naval Hydrodynamics, Washington, D. C.

Gaster, M. and Grant, I. (1975): An Experimental Investigation of the Formation and Development of a Wave Packet in a Laminar Boundary Layer, Proc. Roy. Soc. A., Vol. 347, pp. 253-269.

Ginoux, J.J. (1969): On Some Properties of Reattaching Laminar and Transitional High-Speed Flows, Von Karman Institute for Fluid Dynamics, Tech. Note No. 53, Brussels, Belgium.

Ginoux, J. (1971): Streamwise Vortices in Reattaching High-Speed Flows: Suggested Approach, AIAA Jour., Vol. 9, pp, 759-760 and references therein.

Goertler, H. (1940): Uber eine dreidimensionale Instabilität Laminarer Grenzschichten an Konkaven Wanden, Nachr, Akad, Wiss., Goettingen Math-Physik Vl. IIa, Math-Physik-Chem. Abt. 2, 1-26 (Translated "On the Three-Dimensional Instability of Laminar Boundary Layers on Concave Walls: NACA Tech. Memo. 1375, June 1954).

Görtler, H. (1955): Dreidimensionale Instabilität der ebenen Staupunktströmung gegenüber wirbelartigen Störungen (Three dimensional Instability of the Plane Stagnation Flow with Respect to Vortical Disturbances), Fünfzig Jahre Grenzschicht-forschung (Fifty Years of Boundary Layer Research), edited by H. Görtler and W. Tollmien, Vieweg and Sohn, Braunschweig, pp. 304-314.

Grant, H.L. and Nisbet, I.C.T. (1957): The Inhomogeneity of Grid Turbulence, J. Fluid Mech., Vol. 2, p. 263.

Hainzl, J. (1965): Zur Stabilitätstheorie der Staupunkt-strömung gegenüber Wirbelstörungen vom Taylor-Görtler Typ. (On the Stability of Stagnation Point Flow with Respect to Disturbances of the Taylor-Görtler Type), Deutsche Luft und Raumfahrt Rept. FB 65-64.

Hämmerlin, G. (1955): Zur Instabilitätstheorie der ebenen Staupunktströmung (On Instability Theory of Plane Stagnation Flow), Fünfzig Jahre Grenzschichtforschung (Fifty Years of Boundary Layer Theory), edited by H. Görtler and W. Tollmien, Wieweg and Sohn, Braunschweig, pp. 315-327.

Hassler, H, (1971): Hitzdrahtmessungen von langswirbelartigen Instabilitätserscheinungen im Staupunktgebiet eines Kreiszylinders in turbulenter Anströmung (Hot-Wire Measurements of Occurrence of Longitudinal Vortex Instability in the Stagnation Region of a Circular Cylinder), DLR Mitteilung 71-13, Bericht über die DGLR-Fachausschuss-Sitzung "Laminare and Turbulente Grenzschichtung (Report on the DGLR-Specialist Session: "Laminar and Turbulent Boundary Layers"), Göttingen, pp. 221-239.

Herbert, Th, (1976): On the Stability of the Boundary Layer along a Concave Wall, Archiw. Mech, Stosow., Vol. 28, pp. 1039-1055.

Hodson, P.R. and Nagib, H.M. (1975): Longitudinal Vortices Induced in a Stagnation Region by Wakes — Their Incipient Formation and Effects on Heat Transfer from Cylinders. NASA CR-152850.

Hoshizaki, H., Chou, Y.S., Kulgein, N.G., and Meyer, J.W.: Critical Review of Stagnation-Point Heat Transfer Theory, AF Flight Dyn. Lab. Rept., AFFDL-TR-75-85, Lockheed Palo Alto Res. Lab, 1975.

Hunt, J.C.R. (1973): A Theory of Turbulent Flow Around Two-Dimensional Bluff Bodies, J. Fluid Mech., Vol. 61, 1, pp. 625-706.

Iida, S.I. (1978a): Stability of a Two-Dimensional Stagnation Flow, Bull. Japan, Soc. Mech. Eng., Vol. 21, No. 153, pp. 431-438.

Iida, S.I. (1978b): Non-Linear Stability of a Two-Dimensional Stagnation Flow, Bull. Japan Soc. Mech. Eng., Vol. 21, No. 156, pp. 992-999.

Inger, G.R. (1974): Three-Dimensional Disturbances in Two-Dimensional Reattaching Flows. Virginia Poly. Inst. and State Univ. Rept. VPI-Aero-011, AFOSR TR-74-0610; shortened version in AGARD Conf. Rept. No. 168, 1975.

Inger, G.R. (1977): Three-Dimensional Heat and Mass Transfer Effects Across High-Speed Reattaching Flows, AIAA Jour. Vol. 15, pp. 383-389.

Joseph, D. (1974): Stability of Fluid Motions, Springer Publ., Berlin-Heidelberg-New York.

Joseph, D. (1979): Hydrodynamic Stability and Bifurcation, in Hydrodynamic Instabilities and the Transition to Turbulence, H.L. Swinney and J.P. Gollub, eds., Topics in Current Physics Series, Springer Publ.

Kayalar, L. (1969): Experimentelle und Theoretische Untersuchungen über den Einfluss des Turbulenzgrads auf den Wärmeubergang in der Umgebung des Staupunkts eines Kreiszylinders, (Experimental and Theoretical Investigation of the Influence of Turbulence Intensity on the Heat Transfer in the Vicinity of the Stagnation Line of a Circular Cylinder), Forschung Ingen. Wes, Vol. 35, pp. 157-167.

Kellogg, R.M. (1965): Evolution of a Spectral Local Disturbance in a Grid-Generated Turbulent Flow, Ph.D. Thesis, Dept. of Mechanics, The Johns Hopkins Univ.

Kestin, J. (1966): The Effect of Free-Stream Turbulence on Heat Transfer Rates, Advances in Heat Transfer, Vol. 3, editors, T.F. Irvine and J.P. Hartnett, Academic Press, with earlier references.

Kestin, J. and Wood, R.T. (1969): Enhancement of Stagnation-Line Heat Transfer by Turbulence, Progress in Heat and Mass Transfer (Eckert Volume), Vol. 2, pp. 249-253, based in fact on Wood's Ph.D. Thesis, Brown Univ., 1969.

Kestin, J. and Wood, R.T. (1970): On the Stability of Two-Dimensional Stagnation Flow, J. Fluid Mech., Vol. 44, pp. 461-479.

Klebanoff, P.S. and Tidstrom, K.D. (1958): Evolution of Amplified Waves Leading to Transition in a Boundary Layer with Zero Pressure Gradient, NASA TN D-195.

Knapp, C.F. and Roache, P.J. (1968): A Combined Visual and Hot-Wire Anemometer Investigation of Boundary-Layer Transition, AIAA Jour.Vol 6,pp 29-36.

Koschmieder, E.L. (1975): Effect of Finite Disturbances on Axisymmetric Taylor Vortex Flow, Phys, Fluids, Vol. 18, pp. 499-503.

Kovasznay, L.S.G. (1949): Hot-Wire Investigations of the Wake Behind Cylinders at Low Reynolds Numbers, Proc. Roy. Soc. A, Vol. 198, p. 174.

Kuethe, A.M., Willmarth, W.W., and Crocker, G.H. (1961): Turbulence Near the Stagnation Point of Blunt Bodies of Revolution, Heat Transfer and Fluid Mechanics Institute, p. 10. More detailed information in AFOSR TR60-65.

Lighthill, M.J. (1954): The Response of Laminar Skin Friction and Heat Transfer to Fluctuations in the Stream Velocity, Proc. Roy. Soc. Series A, Vol. 224, No. 1, pp. 1-23.

Loehrke, R.I. (1970): Stimulated Temperature and Velocity Disturbances in a Laminar Boundary Layer, PhD thesis, Mech. & Aerosp. Engin. Dept., Ill. Inst. Tech., available from University Microfilms, 300 N. Zeeb Rd., Ann Arbor, Mich., 48106.

Lowery, G.W. and Vachon, R.I. (1975): The Effect of Turbulence on Heat Transfer from Heated Cylinders, Intern. J. Heat & Mass Transfer, Vol. 18,pp.1229-42.

Mair, W.A. (1955): The Distribution of Pressure on an Aerofoil in a Stream with a Spanwise Velocity Gradient, Aeronaut. Quart., Vol. 6, p. 1.

Marris, A.W. (1963): The Generation of Secondary Vorticity in an Incompressible Fluid, J. Appl. Mech., Vol. 30, Trans. ASME Series E, pp. 525-531.

Miyazaki, H. and Sparrow, E.M, (1977): Analysis of Effects of Free-Stream Turbulence on Heat Transfer and Skin Friction, J. Heat Transfer, Trans. ASME, Series C , Vol. 99, pp. 614-619.

Morkovin, M.V. (1969): Critical Evaluation of Transition from Laminar to Turbulent Shear Layers with Emphasis on Hypersonically Traveling Bodies, USAF Rept. AFFDL-TR-68-149.

Morkovin, M.V. (1978): Instability, Transition to Turbulence and Predictability, AGARDograph AG-236, NATO, France.

Morkovin, M.V. (1979): Observations on Streamwise Vortices in Laminar and Turbulent Boundary Layers, NASA Contractor's Report CR 159061.

Nagib, H.M. and Hodson, P.R. (1977) Vortices Induced in Stagnation Region by Wakes; Aerodynamic Heating and Thermal Protection Systems, L. S. Fletcher, ed., Vol. 59, pp. 66-90, Progress in Aeronautics and Astronautics, AIAA.

Nishioka, M. and Sato, H. (1973): Measurements of Velocity Distributions in the Wake of a Circular Cylinder at Low Reynolds Numbers, J. Fluid Mech., Vol. 65, Part 1, pp. 97-112.

Norman, R.S, (1972): On Obstacle Generated Secondary Flows in Laminar Boundary Layers and Transition to Turbulence, PhD Thesis, MMAE Dept., Ill. Inst. Tech., available from University Microfilms, 300 N. Zeeb Rd., Ann Arbor, Mich. 48106.

Orszag, S.A. and Kells, L.C. (1979): Transition to Turbulence in Plane Poiseuille and Plane Couette Flow, accepted for J. Fluid Mech.

Phillips, O.M. (1960): On the Generation of Sound by Supersonic Turbulent Shear Layers, J. Fluid Mech., Vol. 9, p. 1.

Piercy, N.A.V. and Richardson, E.G. (1928): On the Flow of Air Adjacent to the Surface of an Aerofoil, Res. and Mem. No. 1224, British ARC.

Piercy, N.A.V. and Richardson, E.G. (1928): The Variation of Velocity Amplitude Close to the Surface of a Cylinder Moving Through a Viscous Fluid, Phil. Mag., Series 7, Vol. 6, pp. 970-977.

Piercy, N.A.V. and Richardson, E.G. (1930): The Turbulence in Front of a Body Moving through a Viscous Fluid, Phil. Mag., Series 7, Vol. 9, pp. 1038-1041.

Prandtl, L. (1932): Handbuch der Experimentalphysik, Vol. 4, 2, p. 83, Leipzig.

Reshotko, E. (1976): Boundary Layer Stability and Transition Annual Review of Fluid Mechanics, Vol. 8, pp. 311-350, Annual Reviews, Inc., Palo Alto,Cal.

Roadman, R. (1975); Flow Visualization Studies of the Vortex Flow Module in a Tow Tank, Bach. Sci. Thesis, MMAE Dept., Illinois Institute of Technology.

Sadeh, W.Z., Sutera, S.P. and Maeder, P.F. (1970a): Analysis of Vorticity Amplification in the Flow Approaching a Two-Dimensional Stagnation Point, Z. Angew. Math. Phys., Vol. 21, pp. 699-716.

Sadeh, W.Z., Sutera, S.P. and Maeder, P.F. (1970b): An Investigation of Vorticity Amplification in Stagnation Flow, Z. Angew. Math. Phys., Vol. 21, pp. 717-742.

Sadeh, W.Z., Brauer, H.J., and Garrison, J.A. (1977): Visualization Study of Vorticity Amplification in Stagnation Flow, Project SQUID Tech Rept. CSU-1-PU.

Sadeh, W.Z. and Brauer, H.J. (1978): A Visual Investigation of Turbulence in Stagnation Flow About a Circular Cylinder, NASA Contractor Rept CR 3019.

Schlichting, H. (1968): Boundary-Layer Theory (Translated by J. Kestin), Sixth ed., McGraw-Hill Book Co.

Schlichting, H. (1971): A Survey of Some Recent Research Investigations on Boundary Layers and Heat Transfer, J. Appl. Mech., Vol. 38, pp. 289-300.

Schubauer, G.B. and Skramstad, H.K. (1947): Laminar Boundary-Layer Oscillations and Stability of Laminar Flow, J. Aeron. Sci., Vol. 14, pp. 69-78.

Schuh, H. (1953): A New Method for Calculating Laminar Heat Transfer on Cylinders of Arbitrary Cross-Section and on Bodies of Revolution at Constant and Variable Wall Temperature, Kungl. Tekniska Högskolan, Tech. Note No. 33, Stockholm.

Schwind, R.G. (1962): The Three-Dimensional Boundary Layer Near a Strut (60° Wedge), Mass. Inst. Tech. Gas Turbine Lab. Rept. No. 67.

Smith, A.M.O. (1955): On the Growth of Taylor-Görtler Vortices along Highly Concave Flows, Quart. Appl. Math., Vol. 13, pp. 233-262.

Smith, M.C. and Kuethe, A.M. (1966): Effects of Turbulence on Laminar Skin Friction and Heat Transfer, Phys. Fluids, Vol. 9, No. 12, pp. 2337-2344, based partly on Smith's PH.D. Thesis, Univ. Mich. 1964: The Effect of Free-Stream Turbulence on the Laminar Boundary-Layer Heat Transfer of Flat Plates and Circular Cylinders, with a critique of earlier research.

Snyder, H.A. (1969): Wave-Number Selection at Finite Amplitude in Rotating Couette Flow, J. Fluid Mech., Vol. 35, pp. 273-298.

Stuart, J.T. (1963): Hydrodynamic Stability, Chapter IX of Laminar Boundary Layers, L. Rosenhead, editor. Oxford University Clarendon Press.

Stuart, J.T. (1971): Nonlinear Stability Theory, Annual Reviews of Fluid Mechanics, Vol. 3, pp. 347-370, Annual Reviews, Inc,, Palo Alto, Calif.

Stuart, J.T. (1977): Bifurcation Theory in Nonlinear Hydrodynamic Stability, pp. 127-147 in Applications of Bifurcation Theory, P.H. Rabinowitz, ed., Academic Press, Inc.

Stuart, J.T. and DiPrima, R.C. (1978): The Eckhaus and Benjamin-Feir Resonance Mechanisms, Proc. Roy. Soc. London A., Vol. 362, pp. 27-41.

Sutera, S.P., Maeder, P.F. and Kestin, J. (1963): On the Sensitivity of Heat Transfer in the Stagnation-Point Boundary Layer to Free-Stream Vorticity, J. Fluid Mech., Vol. 16, pp. 497-520.

Sutera, S.P. (1965): Vorticity Amplification in Stagnation-Point Flow and its Effect on Heat Transfer, J. Fluid Mech., Vol. 21, pp. 513-534.

Swigart, R.J. (1977): Effects of Vorticity Amplification in Two-Dimensional and Axisymmetric Stagnation-Point Flows, AIAA Paper 77-72.

Tani, I. (1962): Production of Longitudinal Vortices in the Boundary Layer along a Concave Wall, J. Geophys. Research, Vol. 67, pp. 3075-3080.

Tani, I. (1974): Streamwise Vortices in Stagnation Flow, Study Meeting on Approximate Solution of Nonlinear Equations of Continuum Mechanics, Kyoto Univ.

Tani, I. and Aihara, Y. (1969): Görtler Vortices and Boundary-Layer Transition, Zeit. f. Angew. Math. Phys., Vol. 20, pp. 609-618.

Thwaites, B. Editor (1960): Incompressible Aerodynamics, Oxford Clarendon Press, pp. 548-553.

Van Dyke, M. (1964): Perturbation Methods in Fluid Mechanics, Academic Press, N.Y.

Williams, G. (1968): Enhancement of Heat and Mass Transfer in a Stagnation Region by Free Stream Vorticity, Brown Univ. Rept. for USAF, issued as Rept. ARL 68-0022.

Wilson, S.D.R. and Gladwell, I. (1978): The Stability of a Two-Dimensional Stagnation Flow to Three-Dimensional Disturbances, J. Fluid Mech., Vol. 84, No. 3, pp. 517-527.

Wortmann, F.X. (1964): Experimentelle Untersuchungen Laminarer Grenzschichten bei instabiler Schichtung (Experimental Investigation of Laminar Boundary Layers with Unstable Distribution Profiles), Proc. XI Inter. Congress Appl. Mech., pp. 815-825.

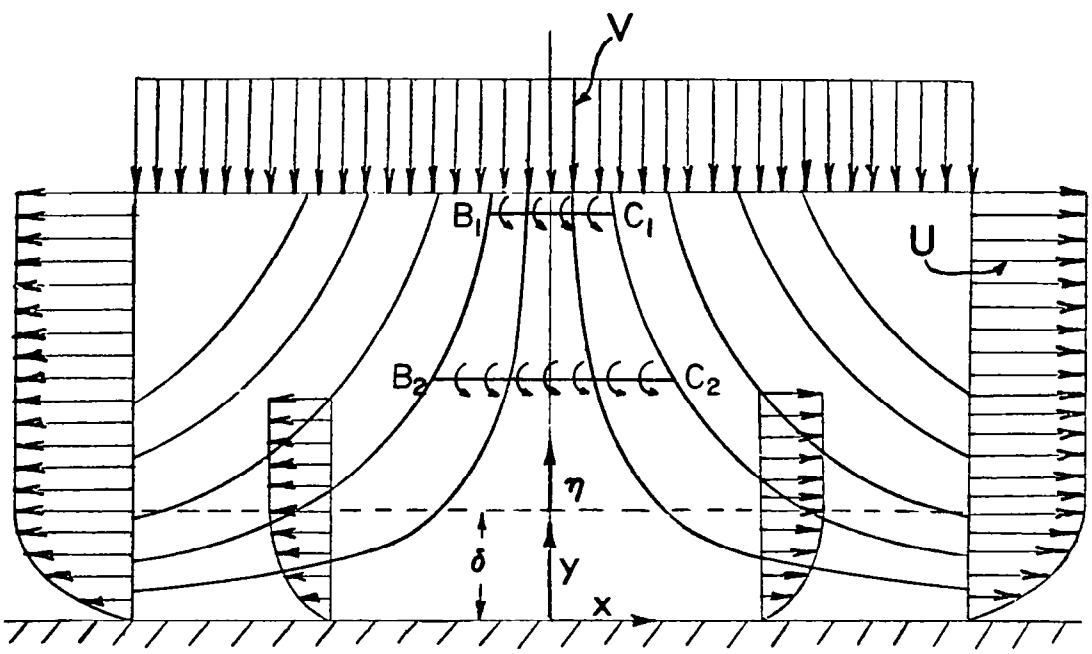

Figure 1. Hiemenz two-dimensional stagnation flow. (After Schlichting,1968.)

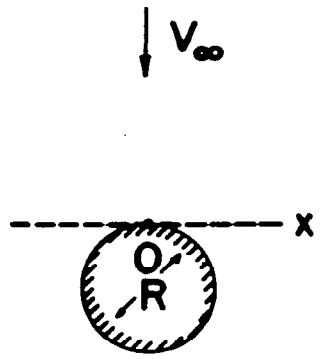

$$U - iV = iV_\infty\left(1 + \frac{R^2}{(Z+iR)^2}\right)$$

$$= V_\infty\left(2\frac{Z}{R} + 3i\frac{Z^2}{R^2} - 4\frac{Z^3}{R^3} + \cdots\right)$$

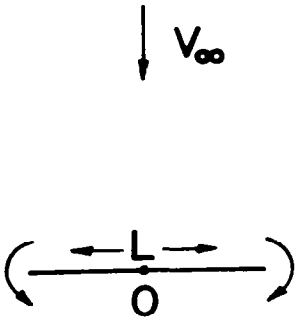

$$U - iV = \frac{V_\infty Z}{\sqrt{L^2 - Z^2}}$$

$$= \frac{V_\infty}{L} Z\left(1 + \frac{1}{2}\left(\frac{Z}{L}\right)^2 + \frac{3}{8}\left(\frac{Z}{L}\right)^4 + \cdots\right)$$

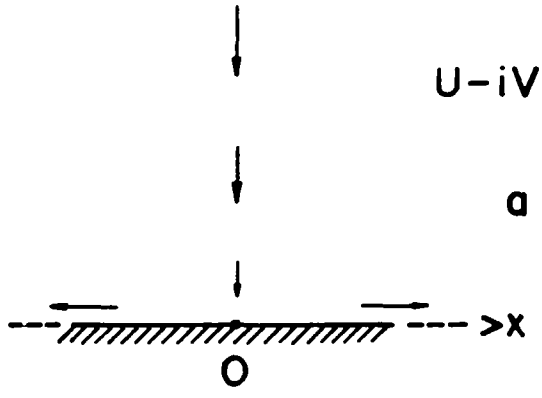

$$U - iV = aZ = a(x + iy')$$

$$a = \left(\frac{\partial U}{\partial x}\right)_0 = \left(\frac{\partial V}{\partial y}\right)_0$$

Figure 2. Examples of imbedding of Hiemenz flow in outer irrotational flows which provide a characteristic length.

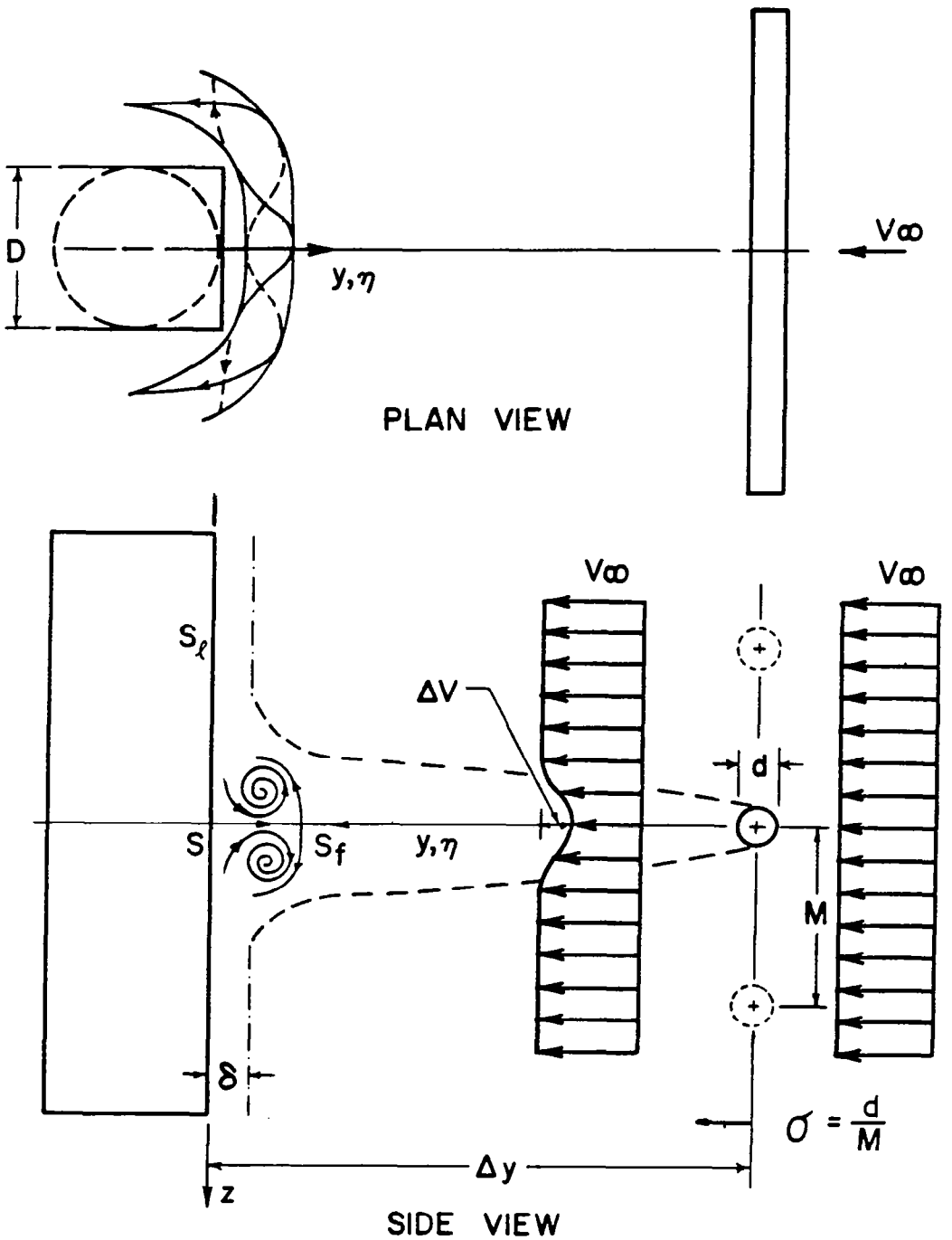

Figure 3. Schematic of counterflow vortex formation due to impingement of steady wakes of "rods" on stagnation region of bluff bodies. (Courtesy of Hodson and Nagib, 1975.)

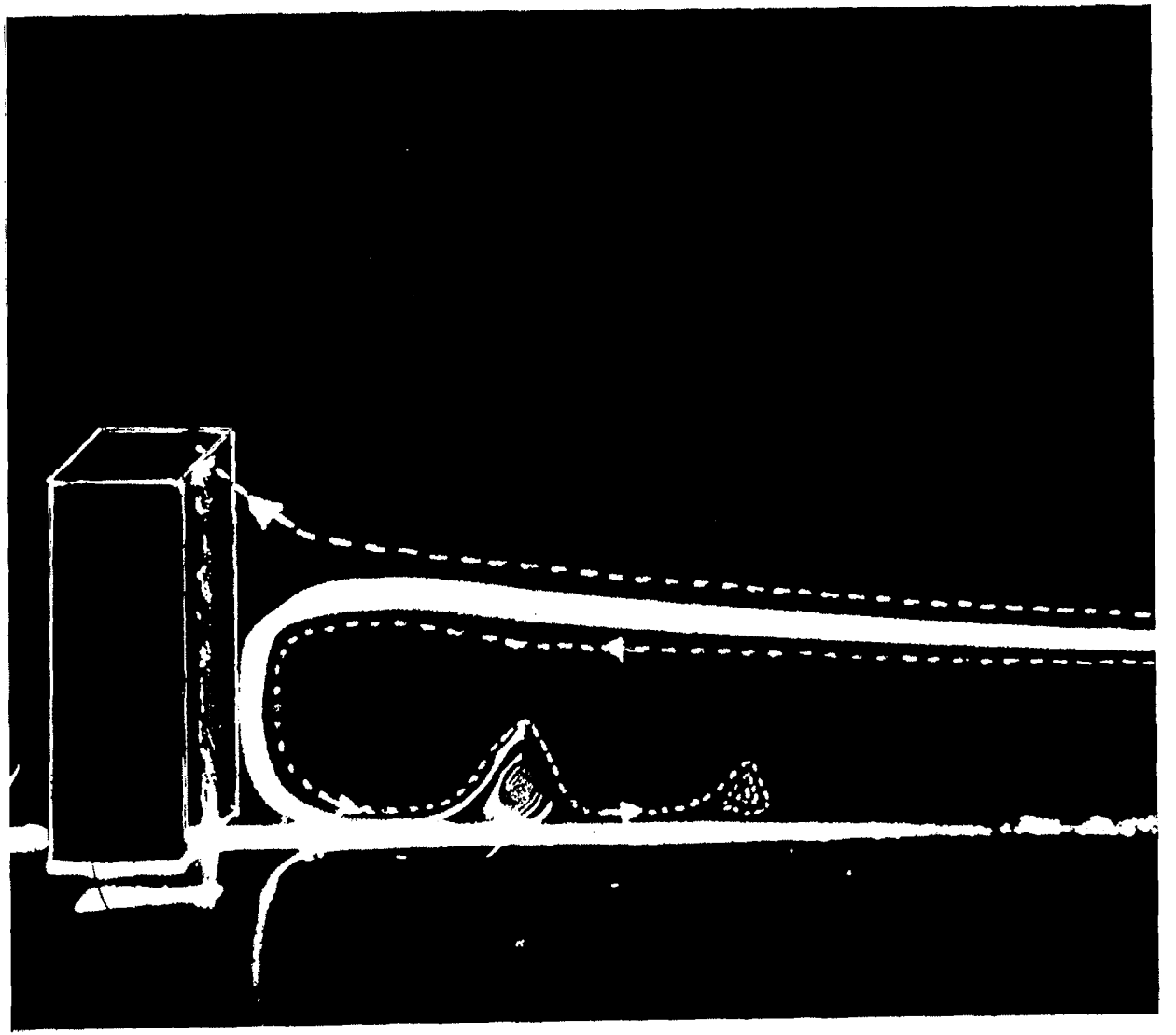

Figure 4. Centerplane smoke visualization of three outer streamlines in counterflow vortex formations caused by placing a prismatic obstacle in a laminar wall boundary layer. (Courtesy of R. Norman, 1972.)

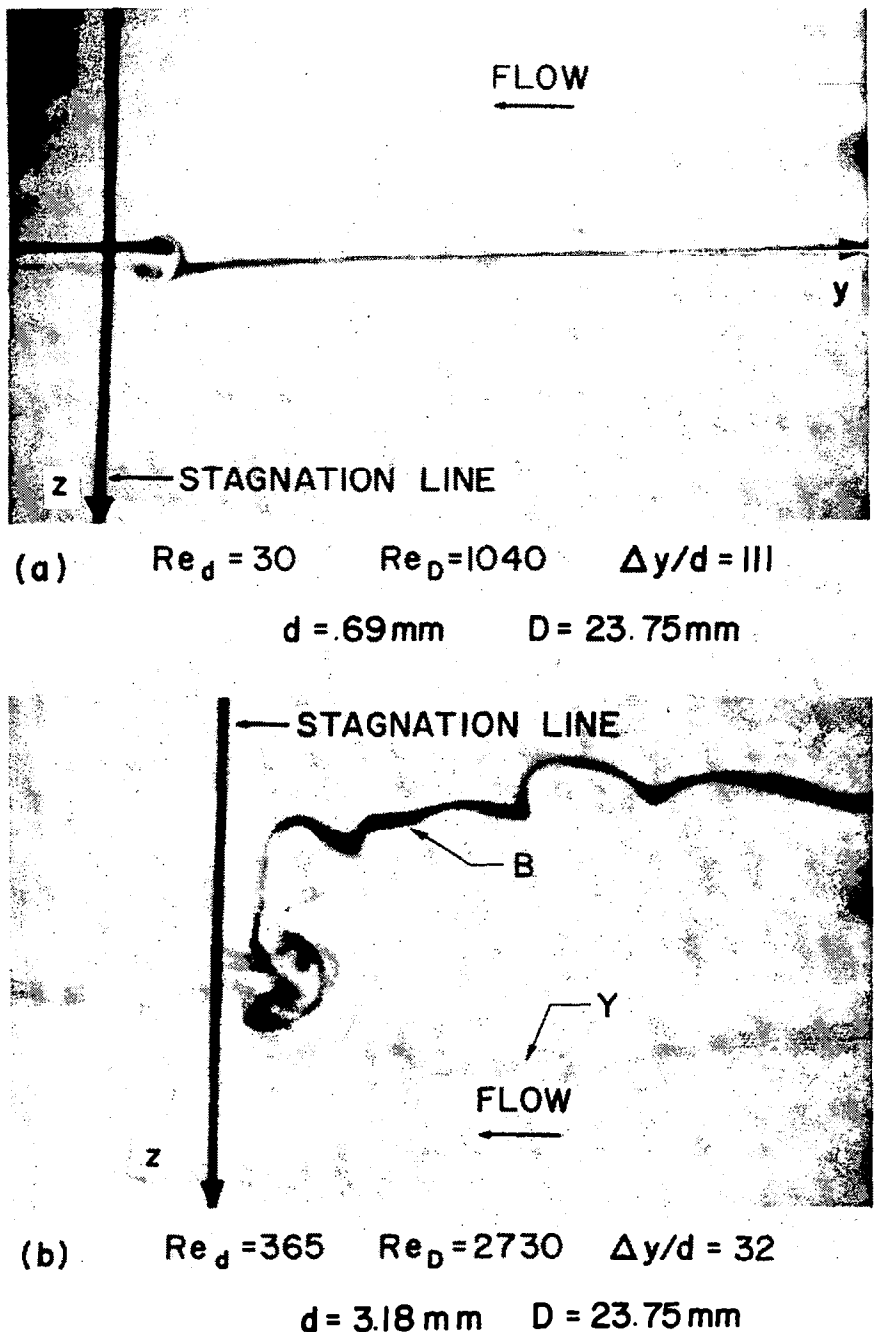

Figure 5. Side-view dye visualization of vortex formation due to a steady and a mildly unsteady single rod wakes. In (b) far-upstream laminar dye injection causes small momentum defects at the edges of the wake which may influence near-singular flow conditions. (Courtesy of Hodson and Nagib, 1975.)

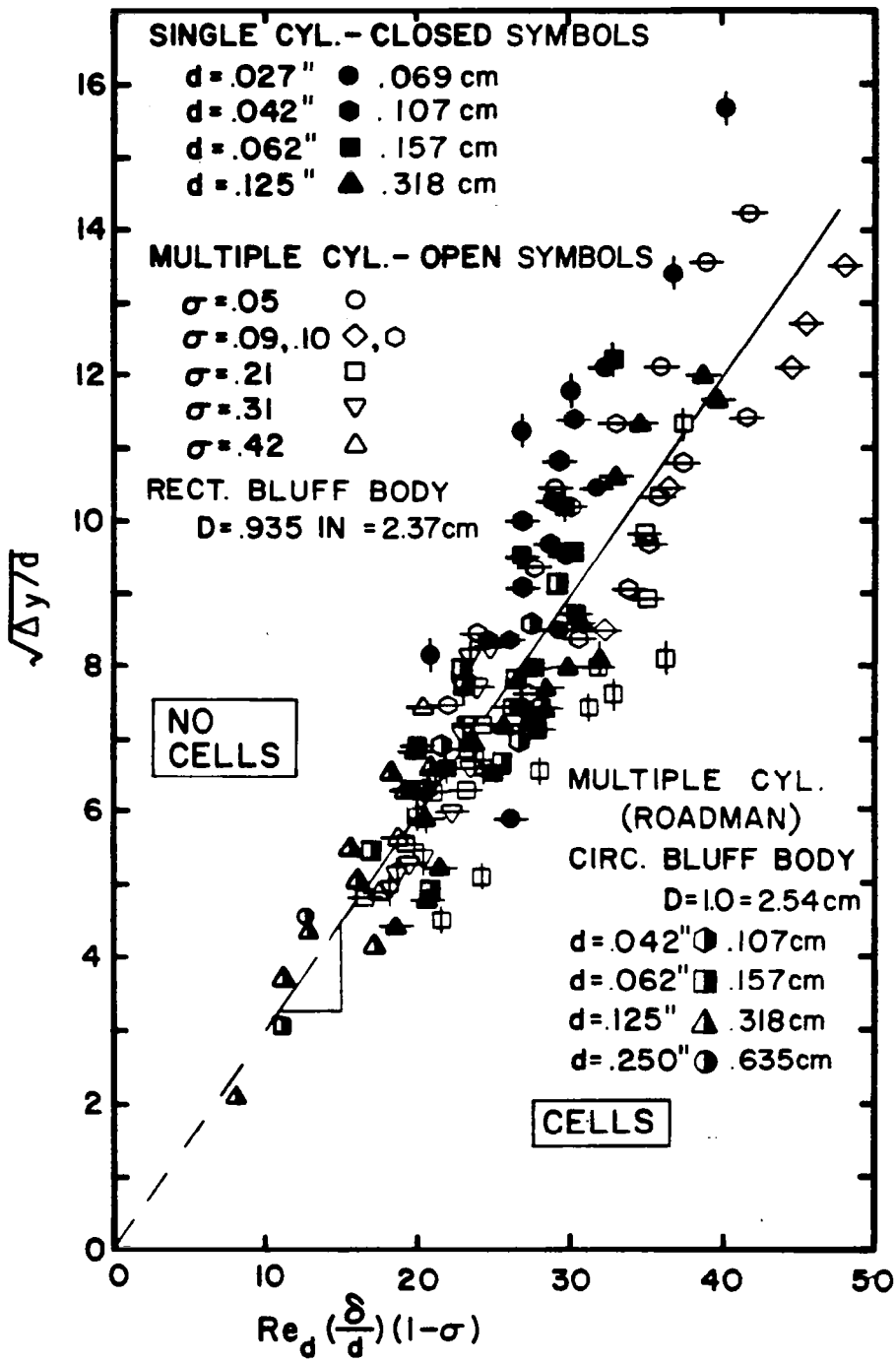

Figure 6. Empirical correlation of threshold conditions for counterflow vortex formation for single and multiple wakes impinging on a rectangular cylinder. (Courtesy of Nagib, Hodson, and Roadman, 1977.)

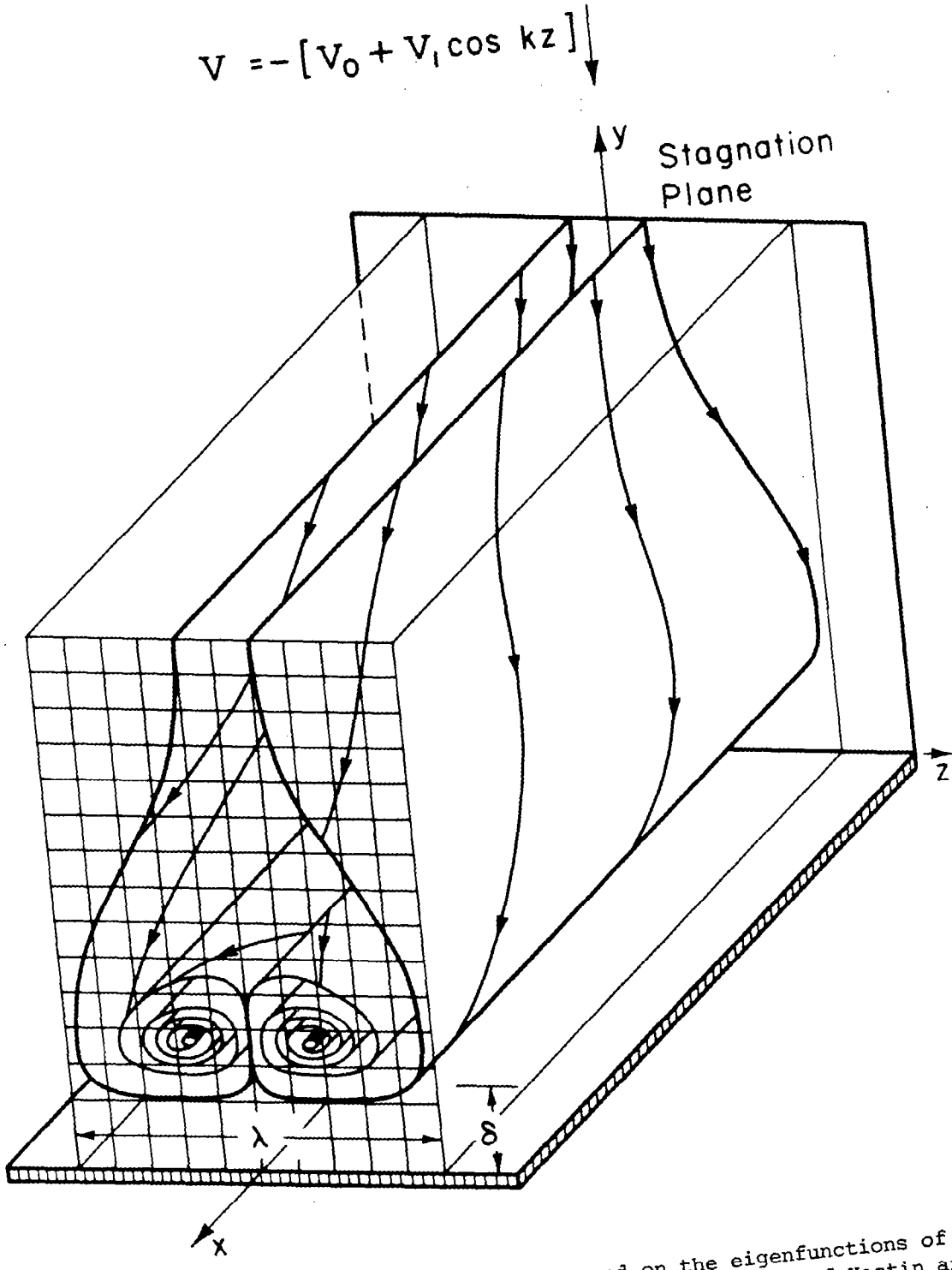

Figure 7. Three-dimensional flow pattern based on the eigenfunctions of the steady vorticity-amplification theory. (Courtesy of Kestin and Wood, 1970.)

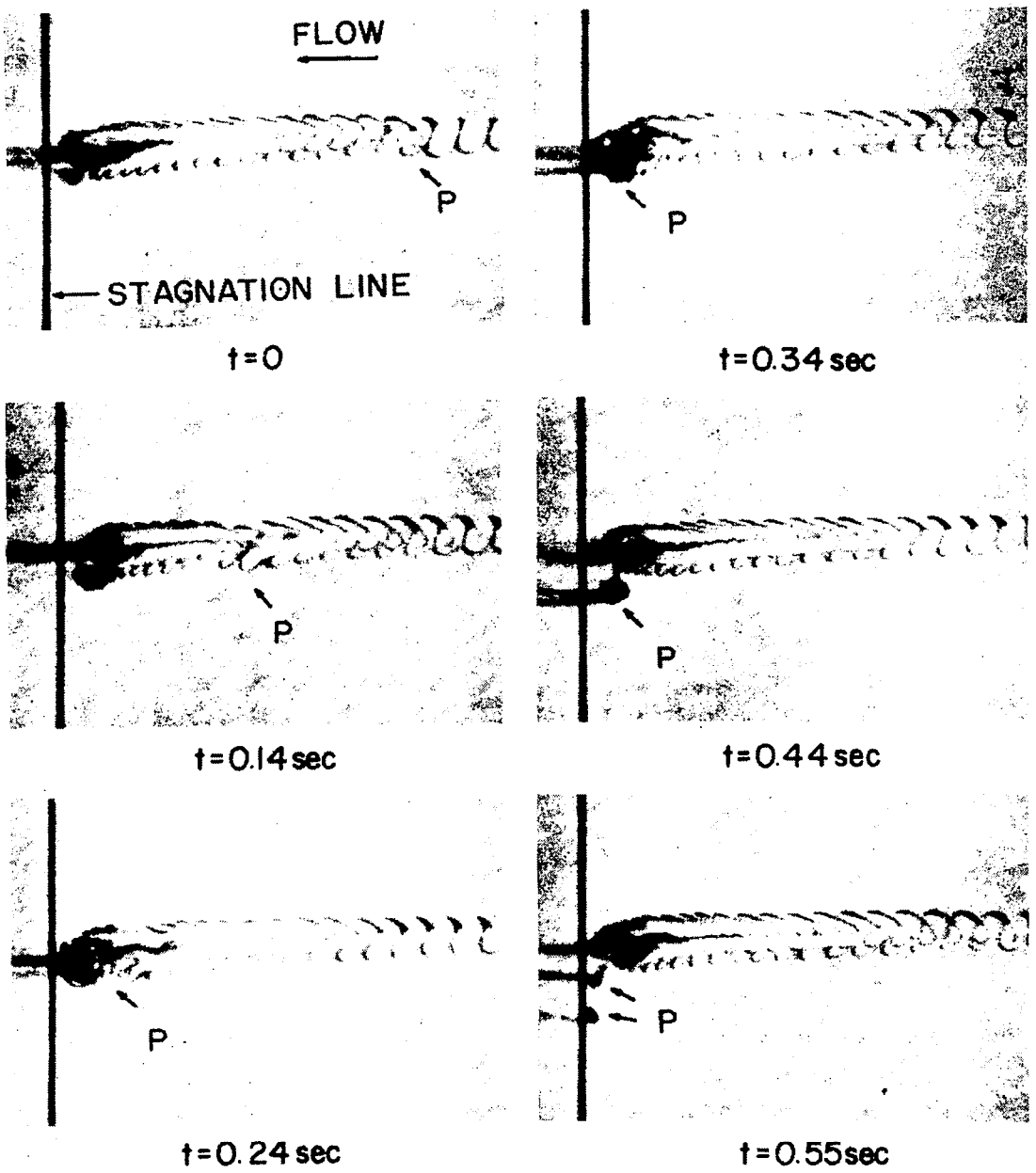

Figure 8. Side-view dye visualization of strong unsteady interaction between a counterflow vortex pair and a "natural" perturbation P of the vorticity in the rod wake at Re_d = 90. (From a movie of Hodson and Nagib, 1975.)

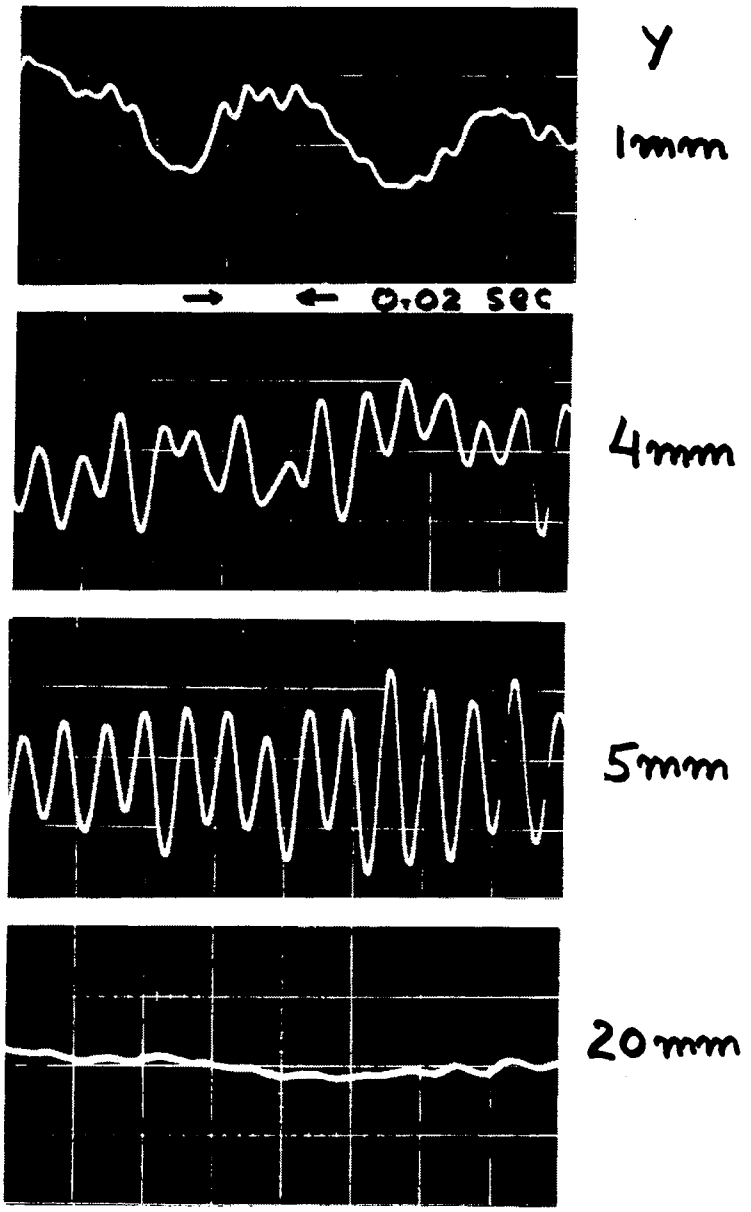

Figure 9. Oscillographs of u'(t), the perturbation velocity perpendicular to a hot wire located at various normal distances y from the cylinder, presumably in the stagnation plane. Water tank experiments: V_∞ = 15 cm/s; δ = 1.8 mm; time = 0,02 sec/div; sensitivity 100mV/div; Tu $\sim$ .85% generated by a screen riding 20 cm upstream of the cylinder; Tu measured 10 cm downstream, and 10 cm above the stagnation plane; screen mesh: 12/cm; wire diameter: 0.31 mm. (Courtesy of H. Hassler, 1971, and private communication.)

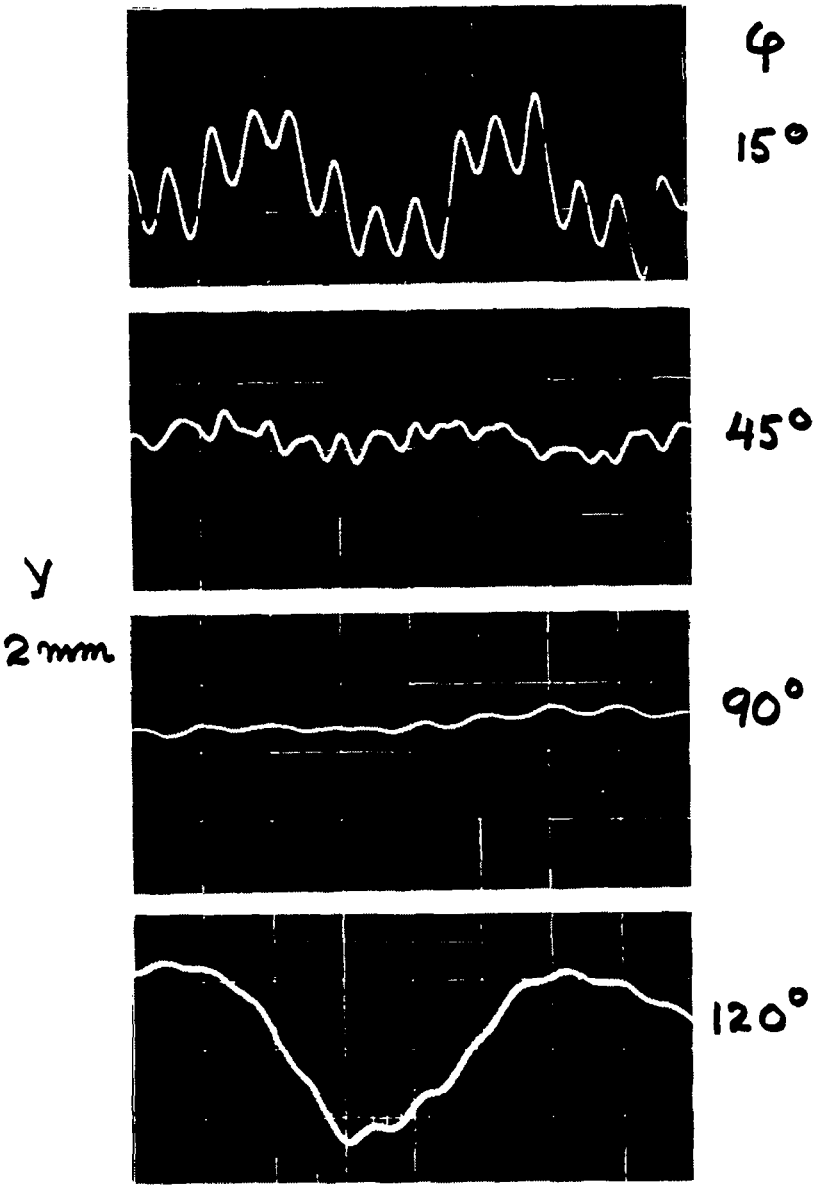

Figure 10. Oscillographs of u'(t), the perturbation velocity perpendicular to a hot wire located at a normal distance y = 2 mm from the cylinder in planes at angles φ from the stagnation plane. Conditions as in Figure 9. (Courtesy of H. Hassler, 1971.)

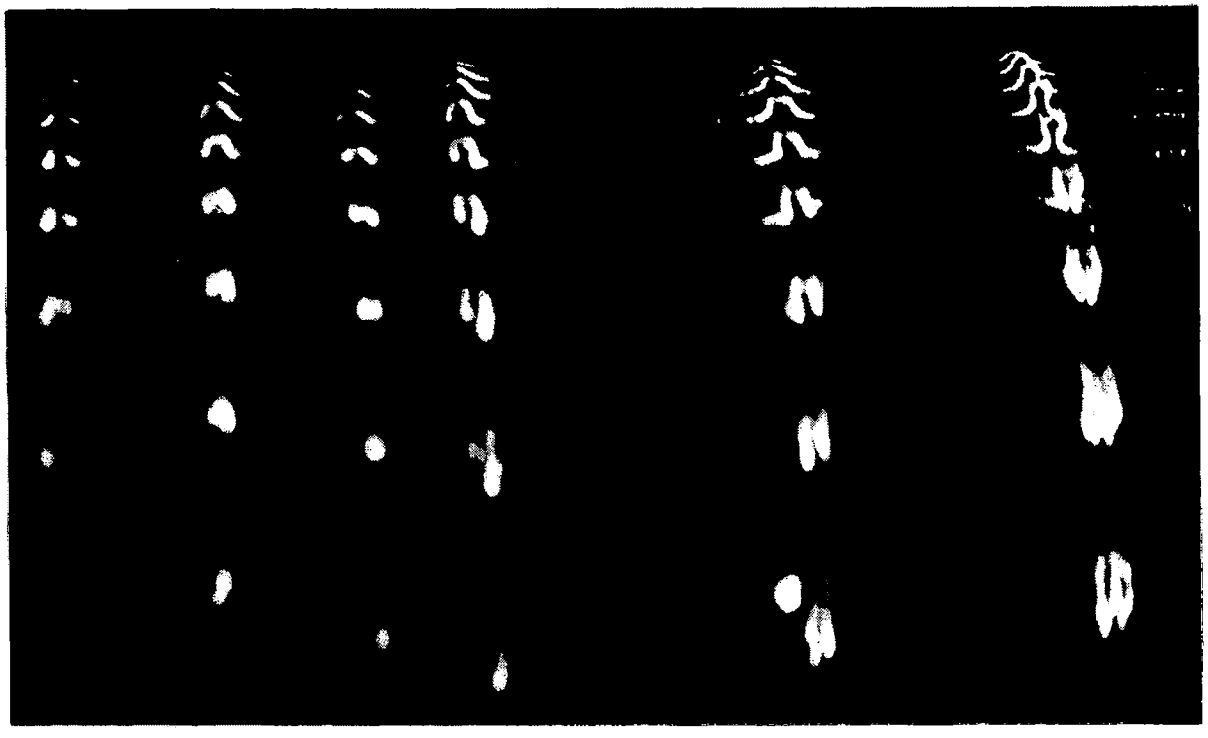

Figure 11. Vertical view downward on the 12 cm diameter cylinder moving in a water tank with V_∞ = 11.9 cm/s into screen-generated turbulence, Tu, of approximately 0.6%. Hydrogen-bubble time lines are formed at a horizontal cathode-pulsed wire location at y = 2mm, $\varphi = 11^\circ$ at the top of the picture. The time lines are progressively deformed by the upwelling motion of an irregular series of unsteady vortex pairs. Originally, the bubbles move towards the plane of symmetry of each pair, are uplifted and then thin out as they move away from the plane of symmetry. Ultimately the bubbles tend to concentrate at the core of the vortices. The time-line shapes near $\varphi = 80^\circ$ correspond to the integrated history of the motion, not to the local vortex strengths. (Courtesy of P. Čolak-Antič, 1971, and private communication.)

Figure 12. Strengthening of vortices with increase in V_{∞} to 19.4 cm/s, other conditions remaining as in Figure 11. Stereoscopic viewing identifies the seemingly closed spirals at left center as a succession of time-line tongues stretched by rotation into mushroom shapes with low bubble density at the top. The concentration of bubbles in the cores develops somewhat irregularly. Stronger vortex pairs often have weak neighbors and there is some amalgamation. (Courtesy of P. Čolak-Antič, 1971, and private communication.)

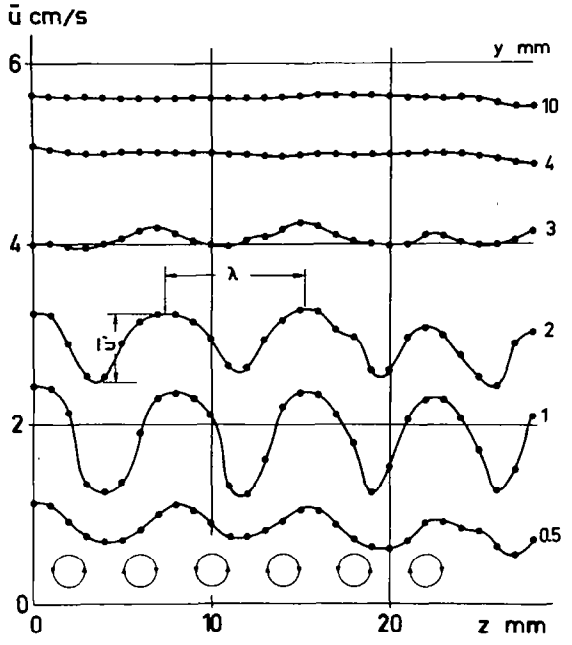

Figure 13. Distribution of $\overline{u}(y,z)$, the short-time averages (over one second) of velocity perpendicular to a hot wire located at spanwise locations z and normal distances y in the plane $\varphi = 4^{\circ}$. Other conditions as in Figure 9. (Courtesy of H. Hassler, 1971.)

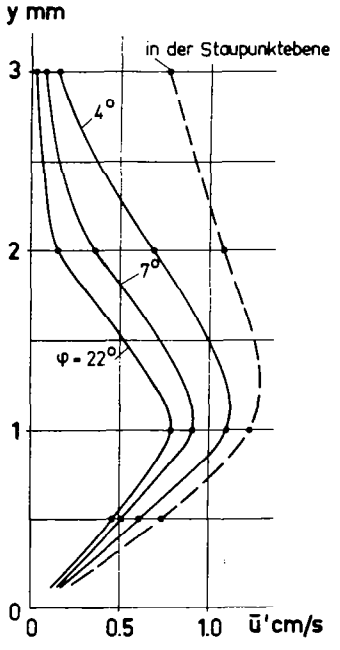

Figure 14. Distribution of one-second averages of velocity $\overline{u}'$ perpendicular to a hot wire at normal distances y from the cylinder, at various φ angles and a fixed z location. Other conditions as in Figure 9. (Courtesy of H. Hassler, 1971.)

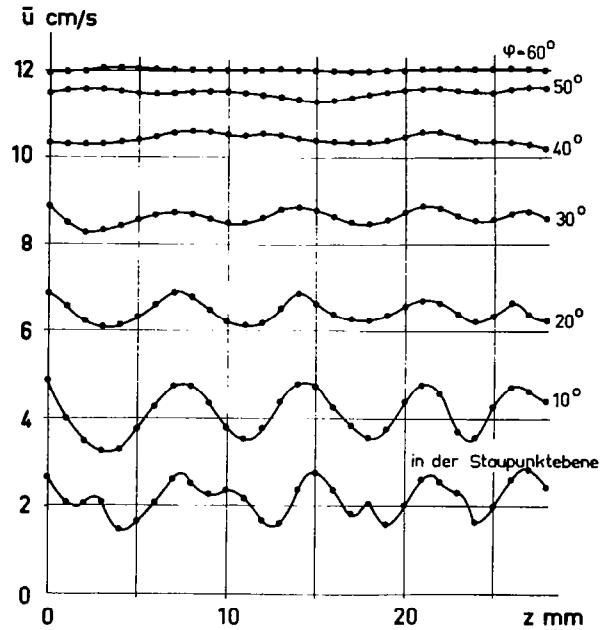

Figure 15. Distribution of one-second averages of velocity $\bar{u}(2,z,\varphi)$ perpendicular to a hot wire located at spanwise locations z, a fixed normal distance y = 2 mm, in planes at angles φ from the stagnation plane. Other conditions as in Figure 9. (Courtesy of H. Hassler, 1971.)

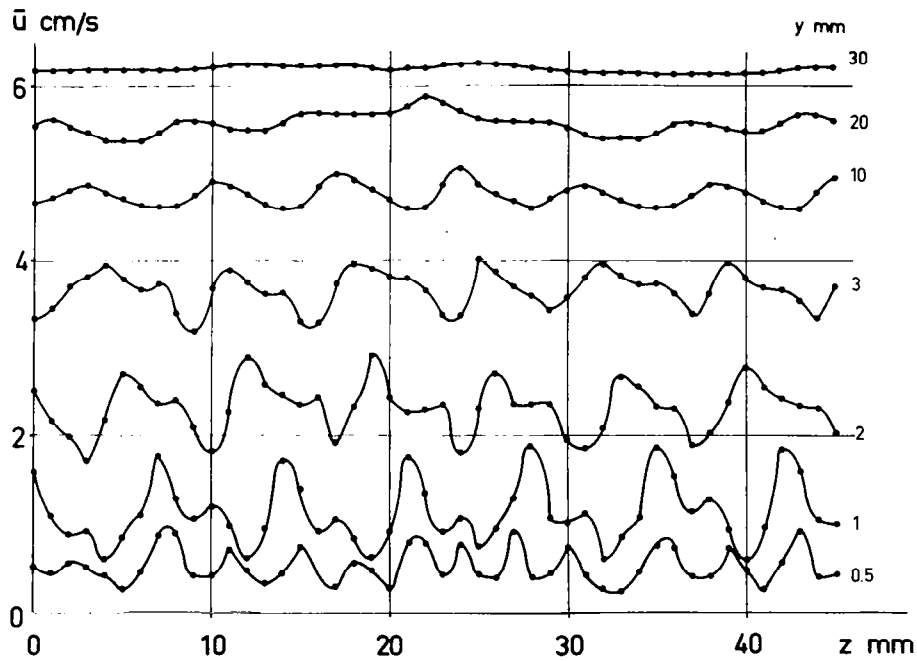

Figure 16. Distribution of one-second averages of velocity $\bar{u}(y,z)$ perpendicular to a hot wire located at spanwise locations z and normal distances y in the stagnation plane $\varphi = 0^{\circ}$. Other conditions as in Figure 9. (Courtesy of H. Hassler, 1971.)

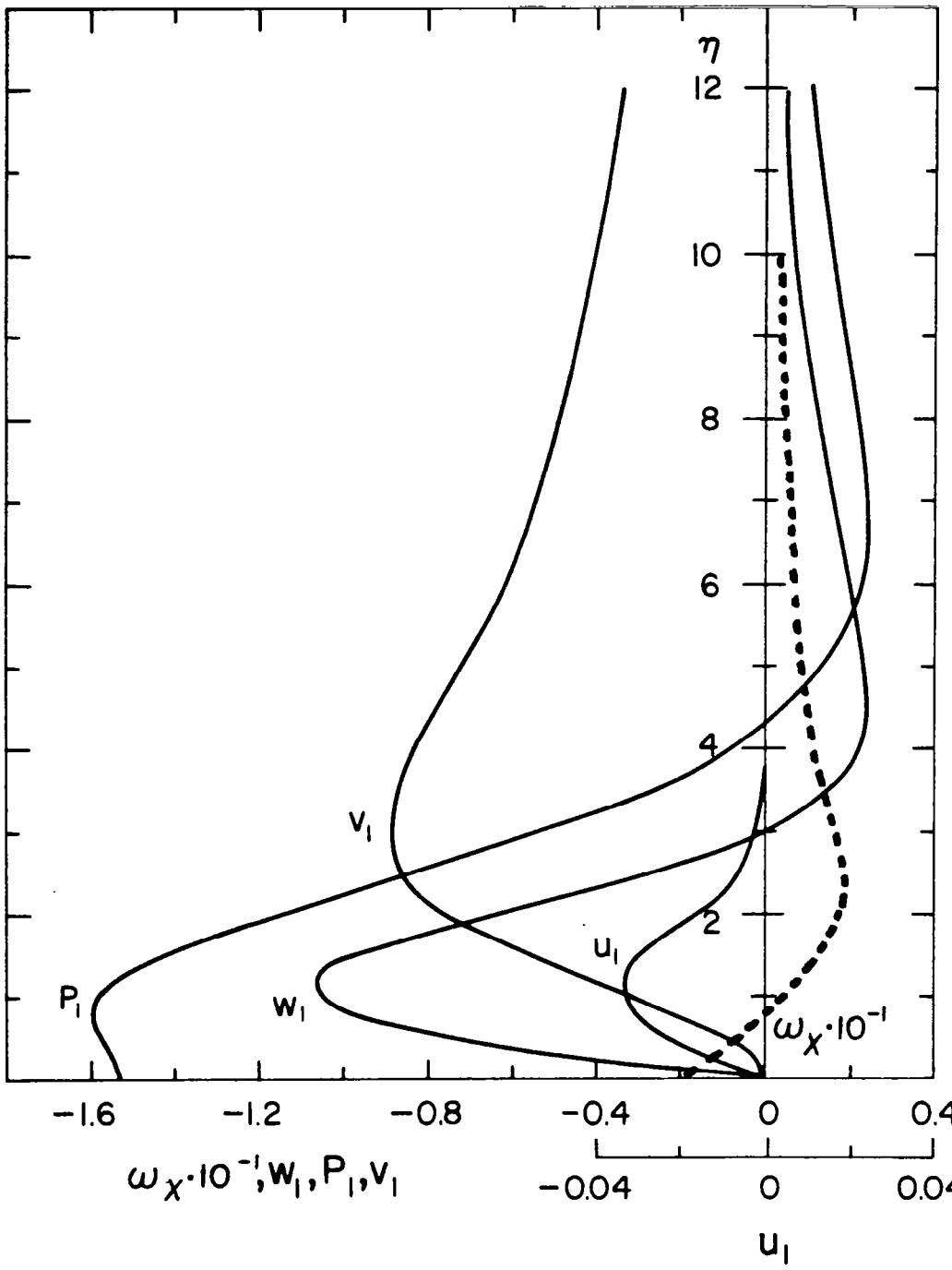

Figure 17. Steady disturbance field profiles of velocity components, static pressure and vorticity; eigenvalues for prescribed wave number k = 2/3. (Courtesy of G, Inger, 1974.)

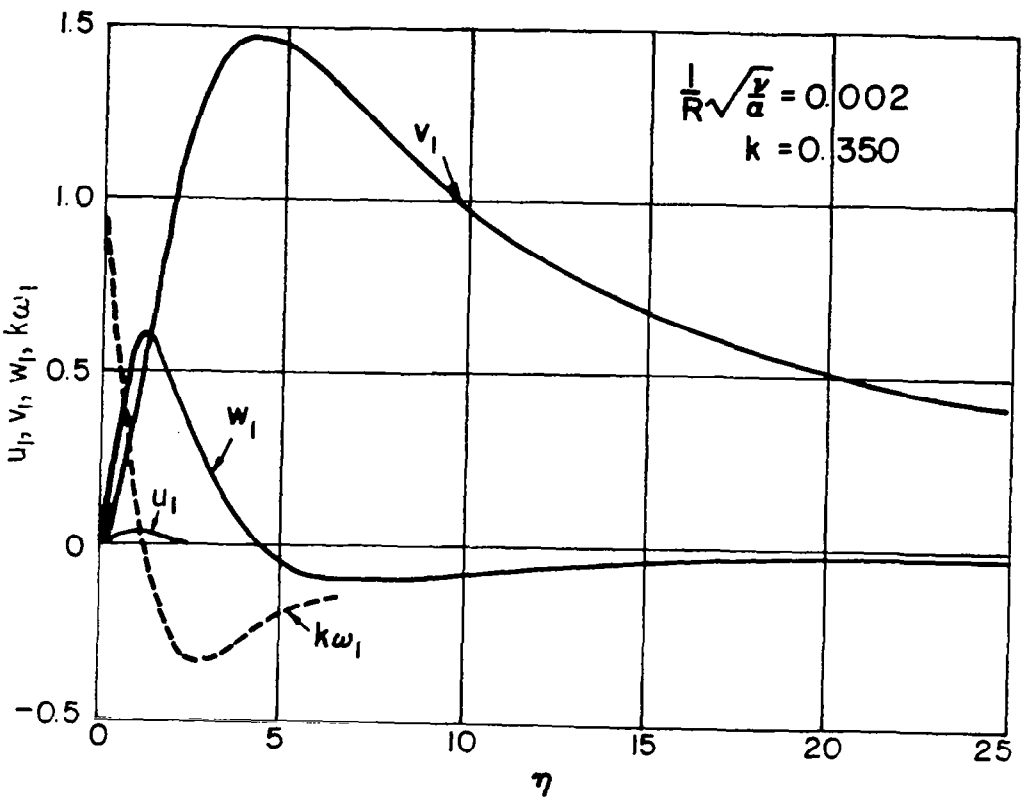

Figure 18. Velocity and vorticity solutions of the steady (neutral) linear eigenvalue problem, subject to asymptotic condition that $V_1(\infty)$ be a minimum. This condition selected k ≈ 0.35. (After Tani, 1974.)

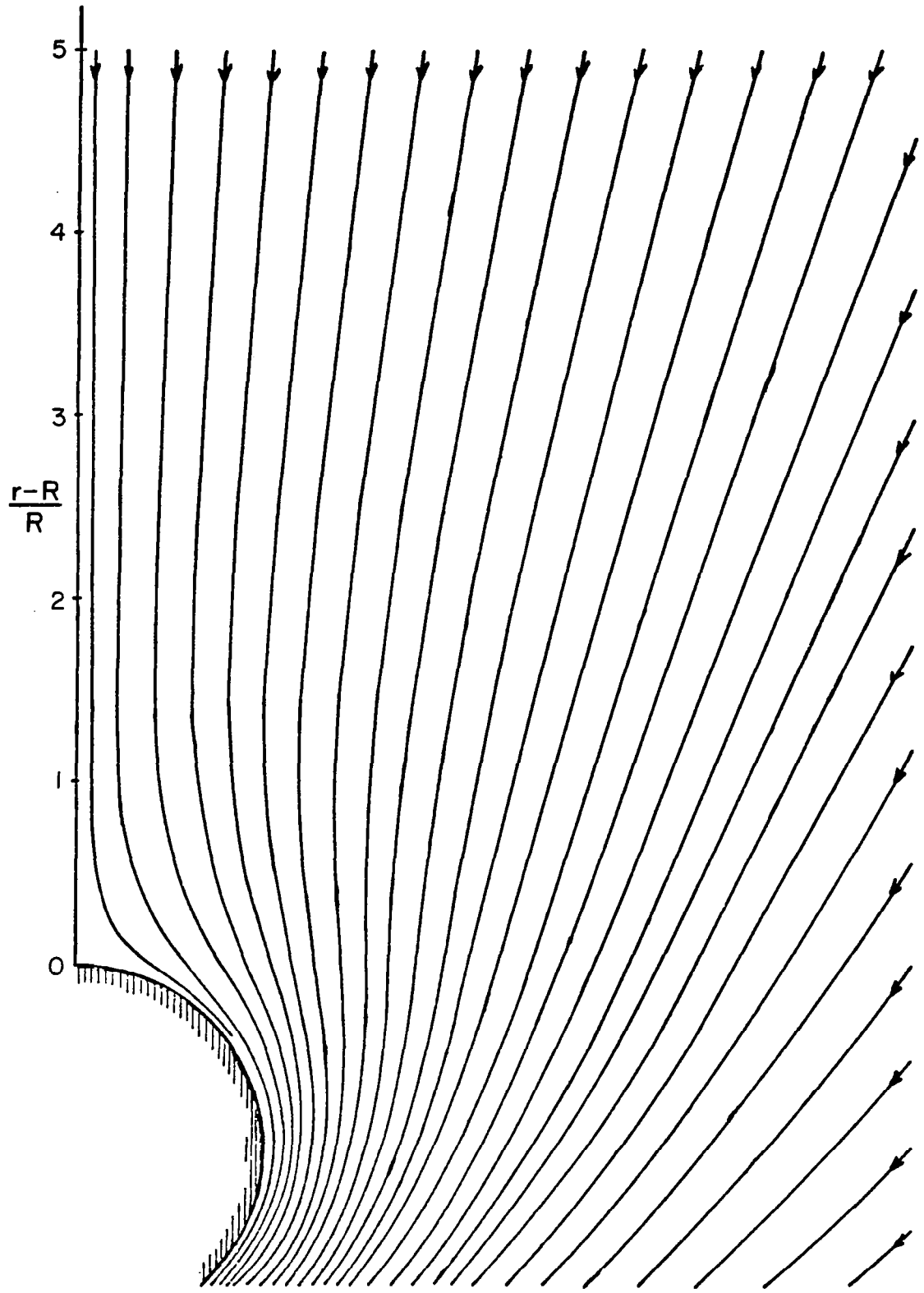

Figure 19. Streamline pattern of Hainzl's base flow, generated by sink distributions along the wake axis. Hammerlin's unstable range $0 < k < 1$ disappeared. (After Hainzl, 1965.)

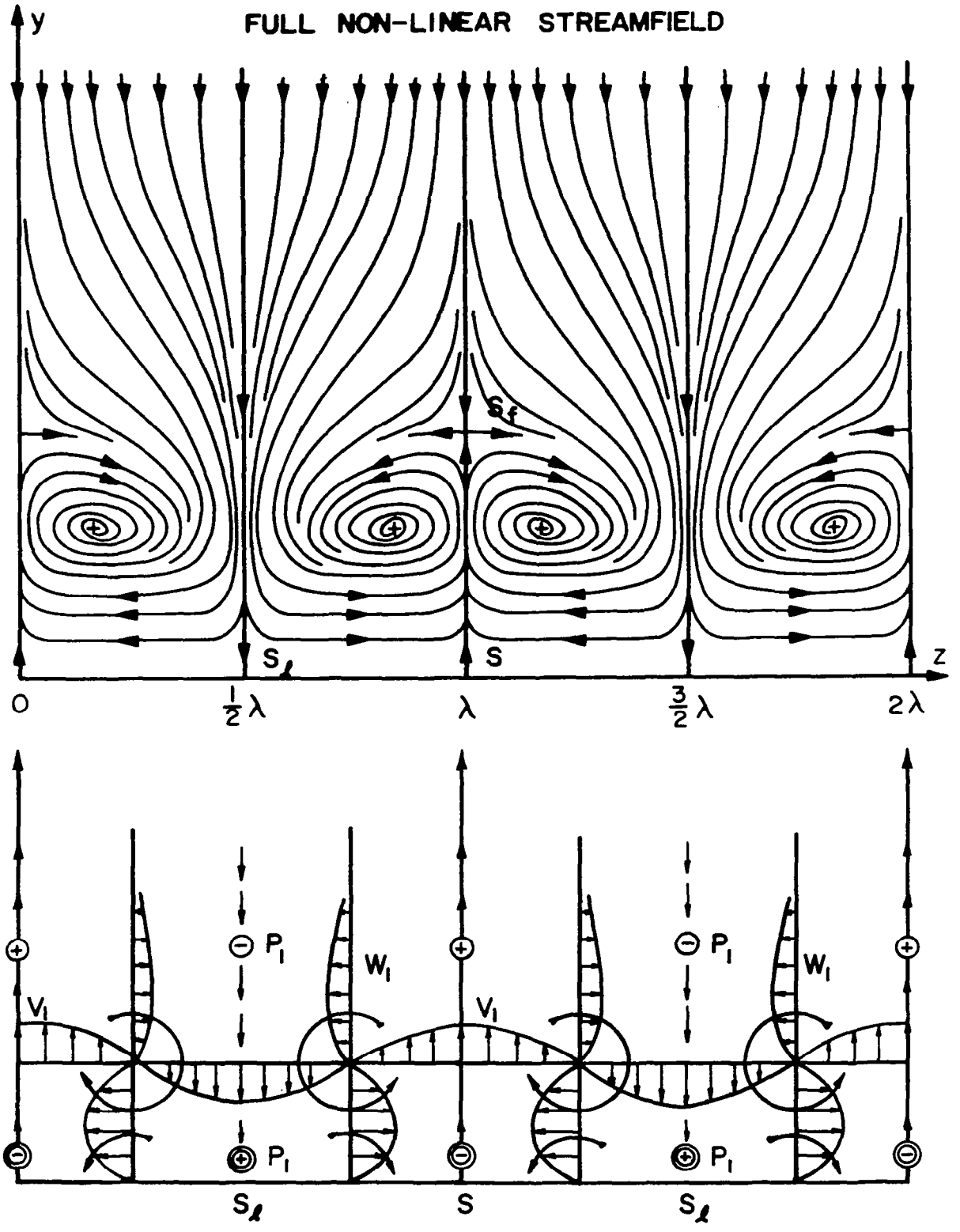

Figure 20. Second-order streamline pattern (Courtesy of Kestin and Wood, 1970) and corresponding linear disturbance fields.

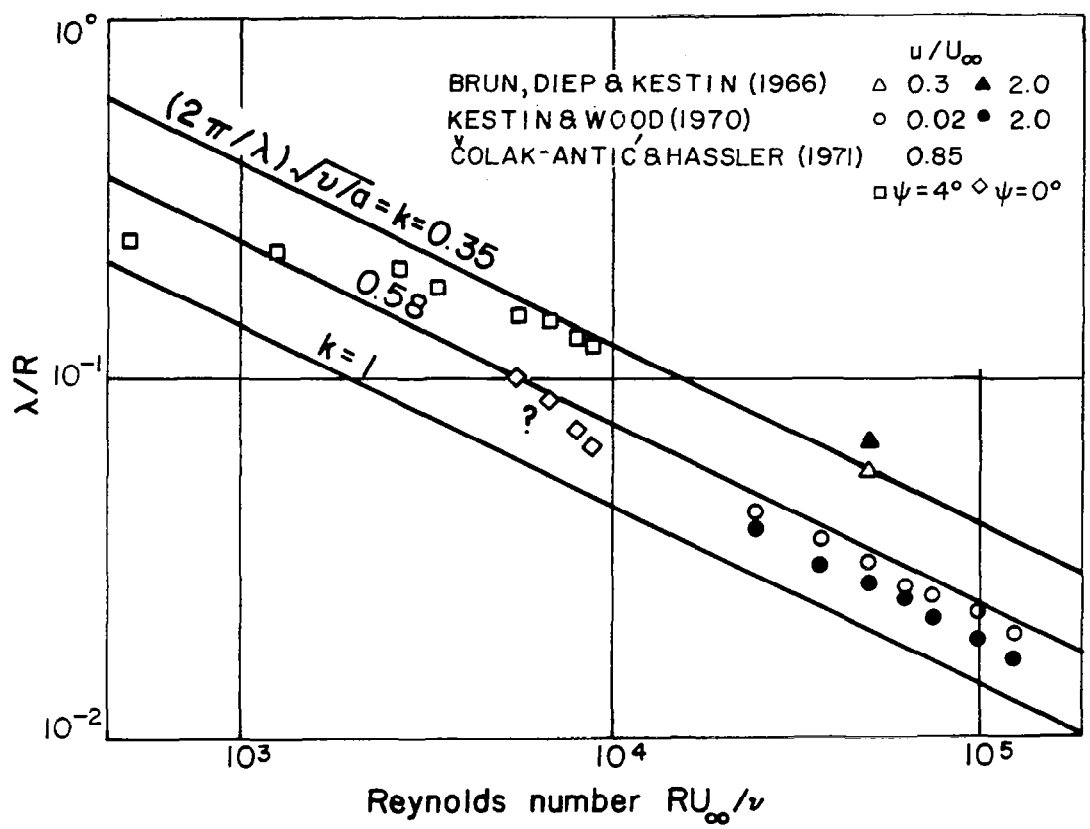

Figure 21. Nondimensionalized, experimentally observed, time-averaged spanwise wavelengths in flows with various turbulence levels as functions of cylinder Reynolds number. (After Tani, 1974.) Diamond-shaped data is from Figure 16 and is probably unreliable because of probe interference.

1. Report No.	2. Government Accession No.	3. Recipient's Catalog No.
NASA CR-3231		

4. Title and Subtitle	5. Report Date
ON THE QUESTION OF INSTABILITIES UPSTREAM OF CYLINDRICAL BODIES	December 1979
	6. Performing Organization Code

7. Author(s)	8. Performing Organization Report No.
Mark V. Morkovin	I.I.T. Fluids and Heat Transfer Report R79-3
	10. Work Unit No.

9. Performing Organization Name and Address	11. Contract or Grant No.
Illinois Institute of Technology MMAE Department Chicago, IL. 60616	NSG-1120

12. Sponsoring Agency Name and Address	13. Type of Report and Period Covered
National Aeronautics and Space Administration Washington, D.C. 20546	Contractor Report 11/15/74 - 4/30/77
	14. Sponsoring Agency Code

15. Supplementary Notes

Langley Technical Monitor: Ivan E. Beckwith

Final report

16. Abstract

In an attempt to understand the unsteady vortical phenomena in perturbed stagnation regions of cylindrical bodies, a critical review of the theoretical and experimental evidence was made. Current theory is revealed to be incomplete, incorrect, or inapplicable to the phenomena observed experimentally. The formalistic approach via the "principle" of exchange of instabilities should most likely be replaced by a "forced-disturbance" approach. Also, many false conclusions were reached by ignoring that treatment of the base and perturbed flows in Hiemenz coordinate η is asymptotic in nature. Almost surely the techniques of matched asymptotic expansions will have to be used to capture correctly the diffusive and vorticity amplifying processes of the disturbances vis-à-vis the mean-flow boundary layer and outer potential field as η and y/diameter approach infinity. There are also serious uncertainties in the experiments which are discussed in detail.

17. Key Words (Suggested by Author(s))	18. Distribution Statement
Instability Theory; Stagnation flow; Flow about a bluff body; Vorticity amplification; Turbulent boundary layer; Laminar boundary layer; Enhanced heat transfer.	Unclassified - Unlimited Subject Category 34

19. Security Classif. (of this report)	20. Security Classif. (of this page)	21. No. of Pages	22. Price*
Unclassified	Unclassified	110	$6.50

* For sale by the National Technical Information Service, Springfield, Virginia 22161

NASA-Langley, 1979